The University of Nottingham

UNITED KINGDOM · CHINA · MALAYSIA

Investigating the Molecular Basis of Biased Signalling at Cannabinoid Receptors

Master by Research Thesis

Author:	Morgan Jane Dennis
Student ID:	14328228
Course:	MRes Pharmacology and Drug Discovery
Level of Study:	Postgraduate Research
Start Date:	October 2021
Supervisor/s:	Prof. Dmitry Veprintsev, Dr David Sykes, Dr Eline Koers
School:	Life Sciences
Faculty:	Medicine and Health Sciences
Email:	mbymjd@nottingham.ac.uk
Total word count:	25, 837

Table of Contents

Abstract

The endocannabinoid system (ECS) comprises both cannabinoid receptor 1 (CB_1R) and cannabinoid receptor 2 (CB_2R), which belong a class of rhodopsin-like G protein-couple receptors (GPCRs) alongside the endogenous ligands, and the respective enzymes for their synthesis and degradation. The ECS and cannabinoid receptors are involved in a number of important physiological processes both in the brain and peripheral tissues, including neuronal development, learning and memory formation, as well as immune cell function and inflammation. It has proven difficult to develop novel selective drugs for the cannabinoid receptors without causing multiple, and often serious, side-effects. In addition, GPCRs such as the cannabinoid receptors couple to one or more trimeric G proteins or arrestin proteins, adding more complexity to drug discovery efforts targeting these receptors. It is now firmly established that certain drugs can trigger pathway-specific signalling, which may enable the development of drugs with greater selectivity for therapeutic pathways and potentially with fewer side effects.

We studied this phenomenon known as *biased signalling* at human cannabinoid receptors using a series of novel ligands, identified via *in silico* docking, and G protein biosensors. Initial competition and saturation binding assays characterised ligand binding to both CB_1Rs and CB_2Rs, while signalling bias investigated via bioluminescent resonance energy transfer (BRET)-based mini-G protein (which mimics a full-length G protein) and β-arrestin recruitment assays (receptor C-terminus tagged with NanoLuc™ donor fluorophore and β-arrestin tagged with a venus acceptor fluorophore). Functional cannabinoid receptor activation was then assessed using G protein activity (Gi-CASE) sensors that use BRET to report the activation-induced dissociation of the G protein.

Among the three novel compounds investigated, two proved to be agonists and one an inverse agonist at CB_1R and CB_2R. Agonist activity in the Gi-CASE assays elicited a decrease in the BRET signal, indicative of receptor activation and G protein dissociation. Inverse agonist activity caused an increase in BRET signal, suggestive of receptor inactivation and the accumulation of inactive G protein. However, the novel ligands appeared relatively unbiased at the cannabinoid receptors due to similar recruitment of mini-G and β-arrestin proteins following receptor activation, both in terms of potency and efficacy. A more complete pharmacological profile of the reference and novel ligands was gained, using confocal microscopy and a diffusion-enhanced resonance energy transfer (DERET) assay, both used to evaluate agonist-induced receptor internalisation at the cannabinoid receptors.

Developing drugs to target CB_1R and CB_2R is valuable because only a few marketed drugs currently target cannabinoid receptors. Rimonabant is a previously marketed CB_1R antagonist and a potent anti-obesity agent, and is associated with significant neurological side effects, which eventually led to its withdrawal from the market. Rimonabant serves as an example of the challenges faced with the development of novel, safe drugs to target cannabinoid receptors in disease.

Unfortunately, we did not identify any ligand bias among any of the three novel compounds under study. However, continued investigation of these and other novel compounds will better characterise their potential to become novel therapies for conditions linked with cannabinoid receptor signalling. Looking forward, we also highlight a novel membrane-based biosensor assay, a step towards creating a high-throughput means to identify novel hits at cannabinoid receptors.

Chapter One: Introduction

1.1 GPCR structure and signalling

The G protein-coupled receptor (GPCR) family encapsulates a vast array of cell membrane receptors. GPCR receptors are membrane receptor proteins consisting of a polypeptide chain that starts with an extracellular amine (N)-terminus, that traverses the membrane and forms seven distinct transmembrane regions connected via intracellular or extracellular loops, before terminating in the intracellular domain with a carboxyl (C)-terminus (Banerjee and Mahele, 2015). The seven transmembrane regions bundle together and form the ligand binding pocket where ligands bind and activate the receptor (Katritch *et al.,* 2013). Different flavours of GPCR exist based on differences in the receptor structure, including type A rhodopsin-like, type B secretin-like, type C metabotropic GPCRs, type D fungal pheromone GPCRs, type E cyclic adenosine monophosphate (cAMP)-like receptors and type F GPCRs which are frizzleds or smoothened receptors (Hu *et al.,* 2017).

GPCRs are associated with intracellular guanine-nucleotide binding proteins, or G proteins, consisting of an alpha (Gα), beta (Gβ) and gamma (Gγ) subunit (Kamato *et al.,* 2015), altogether forming a heterotrimeric Gαβγ protein. Ligands binding to the GPCR causes a conformational change in the receptor, enabling the G protein to bind to the intracellular face of the 7TM receptor core, inducing the dissociation of guanine diphosphate (GDP) from the G protein. GDP is replaced by guanine triphosphate (GTP), causing the heterotrimeric Gαβγ protein to separate into a Gα subunit and Gβγ dimer, which is reformed when GTPase enzymes hydrolyse GTP to GDP (Harrison and Traynor, 2003).

The Gα subunit of the G protein heterotrimer can be stimulatory ($G\alpha_s$) and cause adenylyl cyclase activation, which converts adenosine triphosphate (ATP) to cyclic adenosine monophosphate (cAMP) and stimulates phosphokinase A (PKA) for the phosphorylation of target proteins (Wang *et al.,* 2017). The Gα subunit can also be an inhibitory ($G\alpha_i$) protein which supresses adenylyl cyclase and halts cAMP production and PKA stimulation. Collectively, GPCR signalling via $G\alpha_i$ and $G\alpha_s$ proteins oversees downstream signalling events and enzymes involved in cellular metabolism, gene expression and membrane permeability (Hofer, 2012; Kakkar *et al.,* 1999). G proteins can also signal via the inositol phosphate signalling pathway ($G\alpha_q$) involved in the activity of calcium (Ca^{2+}) channels (Smith *et al.,* 2018), while $G\alpha_{12/13}$ proteins also exist to activate RhoGTPases for altering gene transcription, cell transformation and the cell's actin cytoskeleton (Aittaleb *et al.,* 2010).

β-arrestin recruitment is another vital aspect of GPCR signalling, which is responsible for the activation of extracellular-signal-related kinases 1/2 (Coffa *et al.,* 2011; Shenoy *et al.,* 2006), as well as enabling GPCR signalling to come to an end. GPCR signalling is terminated by receptor phosphorylation and desensitisation, led by G-protein coupled receptor kinases (GRKs) that attach phosphate groups to serine and threonine amino acid residues near the intracellular C-terminus of the GPCR (Smith *et al.,* 2018). GRKs also recruit β-arrestin proteins to the receptor, which blocks the G protein from accessing the GPCR, thus halting G protein activation and signalling (Haider *et al.,* 2022; Shenoy and Lefkowitz, 2011). β-arrestin recruitment also triggers GPCR internalisation via endocytosis by forming clathrin-coated pits (CCPs) (Mohan *et al.,* 2012), formed from the arrestin interacting with clathrin and adaptor protein-2, which are involved in the formation of intracellular vesicles following receptor desensitisation (Chaudhary and Kim, 2021). Once internalised, the GPCR can be degraded or reset and recycled back to the membrane for reactivation.

1.2 Signalling bias at GPCRs

GPCR signalling can be tuned in response to agonist binding, and can result in the receptor preferentially signalling via either the G protein or β-arrestin protein. Termed *biased signalling,* this phenomenon involves pathway-specific signalling and may help drug discovery efforts by making novel drugs with fewer side effects (Kenakin and Christopoulos, 2013). Biased signalling can arise due to *ligand bias,* caused by differences in the strength of the interactions between a ligand and the GPCR binding domain, resulting in a unique conformation and differential GPCR signalling compared to that of another ligand binding and activating the same receptor (Kenakin and Christopoulos, 2013; Kenakin, 2019). In addition, stoichiometric differences in the abundancy of G proteins or β-arrestin proteins for a given GPCR can cause *systems bias*, causing differential signalling via the G protein or β-arrestin based on the tissue or system within which the GPCR is expressed (Sengmany *et al.,* 2019). Lastly, the location and intracellular environment of the GPCR inside the cell can lead to *location bias* and differential GPCR signalling depending on whether it is exhibited on the cell membrane versus inside the cell (Mohammad Nezhady e*t al.,* 2020).

Biased signalling is observed in μ-opioid receptors, where novel biased agonists are designed to target the G protein signalling pathway which is responsible for the analgesic effects of opioid medicines, without recruiting the β-arrestin proteins which may bring about adverse signalling events leading to opioid-induced respiratory depression and gastrointestinal effects (Senese *et al.,* 2020; Gillis & Christie, 2021).

Additional reviews also exist outlining several pre-clinical *in vivo* examples of biased ligands being able to treat for pain and itch, without causing side effects such as sedation or dysphoria, as well as examples of endomorphins as arrestin-biased ligands and morphine as a partially G protein-biased ligand (Kelly, 2013; Ranjan *et al.,* 2017). In fact, oliceridine is a recent FDA-approved μ-opioid agonist, designed to preferentially stimulate G protein signalling. However, concerns remain over the drug's safety and there are debates over whether the drug is biased or simply a partial agonist of G protein activation (Mullard, 2020). Indeed, there seems to be a discrepancy between observed biased agonism in *in vitro* studies versus that seen in *in vivo* studies in both human and other species, suggesting that biased signalling requires a more robust and continued understanding as far as drug discovery is concerned.

As for the cannabinoid receptors, research concerning biased agonism at these receptors is still somewhat in its infancy. However, studies indicative of biased agonism may be useful for drug discovery efforts by revealing more about how these receptors signal. For example, LaPrairie et al. have highlighted that β-arrestin signalling is preferred in cannabinoid receptor type 1 following tetrahydrocannabinol (THC) stimulation on mouse striatal derived cell lines (LaPrairie *et al.,* 2014), and that endocannabinoids tend to be biased towards G protein signalling (LaPrairie *et al.,* 2015). Similar findings on THC have also been found by Zhu et al. based on studies of receptor internalisation and signalling via the phosphorylated ERK1 and 2 pathways in Chinese hamster ovary cells, which may indicate a preference for β-arrestin signalling over the G protein (Zhu *et al.,* 2020). However, Ibsen et al. failed to highlight β-arrestin-favoured signalling with THC stimulation in studies in human embryonic kidney (HEK)-293 cells (Ibsen *et al.,* 2019), indicating how the molecular basis of biased signalling may vary with cellular and experimental conditions. This highlights the need to better define the molecular mechanism of biased signalling at cannabinoid receptors.

1.3 The endocannabinoid system and cannabinoid receptor signalling

The endocannabinoid system (ECS) encompasses cannabinoid receptor types 1 (CB_1R) and 2 (CB_2R), which are type-A, rhodopsin-like GPCRs, and couple to an inhibitory G protein ($G\alpha_i$) to suppress adenylyl cyclase activity and the production of cAMP and PKA (Howlett, 2005). The ECS also includes a number of G protein-like receptors linked to the activity of endogenous cannabinoids that play a role in cognitive function in mouse models of Alzheimer's disease and the control of blood

pressure (Penumarti & Abdel-Rahman, 2014; Blanton *et al.,* 2022; Xiang *et al.,* 2022), as well as including a number of transient receptor potential channels (Muller *et al.,* 2019). The ECS further includes the enzymes responsible for the biosynthesis and degradation of the endogenous cannabinoid ligands *N-arachidonoylethanolamine* (anandamide; AEA) and *2-arachidonoylglycerol* (2-AG), which are derived from membrane phospholipids and arachidonic acid, binding to both receptors with sub-micromolecular affinities (Devane *et al.,* 1992; Mechoulam *et al.,* 1995). The metabolism of AEA primarily involves fatty acid aminohydrolase, cyclooxygenase-2 (COX-2) or *N*-acylethanolamine, though is often carried out by monoacylglyerol. In contrast, 2-AG is degraded by ABH6 and 12, as well as COX-2 (Morcuende *et al.,* 2022), suggesting that inhibitors of COX-2 may benefit endocannabinoid levels.

CB_1R is expressed throughout the central nervous system, primarily on presynaptic neurones, where its expression enables the modulation of neuronal excitation. Specifically, postsynaptic neuronal depolarisation causes an influx of calcium into the neurone and triggers the production of AEA and 2-AG (Brini *et al.,* 2014; Ogura *et al.,* 2016). AEA and 2-AG are then fed back to the presynaptic neurone, where they bind CB_1R couple to $G\alpha_i$ coupling, decreasing the activity of voltage-gated calcium channels and suppress continued neuronal excitation. CB_1R can also couple to stimulatory G ($G\alpha_s$) proteins, increasing the activity of inwardly-rectifying potassium channels to further dampen neuronal excitation (Guerrero-Alba *et al.,* 2019). CB_1Rs are expressed in neurones of the periaqueductal grey matter in the midbrain and the substantia gelatinosa of the spinal cord (Manzanares *et al.,* 2006), suggesting CB_1R may also have a role in the modulation of nociception. Notably, the presence of CB_1R on presynaptic neurones in the central nervous system supports the control of endogenous pain by dampening presynaptic neuronal excitation and neurotransmitter release. This forms the basis of cannabis use for the control of neuropathic pain (Casey *et al.,* 2022), and also supports the use of cannabinoids for treating anxiolytic disorders and epilepsy by reducing neuronal excitation (Berger *et al.,* 2022; Costa *et al.,* 2022). The medicinal use of cannabinoids including cannabis could also ameliorate depression and similar conditions by targeting CB_1R (Hernández-Hernández and Garcia-Fuster, 2022; Zer-Aviv *et al.,* 2022), further justifying the importance of elucidating the therapeutic potential of the ECS.

However, targeting CB_1R is a double-edged sword, and the long-term use of cannabis can be detrimental to mental and physical health and can worsen psychological disorders in affected people (Karila *et al.,* 2014). Furthermore, *rimonabant,* which was

previously marketed as a potent anti-obesity agent and CB_1R antagonist to block appetite, has caused significant psychiatric effects and suicidal tendencies in patients (Blum *et al.,* 2021). As a result, finding efficacious treatments at CB_1R is challenging, and drug discovery efforts may be best directed to targeting CB_2R instead. CB_2R is located mainly in peripheral tissues and at lower levels in the brain, and is expressed on immune cells including microglia (Turcotte *et al.,* 2016). CB_2R has anti-inflammatory properties in mice, where it helps reduce the activation and infiltration of pro-inflammatory M1 macrophages (Du *et al.,* 2018), and regulates the release of pro-inflammatory cytokines such as interleukin-1β (Liu *et al.,* 2022), and may ameliorate emotional behaviour and cognition in response to inflammation (Morcuende *et al.,* 2022). Activating CB_2R can also alleviate oxidative stress in psoriatic skin lesions (He *et al.,* 2023), while also having an antinociceptive effect in a number of animal models (Wen *et al.,* 2023; Wilkerson *et al.,* 2022; Zhou *et al.,* 2023), indicating the beneficial role of CB_2R for which we have only just scratched the surface. It is therefore important to develop novel and effective therapies for the cannabinoid receptors that can better target specific signalling pathways to minimise systemic side effects.

1.4 Current methods and limitations to studying G protein activation

Discovering novel hits at GPCRs, including the cannabinoid receptors, typically incorporates a whole-cell approach. Using whole cells can be challenging due the requirements of culturing cells, as well as differences in receptor expression and variability in drug response, thus hampering screening efficiency and delaying the identification of novel hits between assays.

As a result, drug discovery efforts employing membrane-based assay alternatives could increase the screening throughput of novel compounds to target receptors, thus accelerating the identification of new treatments. For example, the [^{35}S]GTPγS assay is a useful membrane-based assay for studying agonist efficacy and potency at $G\alpha_i$-coupled GPCRs, which works by replacing GTP bound to $G\alpha_i$ with a radioactive ^{35}S-labelled guanosine 5'-o-(3-thio) triphosphate ligand (DeLapp *et al.,* 2012). The label is resistant to GTPase hydrolysis, which in turn prevents the rebinding of GDP and hence the reformation of the original heterotrimeric G protein. This results in $G\alpha_i$ accumulation which can be quantified alongside the radioactivity count as a marker of agonist activity (Harrison and Traynor, 2003). Despite this, running the assay in whole cells is not easy because the radioactive label cannot readily permeate the cells without permeabilizing the cell membrane, which may compromise cellular functions. The [^{35}S]GTPγS assay is best suited to $G\alpha_i$-coupled GPCRs, although responses

have been reported before at low levels in membrane preparations of $G\alpha_s$-coupled receptors (Harrison & Taylor, 2003). Low-level responses in $G\alpha_s$-coupled receptor membranes could arise due to differences in G protein lipidation (Vögler *et al.,* 2008), and because $G\alpha_s$ proteins may be less abundant than $G\alpha_i$ proteins (Milligan, 1988). Furthermore, $G\alpha_s$ protein activation may occur more slowly compared to $G\alpha_i$ proteins (Milligan, 1988), resulting in the assay being more favourable for $G\alpha_i$-coupled GPCRs.

The cAMP assay is another useful tool for studying $G\alpha_i$-coupled GPCR activation (Gilissen *et al.,* 2015), which involves using forskolin to activate cAMP production before stimulating the receptor, the result of which can inhibit or enhance cAMP production due to the coupling of the respective G protein (Seamon *et al.,* 1981). Other forskolin-free methods have more recently been developed (Gilissen *et al.,* 2015), and there are also a number of examples where $G\alpha_s$-coupled receptors have been successfully screened using cAMP (Chen *et al.,* 2013; Titus *et al.,* 2008). However, cAMP-based assays require precise amounts of forskolin, and membrane-based assay formats require cAMP regeneration buffers and enzymes, making the assay technical, variable and complex.

Biosensors of G protein activity have been recently refined and improved by the Schulte lab to account for all subtypes of Gα protein. G protein tricistronic activity sensor (G-CASE) biosensors utilise the properties of BRET, encoding a NanoLuciferase luminescent donor tag on the N-terminus of the Gα protein and a venus luminescent acceptor tag on the C-terminus of the Gγ subunit (Schihada *et al.,* 2021). G protein activation and dissociation causes a decrease in BRET signal between the donor and acceptor fluorophores, based on the increased spatial proximity between the Gα and Gβγ subunits, and so a reduced ability for resonance energy transfer to occur. However, these biosensor assays currently run in whole cells and have not yet been used in membrane-based assays investigating agonist-induced G protein activation for drug discovery. However, it may be possible to modify these biosensors and anchor the G protein to the inner leaflet of the plasma membrane to support the development of a membrane-based, miniaturised assay format that allows the study of G protein activity when screening novel hits at GPCRs.

1.5 Aims and objectives of the investigation

This project involved investigating biased signalling at cannabinoid receptors using novel compounds discovered in a docking screen and standard reference compounds. The first objective was to determine the equilibrium K_d of our fluorescent

tracer at CB_1R and CB_2R using saturation binding assays, before determining the affinity and selectivity of three novel compounds (compound 005, 009 and 025) for CB_1R and CB_2R compared to a positive control (rimonabant for CB_1R and SR-144,528 for CB_2R), via competition binding assays

The second objective of this investigation was to study ligand bias among the three novel compounds. This phenomenon will be studied using functional assays including mini-G and β-arrestin recruitment assays, where the response of the novel compounds will be considered relative to an appropriate positive control. We hoped to find a degree of bias towards G protein or β-arrestin recruitment at CB_1R or CB_2R with the novel compounds. The mini-G and β-arrestin recruitment assays will be complemented with assays using a biosensor for $G\alpha_i$-coupled GPCRs (Gi-CASE) (Schihahda *et al.,* 2021) to better elucidate G protein activity in response to agonist stimulation relative to a positive control. These assays will indicate the mechanism of action of the three novel compounds, which cannot be depicted in the saturation and competition binding experiments, thus providing a good insight into how the novel compounds cause G protein activation and signalling.

After studying G protein activation, we will then consider β-arrestin recruitment in more detail by conducting assays into CB_1R and CB_2R internalisation, which is thought to be mediated by β-arrestin activity. Studies of receptor internalisation will involve using confocal microscopy to visualise agonist stimulation on GFP-labelled cells with the novel compounds and a positive control. Diffusion-enhanced resonance energy transfer (DERET) assays will also be conducted as an additional means to track receptor internalisation. Concentration-response curves should look similar to those obtained in the β-arrestin recruitment assays and will help us to gain a full pharmacological profile of the novel compounds in the presence of the positive control.

As a side project, we attempted to miniaturise the Gi-CASE assay by creating a lipid anchor for the fluorescent G protein to increase its concentration in the plasma membrane, thus promoting the development of a membrane-based assay to study functional G protein activation in response to agonist stimulation. Preliminary experiments using membranes with the lipidated G protein should show a response that is similar to that seen in the assay conducted in whole cells. The assay can then be optimised in future to accelerate the identification of novel agonists for the cannabinoid receptors, which could be applied to other GPCRs.

Chapter Two: Materials and Methods

2.1 Materials

Mammalian cell culture reagents

HEKT-REx™-293 Cell lines were purchased from Invitrogen (CA, USA). HEKT/17 cells were purchased from American Tissue Culture Collection (ATCC) (VA, USA). T75 and T175 mammalian cell culture flasks were purchased from Fisher Scientific (Loughborough, UK). Cell culture reagents from Sigma Aldrich (St. Louis, MO, USA) include foetal calf serum (FCS), Dulbecco's Modified Eagle's Medium (DMEM) 500mL – high glucose (catalog no. D6429), Dulbecco's Phosphate Buffered Saline (PBS), Hank's Buffered Saline Solution (HBSS), 4- (2-hydroxyethyl)-1-piperazineethanesulfonic acid) (HEPES) sodium salt (catalog no. RDD035-100G), bovine serum albumin, trypsin/EDTA solution 100mL (catalog no. R001100). Reagents purchased from Gibco™ (MA, USA) included Opti-MEM™ Reduced Serum Medium (catalog no. 31985062), Blasticidin™ Selection Reagent HCl 10mg/mL (catalog no. 12172530), Zeocin™ Selection Reagent 100mg/mL (catalog no. R25005), Geneticin™ Selective Antibiotic (G-418 Sulfate) 50mg/mL (catalog no. 10131035), Tryan Blue Solution, 0.4% (catalog no. 15250061). Sheared Salmon Sperm DNA was purchased from Invitrogen (CA, USA) (10mg/mL; catalog no, AM9680). Reagents from Corning® (Corning, NY, USA) include Corning® 100mL Cellstripper™, liquid (catalog no. 25-056-Cl). Reagents from Lonza (Allendale, NJ, USA) include cryoprotective freezing medium, 100mL (catalog no. 12-132A). Cell culture reagents from Cisbio (Codolet, France) include LabMed buffer and HTRF Tag-lite SNAP-Lumi4-Tb labelling reagent (5X) (100mL LABMED). Polyethylenimine (PEI) was obtained from Polysciences Inc (PA, USA). 96-well plates Cellstar ® tissue culture plates were purchased from Greiner Bio-One (Kremsmünster, Austria).

Molecular biology reagents

Molecular biology reagents from Thermofisher (MA, USA) include SYBR™ Safe DNA Gel stain (catalog no. S33102). Reagents from Invitrogen (CA, USA) include LB Agar, powder (catalog no. 22700041).

Compounds

Reference ligands from Bio-Techne® Tocris (Abingdon, Oxfordshire, UK) include HU-210 ((6a*R*)-*trans*-3-(1,1-Dimethylheptyl)-6a,7,10,10a-tetrahydro-1-hydroxy-6,6-dimethyl-6*H*-dibenzo[*b*,*d*]pyran-9-methanol) (catalog no. 0966), HU-308 ((1*S*,4*S*,5*S*)-4-[4-(1,1-Dimethylheptyl)-2,6-dimethoxyphenyl]-6,6-dimethylbicyclo[3.1.1]hept-2-ene-2-methanol) (catalog no. 3088), anandamide (AEA) (*N*-(2-Hydroxyethyl)-5*Z*,8*Z*,11*Z*,14*Z*-eicosatetraenamide (catalog no. 1339), 2-Arachidoylglycerol (2-AG)

(5*Z*,8*Z*,11*Z*,14*Z*)-5,8,11,14-Eicosatetraenoic acid, 2-hydroxy-1-(hydroxymethyl)ethyl ester (catalog no. 1298), SR-144,528 (5-(4-Chloro-3-methylphenyl)-1-[(4-methylphenyl)methyl]-*N*-[(1*S*,2*S*,4*R*)-1,3,3-trimethylbicyclo[2.2.1]hept-2-yl]-1*H*-pyrazole-3-carboxamide) (catalog no. 5039) and rimonabant (SR-141716A) (*N*-(Piperidin-1-yl)-5-(4-chlorophenyl)-1-(2,4-dichlorophenyl)-4-methyl-1*H*-pyrazole-3-carboxamide hydrochloride) (catalog no. 0923).

We tested three novel compounds, including compounds 005, 009 and 025. The three compounds were derived from a primary batch of compounds identified as novel hits from docking studies using *ZINC database*. Initial hits from the first batch of compounds were taken and the database was used to further explore and compare similarities in the compounds' structure with other existing structures. The novel hits in the primary batch were then taken and a second batch including the three compounds tested in this project were purchased and tested at the cannabinoid receptors. D77, a fluorescent tracer based on the structure of THC was also used, the kinetics and binding time profile of which have been characterised by a former PhD student working in the Veprintsev lab (unpublished data).

DNA constructs

HEK293TR cells expressing CB_1R, CB_2R and truncated CB_1R (91-472) were transfected with the Gi-CASE plasmid, which was obtained from Addgene (catalog no. 168120) (Teddington, UK) and is available as Addgene: Gi1-CASE (Schihada *et al.,* 2021). Original Gi-CASE constructs were made using pcDNA™3.1 mammalian vectors Invitrogen™ (CA, USA) (catalog no. V79020). HEK293TR cells were made to express CB_1R and CB_2R using pcDNA™4/TO mammalian vectors ((catalogue no. V102020) Thermofisher Scientific (MA, USA), expressing the gene for CB_1R using CNR1 and the gene for CB2R using CNR2. Later, the Gi-CASE plasmid, as well as the Gs-CASE and Gq-CASE plasmids, were modified as part of our attempt to create a membrane-based biosensor assay. The DNA sequence of these plasmids reflects the DNA sequence of $G\alpha_i$, $G\alpha_s$ and $G\alpha_q$ proteins, so we targeted the amino acids in these plasmids in order to modify the actual G protein linked to the receptor, promoting palmitoylation and myristoylation at the Gα subunit N-terminus. Benchling was used as a tool to visualise the plasmids. PCR primers, for the insertion of the nucleotides at the extreme N-terminus of the Gα subunit, were designed using AAScan (Sun *et al.,* 2013). The N-terminus of the Gαi protein-encoding region had the original DNA sequence TACCCGACGTGTGACTCGCGA which encoded the amino acid sequence MGCTLSA. The N-terminus of the Gs-CASE plasmid had the original DNA sequence

as follows: TACCCGACGGGAGCCGTTGTCATTC for the first eight amino acids for the sequence MGCLGNSK. The original DNA sequences were then modified for the sequence: TACCCGACGACAACGTCGTTT and encoded the amino acids sequence MGCCCSK. For the Gq-CASE plasmid, the DNA sequence of the N-terminus of the Gα protein was TACTGAGACCTCAGGTAGTAC and encoded the amino acid sequence MTLESIM. The original DNA sequence was then modified for the sequence TACCCGGAACTTAGATCGTTT and encoded the amino acid sequence MGLESSK. The insertion of nucleotides at the N-terminus sequences was enabled using CoIE forward and reverse primers. Constructs were transformed into OneShot™ TOP10 Chemically Competent E.coli cells from Invitrogen (catalog no. C404010) (CA, USA).

2.2 Methods

PCR reactions and DNA elution

The PCR of constructs was performed by preparing 1 µL of 0.1 ng/µL template DNA, 1.25 µL of 6 µM CoIE forward and reverse primers, 9 µL deionised water and 12.5 µL Primestar HS polymerase (premix). Forward and reverse primer solutions were prepared separately. Products were then prepared for purification and plasmid assembly by digestion of the recognition sequences by adding 0.5 µL (5 units) Dpn1 restriction enzyme (Promega) to each PCR product, followed by incubation using a PCR reactions were carried out using a PCRmax® (Stone, Staffordshire, UK) ALPHA Cycler 2 Thermal cycler as follows: 37 °C for 3 hours, then at 16 °C for 11 hours. Dpn1 digestion was performed so as to leave behind the constituent parts of the plasmid with blunt ends. The plasmid components were then purified using a QIAGEN® Mini-Elute Reaction Clean-up Kit following the attached instructions and were then eluted in 10 µL distilled water. The eluted DNA was then quantified using a DeNovix Ds-11 FX spectrophotometer.

Plasmid assembly was completed using Gibson Assembly® an established method (Heydenreich *et al.,* 2017). A molar ratio of 3:1 of insert: backbone was used, in which the total amount of DNA used was equal to 50 ng. Plasmids were typically made in two halves before being assembled. A total assembly volume of 10 µL was used, and Gibson Assembly mixtures were incubated at 4 °C for two minutes, at 50 °C for fifteen minutes, and then at 37 °C for one hour. Then, the temperature was returned to and held at 4 °C at the end of the assembly.

The outcome of PCR reactions, and the successful insertion of DNA sequences into the template DNA plasmid constructs, was confirmed via DNA gel electrophoresis. A

1% agarose solution was made in which an appropriate amount of agarose powder was dissolved in 1x Tris-acetate-EDTA (TAE) buffer via boiling. The boiled solution was then gradually cooled to approximately 60°C before adding 5 µL SYBR™ Safe DNA Gel Stain (Invitrogen™). The liquid gel was then poured and left to set in a Fisherbrand™ Sub-Gel Midi Horizontal Gel Electrophoresis Unit and was submerged in TAE buffer. 2 µL of GeneRuler™ 1kb DNA ladder was used as a ladder control. Then, a mixture of each PCR product was made, which included 2 µL PCR product, 2 µL distilled water and 1 µL loading dye (Thermofisher Scientific). Samples were then loaded into the gel, before running using an electric field created with a Cleaver Scientific NANOPAC-300P power supply (400mA, 90V) for 40 minutes. The gel was then analysed using a gel imaging analysis system as an indicator of successful PCR reactions and as a deciding factor in whether the PCR should be repeated if bands were too faint or not visible.

Transformation in bacteria

Assembled plasmids were transformed using One Shot® TOP10 Chemically Competent E.coli (Thermofisher, MA, USA) stored at -80 °C, and pre-treated with manganese chloride to aid plasmid uptake. Cells were thawed on ice before 4 µL of Gibson Assembly contents was added and the Eppendorf tube was flicked to ensure the plasmid was taken into and distributed in the E.coli suspension. The suspension was put on ice for 25 minutes, then was given a heat shock for 30-40 seconds at 42 °C, before being placed back on the ice for two minutes.

For plasmids containing G protein tricistronic activity sensor (G-CASE) inserts, in which kanamycin was a selective agent to isolate bacteria that have successfully taken up the plasmid, a 1-hour recovery step was taken before plating. This involved adding 500 µL autoclaved Luria broth (LB) to the plasmid suspension and incubating for one hour at 37 °C. The recovered cells were then centrifuged at 1,000 RPM for 3 minutes at 4 °C, after which all but 50 µL of supernatant was discarded. For plasmids in which carbenicillin was the selection agent, the recovery step and centrifugation were not included in the transformation. The pellet was then re-suspended in the 50 µL supernatant and then spread onto the agar jelly in a petri dish, under sterile conditions.

Agar Petri dishes were prepared using liquified 12.5 mL LB-agarose containing 100 µg/mL of the appropriate antibiotic, dispersed evenly, and left to sit for 20 minutes. After take-up into the E.coli host, the suspension was then spread onto the agar jelly and distributed across the plate using an inoculating loop to create a set of three

zigzag lines to dilute the bacteria to single colonies. The Petri dish was then placed face down in an incubator at 37 °C overnight before a Gilson p200 pipette tip was used to pick a single colony the day after. Single colonies were placed into a cell culture tube containing 5 mL LB and 100 µg/mL of the correct antibiotic, then sealed with foil and placed in a shaking incubator at 37 °C at 230 RPM for up to 20 hours.

Plasmid DNA extraction using Qiagen

A mini-prep was first carried out using a QIAGEN® mini-prep kit and protocol to confirm that we had the correct sequence, before carrying out a midi-prep using a QIAGEN® kit once we had the right plasmid. Following 24 hours of incubation at 37 °C, a single E.coli colony was picked using a Gilson p100 pipette tip. Tips were then placed into cell culture tubes containing 5mL LB (10% of the correct antibiotic selection agent). Then, tubes were sealed and placed into a shaking incubator at 37 °C overnight. Following incubation, plasmids were extracted from the E.coli vector using QIAGEN® Midi-prep kits (Qiagen, Hilden, Germany). Briefly, plasmids were placed in a resuspension buffer, the cells were lysed and the solution neutralised, before being centrifuged at 20,000*g* for 30 minutes at 4 °C, using a Thermofisher Scientific *fiberlite* fixed angle rotor container, to separate the DNA from the cell host. The supernatant was then transferred to an equilibrated QIAGEN-tip 500 tube and was left to filter into a universal attached to the bottom, using gravity. A wash buffer was then added to the sample, before adding the DNA elution buffer, then isopropanol and ethanol to elute the DNA. The samples are then centrifuged once more under the same conditions, and the pellet was then air-dried before being re-suspended in 20 µL distilled water. The DNA concentration is then quantified using spectrophotometry and is stored at -20°C.

Spectrophotometry and DNA quantification

Purified DNA prepared by transformation into E.coli was quantified using a DeNovix DS-11 FX+ Cuvette Spectrophotometer. Using 1 µL distilled water as a blank sample, the spectrophotometer was calibrated, before a 1 µL sample of the eluted DNA was placed on the reader and the concentration of DNA was measured. The spectrophotometer was re-calibrated in between using different DNA samples.

2.3 Cell culture

Cultured cells were maintained in a humidified incubator at 37 °C and 5% CO_2 in Dulbecco's modified Eagle's medium (DMEM) (Sigma-Aldrich) containing 10% foetal calf serum (FCS). Cells were maintained via passaging once reaching approximately

70% confluency. DMEM media was aspirated off and cells were washed with 5 mL Phosphate buffered saline (PBS). The PBS was aspirated off and 2 mL trypsin was added to the flask in order to remove the cells from the bottom of the flask, which typically is coated with poly-d-lysine in order to encourage the adherence of cells to the flask when culturing. After dislodging the cells, the trypsin was neutralised using 8 mL DMEM, and the cell media mixture was made uniform via pipetting.

For cell passaging, an appropriate portion of the 10 mL cell suspension was carried into another T175 flask and made up to a total volume of 15 mL using additional DMEM. When freezing cells, the 10 mL cell suspension was transferred to a universal tube and centrifuged at 350*g* for 3 minutes. The supernatant was then aspirated off and the pellet was resuspended in a suitable amount of cell freezing media (50% DMEM, 50% cryoprotective medium) enough to make 3-4 aliquots containing 0.5 mL cells. Cells were then gradually frozen down to -80 °C using a CoolCell™ LX Cell Freezing Vial Container (Corning).

When plating cells, a similar protocol was followed as per harvesting cells, but the pellet formed as a result of centrifugation was instead re-suspended in 10 mL DMEM. Cells were then counted in order to determine the number of cells per millilitre of DMEM, using a Countess™ II FL Automated Cell Counter (Invitrogen™). 10 µL cells were taken from the cell suspension and mixed with 10 µL trypan blue solution (Gibco™). 10 µL of this solution was then inserted into the glass chamber of a haemocytometer mounted with a glass slide, and cell viability was then read. Cells were plated at a density of 50,000 cells/well. Penicillin-streptomycin (pen-strep, 1 µg/mL) and tetracyclin (1 µg/mL) were also added to prevent bacterial contamination and to induce expression in pcDNA™4/TO vectors, respectively. Cells were plated in a clear-bottomed 96-well OptiPlate™ (PerkinElmer), in which the wells had been coated with poly-d-lysine (5 mg/mL) in PBS prior to plating.

2.4 Generating stable cell lines

Stable cell lines were created using a 3:1 ratio of polyethylenimine (PEI): DNA, in which 5 µg DNA obtained from the prior transformation of the plasmid in E.coli had been purified and appropriately diluted. Separate vials of PEI and DNA containing 250 µL Opti-MEM serum-reduced media were prepared, before the two vials were combined, vortexed, and incubated at room temperature for 25 minutes. Following incubation, the contents of the PEI-DNA vial were added to a T75 flask (Thermofisher Scientific) containing the cells of interest. The flask was then returned to the incubator

for 24 hours, after which an additional 10 mL DMEM was added to the flask. After another 24 hours, the cells were split and maintained as stable cell lines or were harvested when generating transient cell lines.

To generate stable cell lines expressing the receptor of interest, antibiotics including blasticidin (5 µg/mL; Invitrogen™) and Zeocin™ (20 µg/mL; Invitrogen™) were used as selection agents to create cell lines transfected with pcDNA™4/TO mammalian vectors encoding the appropriate GPCR sequence (Thermofisher Scientific, UK). Other selection agents, namely Geneticin® (G-418 sulphate, 200 µg/mL), were used to select for cells containing pcDNA™ 3.1 mammalian vectors (Invitrogen™), used in the creation of the Gi-CASE-expressing cell lines. A mixed population of stable cells was produced with cells having resistance to the appropriate selection agent.

2.5 Fluorescent ligand binding experiments

HEK293T-Rex cannabinoid receptor expression was induced through the application of tetracycline (1µg/mL) 48 hours before cell harvesting. DMEM culture media was aspirated from T175 flasks containing HEK293T-Rex cells expressing the SNAP-tagged CB_1Rs and CB_2Rs, when approximately 90% confluent. The cells were then washed in 10 mL PBS (Gibco Carlsbad, CA) followed by washing in HTRF Tag-lite buffer (LABMED 5mL, Cisbio, PerkinElmer), in order to remove residual DMEM/D-PBS and pre-coat the flask and cells in LABMED. Terbium labelling was then carried out by adding to the cell flask 10 mL of LABMED buffer solution containing 100 mM SNAP-Lumi-Tb. Labelled flasks were then incubated for 1 hour at 37 °C with 5% CO_2. Following incubation, the terbium-containing LABMED solution was aspirated from the cells, and the cells were washed with 5 mL PBS in order to remove residual buffer solution. To harvest the cells, 5 mL Gibco enzyme-free Hank's-based cell dissociation buffer (Gibco, Carlsbad, CA) was added to the flask in order to detach the cells from the flask wall. The dissociation buffer was then neutralised with 5 mL DMEM (10% FCS), which was then added to a collection vial. The collection vial was then centrifuged at 200*g* for 5 minutes, the supernatant was removed and the pellets were frozen at -80 °C.

Membrane preparations of CB_1R and CB_2R-expressing cells involved re-suspending the pellet in 20 mL of ice-cold assay buffer consisting of 10 mM HEPES and 10mM EDTA adjusted to pH 7.4. The cell suspension was homogenised using a Polytron homogeniser (Ultraturrax setting 6, 6x 1 second pulses). The solution was then centrifuged at 200g for 3 minutes, after which the supernatant was taken and

centrifuged for 30 minutes at 48,000*g* at 4 °C using a Beckman Avanti J-251 ultracentrifuge (Beckman). For the Gi-CASE membranes, the resulting pellets were re-suspended in 10 mM HEPES and 0.1 mM EDTA, and aliquoted into 250 µL portions. In the case of the Tb-labelled receptors, a second wash step was performed in 10 mM HEPES and 10 mM EDTA, before being re-suspended in 10 mM HEPES and 0.1 mM EDTA. The Bicinchoninic Acid Kit (Thermofisher scientific) was used for protein determination, before storing the aliquots at -80 °C.

Saturation binding assays

Saturation binding assays were performed in order to determine the affinity of the tracer D77 for CB_1R and CB_2R and to calculate the affinity of the unlabelled compounds for the individual cannabinoid receptors in subsequent competition binding experiments. Saturation analysis was carried out at equilibrium and the affinity of the tracer D77 was calculated from the resulting specific binding. Specific receptor binding was determined by subtracting nonspecific binding from total binding. The non-specific receptor binding of the tracer D77 was defined as the amount of HTRF signal detectable in the presence of CB_1R and CB_2R membranes and the known CB_1R or CB_2R high-affinity antagonists (1 µM rimonabant or 1 µM SR-144,528, respectively). Total binding was measured using membranes treated with DMSO (the vehicle for high affinity antagonists), and increasing concentrations of the fluorescent tracer D77 which was added to all wells.

Fluorescent ligand-binding assays

The affinity of unlabelled ligands for CB_1R and CB_2R was determined using a competition binding assay, which typically involves adding (i) increasing concentrations of ligands to CB_1R and CB_2R in the presence of (ii) a fixed concentration of the fluorescent ligand, to preparations of membrane containing the receptor of interest. These experiments were performed using 384-well OptiPlate™ plates (PerkinElmer) with a total assay volume of 40 µL, using HBSS buffer containing 5 mM HEPES, 0.5% BSA and 0.02% Pluronic acid at a pH 7.4.

Serial dilutions of reference and novel compounds were prepared and added to assay wells containing buffer, before the addition of the fluorescent ligand (900 nM). The reference compounds included rimonabant for CB_1R and SR-144,528 for CB_2R. Novel ligands included compounds 005, 009 and 025 derived from *in silico* docking scoring. Lastly, 0.5 µg/well of membrane preparations containing CB_1R or CB_2R and 400 µM 5'-guanylylimidodiphosphate (GppNHp), were added to the OptiPlate™. GppNHp is a stable, non-hydrolysable analogue of guanine triphosphate (GTP), which was used

to bind and irreversibly activate the receptor G protein, causing its dissociation from the receptor. The plate was then incubated at 37 °C for 15 minutes to allow equilibrium to be reached. The plate was then read for 30 minutes using a PHERAstar FSX microplate reader (BMG Labtech, Offenburg, Germany), using a TRF 337 620 520 optic module to detect the HTRF signal.

Mini-G protein and β-arrestin recruitment assays in CB_2R-expressing cells

Following the competition binding experiments, HEK293TR-CB_2R-nLuc cells expressing fluorescently labelled miniG (mG) protein and β-arrestin were used to assess effector recruitment. Cultured cells were harvested upon reaching 70% confluency. DMEM culture media was aspirated off the cells, which were then washed in 5 mL PBS, and the cells were detached from the flask wall using 2 mL trypsin. The trypsin was then neutralised with 8 mL DMEM, creating a 10 mL cell suspension. An appropriate portion of the cell suspension was transferred into a fresh t175 flask (Thermofisher Scientific), alongside an appropriate amount of DMEM in order to continue the cell line. The rest of the cell suspension was centrifuged at 350*g* for 3 minutes, the supernatant was aspirated off and the pellet was re-suspended in 10 mL fresh DMEM containing 1 µg/mL tetracycline. 10 µL of cells were then taken and mixed with 10 µL trypan blue, counted, and plated with 50,000 cells per well using a standard protocol (see section 2.3).

The plated cells were stored in a humidified incubator (37°C + 5% CO_2) for 48 hours, until the cells reached confluency such that the wells are covered in a carpet of cells. Media was then aspirated off and the wells were washed in 100 µL/well PBS, then 90 µL/well assay buffer (HBSS, 0.5% BSA, 5 mM HEPES) with 10 µM furimazine. The plate was then incubated for 15 minutes in order to allow the furimazine to enter the cells. Three BRET cycles were carried out on the plate as an initial reading, after which 10 µL of compounds diluted in assay buffer were added to the plate, and the plate was read at 1-minute intervals for 30 minutes. Compounds included serial dilutions of synthetic CB_2R agonist HU-308, endogenous CB_1R and CB_2R agonists AEA and 2-AG, a synthetic CB_2R inverse agonist SR-144,528, the three novel compounds (005, 009, and 025). 1/3 serial dilutions in DMSO were made, before a 1/10 dilution in assay buffer and a further 1/10 dilution on addition to the assay plate. A final log molar (logM) concentration of -4 was used for AEA, 2-AG, 005, and 009, -5.5 was used for HU-308 and 025, and -6 was used for SR-144,528 (figure 1). Buffer containing 10% DMSO (1% final) served as the vehicle control and 3µM HU-308 was the positive control to which all responses were normalised.

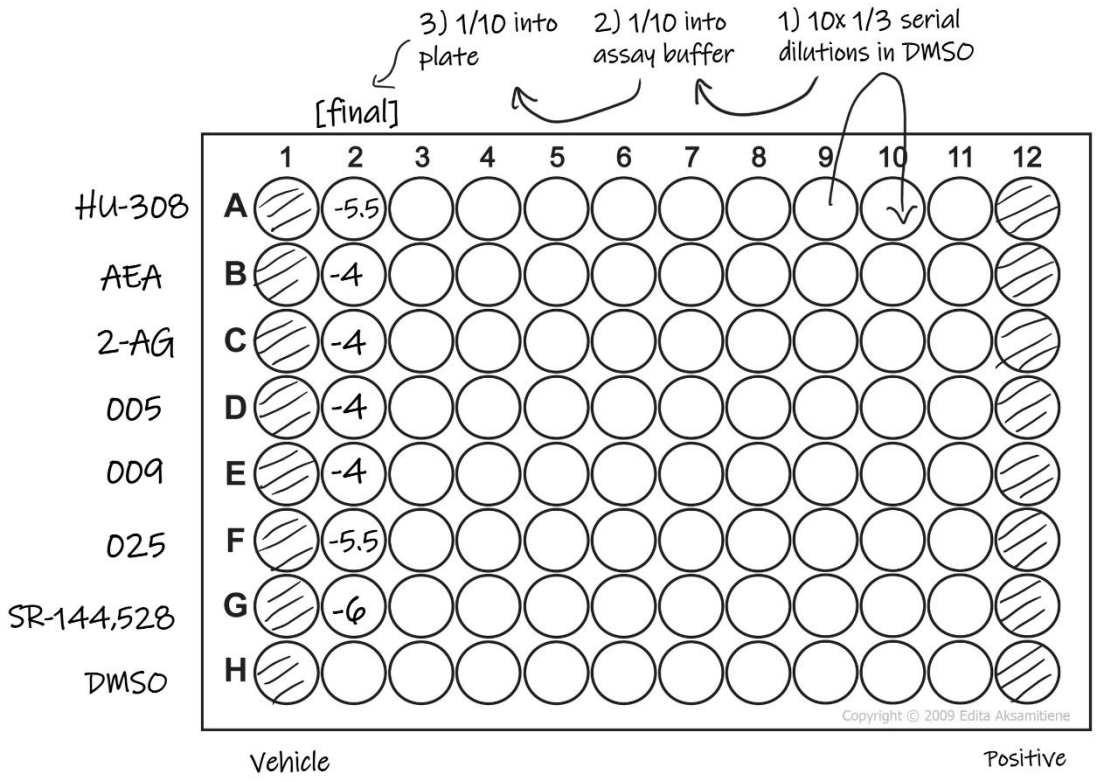

Figure 1: **Mini-G protein and β-arrestin assay set-up to study signalling bias**. Assays included serial dilutions of the compounds in DMSO and assay buffer tested on HEK293TR cells expressing cannabinoid receptor-2. The image is taken from *playbestonlinegames.com.*

2.6 Biosensor assays

Transient transfection with Gi-CASE biosensor plasmid

Following mG protein and β-arrestin recruitment assays, a similar assay setup was used to assess functional receptor signalling at CB_2R and CB_1R using a novel $G\alpha_i$ protein activity (Gi-CASE) biosensor described previously (Schihada *et al.,* 2021). As a preliminary experiment, HEK293TR-SNAP-CB2-TS-1D4 cells were transiently transfected with the biosensor plasmid. A 100 ng/µL stock of the Gi-CASE plasmid DNA was prepared, alongside a 100 ng/µL salmon sperm DNA stock as a control. We performed a 24-well transfection for six different transfection ratios, using a 36 µL total transfection volume equalised with an appropriate amount of salmon sperm DNA depending on the transfection condition (table 1). Six separate solutions of 200 µL opti-MEM and 3 µg DNA mixture were prepared, vortexed and added to a separate solution of 200 µL opti-MEM with to 9 µL PEI, such that the ratio of DNA:PEI was 1:3. The DNA solution was added to the PEI solution, which was then thoroughly vortexed and incubated at room temperature for 20 minutes.

Transfection condition	Gi-CASE DNA (100 ng/μL)	Salmon sperm DNA (100 ng/μL)
1	1400	0
2	1200	200
3	1000	400
4	800	600
5	600	800
6	400	1000

Table 1: **Summary of the six transfection ratio conditions** used for the preliminary transient transfections of a novel G protein activity biosensor in HEK293TR-CB_2R cells.

Cultured cells were then trypsinized and centrifuged at 350*g* to form a pellet. Cells were counted and the cell suspension was diluted to contain 500,000 cells/mL. Receptor expression was induced using 1 μg/mL tetracycline, alongside 1 μg/mL penicillin-streptomycin solution (pen-strep) to prevent contamination. The cell suspension was then portioned into six, sufficient for a 100 μL/well 24-well transfection. The contents of the first transfection tube were added to the first portion of cell suspension, which was repeated for the other five transfection tubes. A 100 μL cell suspension from each transfection condition was dispensed into 24 wells of a 96-well assay plate. The plate was then incubated for 48 hours (37 °C + 5% CO_2). After incubating, the cell culture media was aspirated off and the cells were given one washing of 100 μL/well PBS. 90 μL/well assay buffer containing 10 μM furimazine was then added. After a 15-minute incubation period, three BRET cycles were carried out, and then 10 μL/well HU-210 was added to the plate. HU-210 was firstly serially diluted by 1/10 in DMSO, which was then diluted 1/10 in assay buffer (HBSS, 0.5% BSA) for a final HU-210 logM concentration of -5. A SR-144,528 was used as a positive control (1 μM) which is a CB_2R inverse agonist, in addition to vehicle control (10% DMSO).

Gi-CASE stable cell lines: assays with reference compounds

Transient transfections of the Gi-CASE plasmid were followed by stable transfections of the plasmid into HEK293TR-SNAP-CB1-TS-1D4, HEK293TR-SNAP-CB2-TS-1D4 and truncated HEK293TR-SNAP-CB1-TS-1D4 (91-472) cells using a typical stable transfection protocol (see section 2.4). Cells were cultured, harvested, and plated as per the protocol used for the mG-protein and β-arrestin recruitment assays (see section 2.5), but were incubated for 72 hours rather than 48 hours.

Receptor activation of CB_1R, truncated CB_1R and CB_2R-expressing cells with the Gi-CASE biosensor was first characterised using serial dilutions of reference compounds. After 72-hour incubation, cell culture media was aspirated off and the cells were washed in 100 µL/well PBS. 90 µL/well assay buffer (HBSS containing 0.5% BSA, 5 mM HEPES) with 10 µM furimazine was dispensed into the wells and the plate was incubated for 15 minutes. Then, three BRET cycles were carried out before adding 10 µL of compound to the plate. Compounds included serial dilutions of synthetic CB_1R and CB_2R agonists HU-210 and HU-308, and synthetic CB_1R and CB_2R inverse agonists rimonabant and SR-144,528. 1/3 dilutions were made in DMSO, then a 1/10 dilution was made in assay buffer, followed by an additional 1/10 dilution when the compounds were added to the plate. Thus, a final logM concentration of -5 for HU-210, HU-308 and rimonabant, and -6 for SR-144,528 was used (figure 2). Buffer was also used as a vehicle control. Positive controls included 10µM HU-210 for CB_1R or truncated CB_1R cells, and 10 µM HU-308 for CB_2R cells.

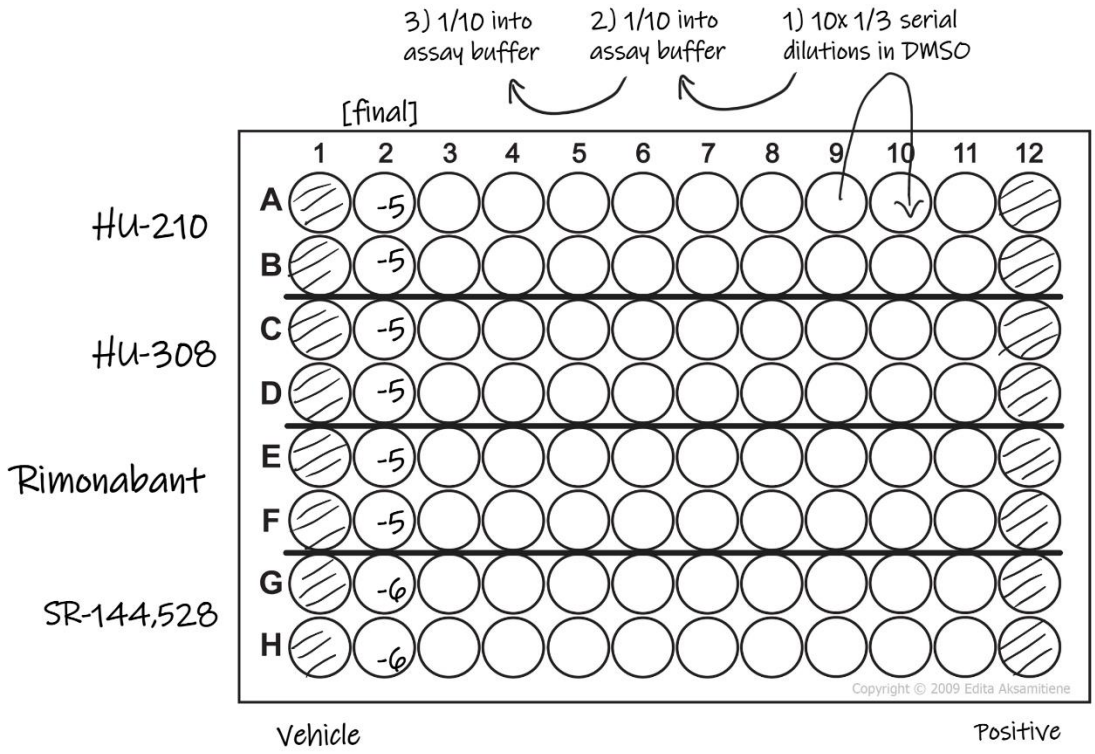

Figure 2: **Initial G protein biosensor assay set-up**. The assay used serial dilutions of the compounds in DMSO and assay buffer to characterise receptor activation of cells expressing full-length and truncated cannabinoid receptor-1, and full-length cannabinoid receptor-2. The image is taken from *playbestonlinegames.*

Gi-CASE stable cells lines: assays with novel compounds

Following characterisation of the Gi-CASE system, novel ligand activation of CB_1R, truncated CB_1R and CB_2R was investigated using serial dilutions of synthetic CB_1R and CB_2R agonists (HU-210 for full-length and truncated CB_1Rcells and HU-308 for full-length CB_2R cells), endogenous CB_1R and CB_2R agonists AEA and 2-AG; a synthetic CB_1R and CB_2R inverse agonist SR-144,528, plus the three novel compounds (005, 009, and 025) and DMSO to account for non-specific plating effects. 1/3 serial dilutions of the compounds were made in DMSO, followed by a 1/10 dilution in assay buffer (HBSS, 0.1% BSA, 5 mM HEPES). A final logM concentration of -4 was used for AEA, 2-AG, 005 and 009, -5.5 was used for 025 -6 was used for SR-144,528 and -7 for HU-210 in CB_1R cells or -5 for HU-308 for CB_2R cells. Responses were normalised to a positive control 10 μM HU-308 for full-length CB_2R cells and 10μM HU-210 for full-length and truncated CB_1R cells (figure 3). Cell culture media was aspirated from the plate and the cells were washed in 100 μL/well PBS. PBS was aspirated off and 90 μL/well assay buffer containing 10μM furimazine was added. After storing for 15 minutes in the incubator, three cycles of BRET were carried out, before adding 10 μL/well of the compounds preparations to the plate.

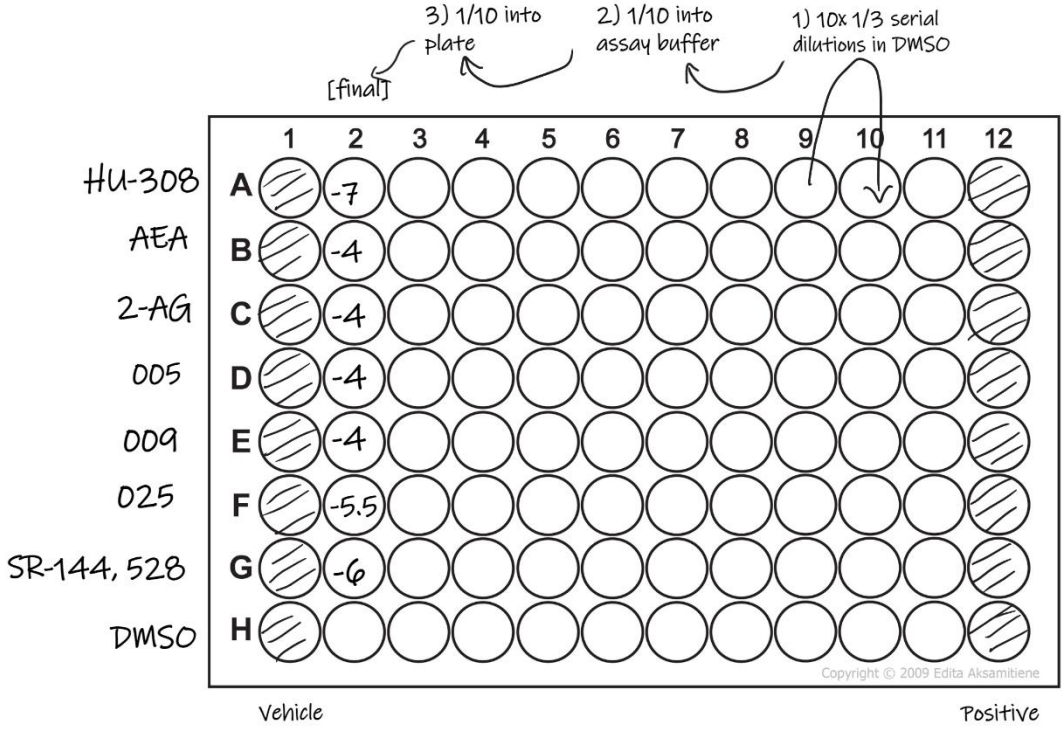

Figure 3: **G protein biosensor assay set-up for the novel compounds**. Assays used serial dilutions of the compounds in DMSO and assay buffer to characterise receptor activation of cells expressing full-length and truncated cannabinoid receptor-1, and full-length cannabinoid receptor-2. The image taken from *playbestonlinegames.*

2.7 Receptor internalisation assays

GFP-based internalisation assay

Internalisation assays were performed on a confocal microscope, using HEK293TR-CB_2R-egfp cells plated in a black, clear-bottomed 96-well Greiner Bio-One CELLSTAR µClear™ microplate. The plate was prepared by coating the wells in 50 µL poly-d-lysine in PBS (5 mg/mL) and incubating at room temperature for 30 minutes. The solution was then aspirated off and each well was washed one washing with 100 µL PBS. The PBS was then aspirated off and the coated plates were then stored in the fridge prior to use. A typical plating protocol was followed (see section 2.3), but we instead seeded the cells at 40,000 cells/well.

Once cells had reached approximately 70% confluency, cell growth media was aspirated off and the cells were washed in assay buffer (HBSS, 0.5% BSA, 5 mM HEPES), and were stimulated for 1 hour in a humidified incubator (37°C, 5% CO_2) with HU-308 and SR-144,528 and DMSO, based on a similar prior assay setup (see section 2.6 and figure 3). Only the centre 60 wells of the black 96-well Greiner microplate were used.

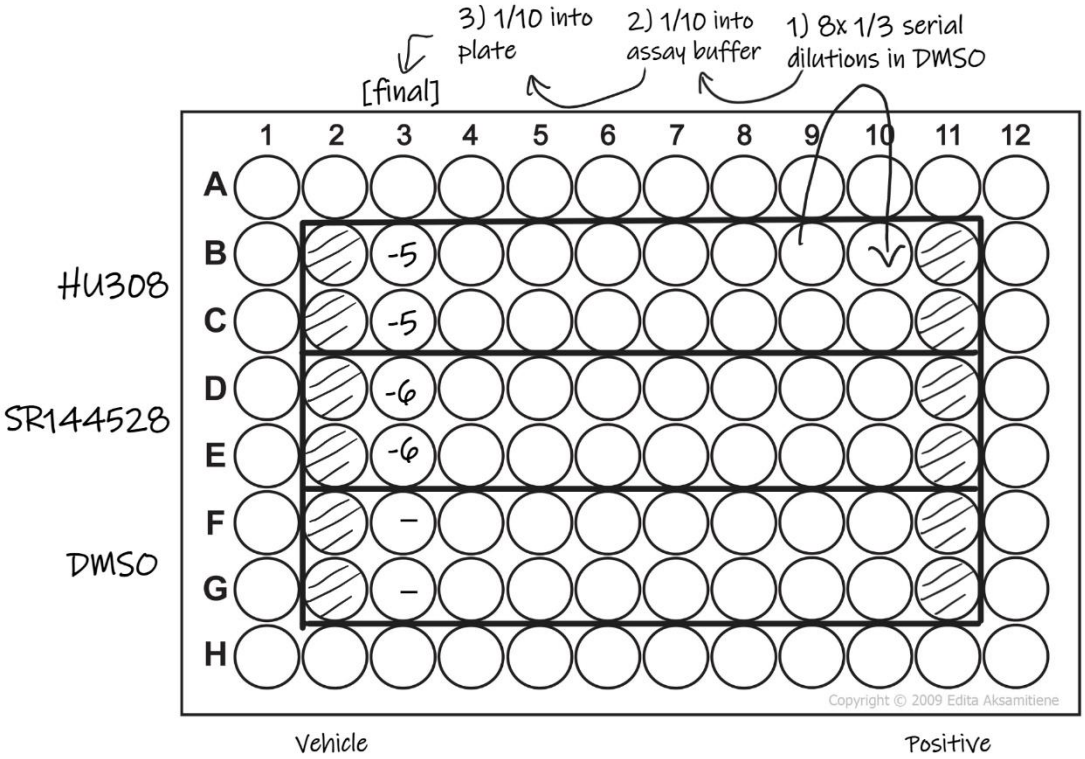

Figure 4: **Green fluorescent protein internalisation assay set-up.** Included serial dilutions of the compounds in DMSO and assay buffer to study the agonist-induced receptor internalisation of HEK293TR cells cannabinoid receptor-2. The image is taken from *playbestonlinegames.*

After stimulation, the assay buffer containing the reference compounds was aspirated off and the cells were fixed. Cell fixing involved washing each well with 100 µL PBS, then adding to each well 100 µL of 2% PFA in PBS fixative solution, and incubating the plate at room temperature for 15 minutes. The plate was then washed with two washings of 200 µL/well PBS, before adding 100 µL/well of 1 µM Hoechst stain and incubating at room temperature for 15 minutes. Two further PBS washings were performed, before adding 100 µL/well of PBS. The plate was then sealed in foil and stored in the fridge until imaging on a confocal microscope. After stimulating with rimonabant and SR-144,528, HU-308, SR-144,528 and the three novel ligands were tested against CB_2R. The same protocol was followed as per before to prepare the compounds. A final logM concentration of -6 logM was used for HU-308 and SR-144,528, -4 logM for compounds 005 and 009, -5.5 logM for compound 025.

DERET assay

Confocal microscopy experiments were complemented with diffusion-enhanced resonance energy transfer (DERET) assays, using SNAP-tagged HEK293TR-CB_1R and HEK293TR-CB_2R cells. Since the DERET assay is a TR-FRET assay, our cells expressed a SNAP-tag as opposed to an eGFP tag in order to allow terbium labelling. Cells were plated in a white, opaque-bottomed 96-well cell culture plate, which had been coated in poly-d-lysine before use, at a density of 50,000 cells/well and stored in a humidified incubator (37°C + 5% CO_2) for 48 hours.

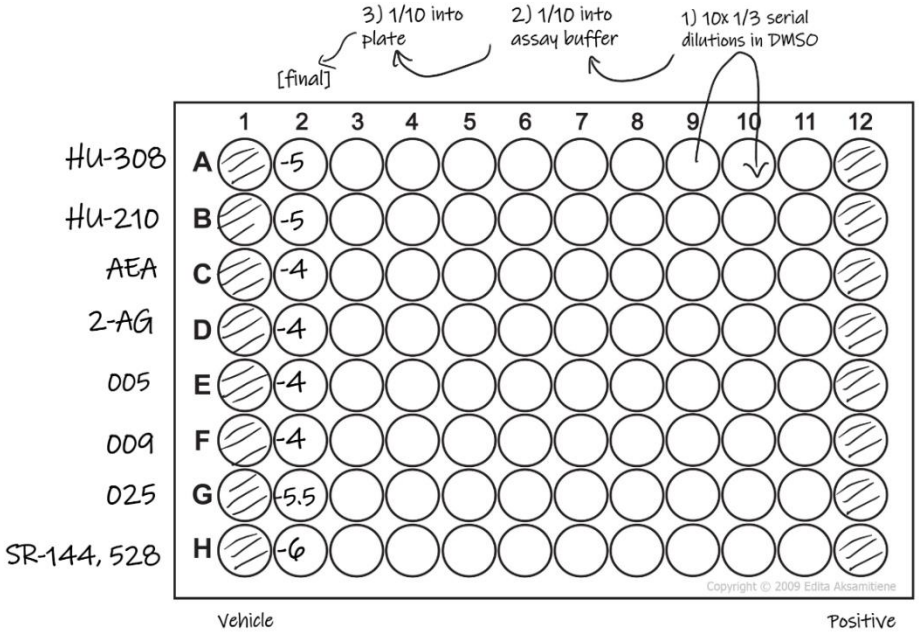

Figure 5: **Diffusion-enhanced resonance energy transfer (DERET) assay set-up**. The asays used compound serial dilutions in DMSO and assay buffer to study

receptor internalisation following agonist stimulation of HEK293TR cells expressing cannabinoid receptor-1 and -2. The image is taken from *playbestonlinegames.*

After 48 hours, the cell culture media was aspirated off and the cells were washed in 100 µL/well PBS. PBS was then aspirated off and 100 µL/well 1x LABMED was added to the plate. Specifically, the LABMED solution contained a ratio of 1:4 parts LABMED:deionised water, alongside 5 mM HEPES and 0.5% BSA. LABMED was then aspirated from the wells and Lumi4-Tb solution was added at 50 µL/well, and the cells were incubated for 1 hour at 37 °C. The solution was then removed and the cells were then given 3x washings of 100 µL/well PBS. Finally, 90 µL/well of 60 mM fluorescein was added to assay buffer (HBSS + 0.5% BSA + 5 mM HEPES adjusted to pH 7.4) for a 6 mM solution. A backing seal was added to the plate and three cycles of BRET were carried out on the plate reader before adding 10 µL of the compounds.

2.8 Membrane-based assay preparation

G protein modifications for plasma membrane lipidation

Cultured HEK293TR-CB_1R, -CB_2R and truncated -CB_1R (91-472) cells with 70% confluency were transfected with a modified Gi-, Gs- and Gq-CASE biosensor and put under selection with G-418, Zeocin® and Blasticidin. When the cells were stably expressing the biosensor, cell membranes were prepared using a repeated protocol (see section *2.5.1*). The biosensor was a modified version of the original G-CASE plasmid for $G\alpha_i$, $G\alpha_s$ and $G\alpha_q$ proteins. The modified G-CASE biosensor for $G\alpha_s$ and $G\alpha_i$ contained a modified Gα N-terminus in which the first seven amino acids were replaced with the sequence ‘MGCCCSK’, while the N-terminus of the Gα subunit of the Gαq was substituted with the amino acid sequence ‘MGLESSK’. stable lines for each modified plasmid were established across CB_1R-, truncated (91-472) CB_1R- and CB_2R-expressing HEK293TR cells.

2.9 Signal Detection and Data Analysis

Raw experimental data was collected using MARS data analysis software (BMG Labtech, Offenburg, Germany), and processed in Microsoft Excel. All analysis was carried out in GraphPad PRISM 9.0. All data are normalised, either to a positive control or the lowest concentration of drug used, dependent on whether or not the assay was affected by the edge-well effect (Mansoury *et al.,* 2021).

Cheng-Prusoff equation: Dissociation constant (K_i) = $\frac{IC50}{1+([S]\div Kd)}$

Specific binding = total binding – non-specific binding

Sigmoidal dose-response: $Y = Bottom + \frac{(Top-Bottom)}{1+10^{LogEC50-X}}$

For functional data fitted with a sigmoidal curve, the slope was fixed to 1, which assumes a slope of unity such that there is a direct relationship between ligand-receptor binding and function. Often agonist curves have a slope of less unity, suggesting no proportionate increase in receptor function despite increased binding, which may be the result of changes in the state of the receptor, such as receptor phosphorylated and desensitisation. In this project, the responses were small, so in order to fit the curves we assumed there was a direct relationship between ligand-receptor binding and receptor activation, hence we fixed the slopes unity. Any EC_{50} values derived should be reflective of compound potency. However, a free-fitting slope parameter would allow potency estimates to be more accurate.

Chapter Three: Characterisation of novel ligand-binding at CB_1R and CB_2R, using FRET-based technologies

3.1 Introduction

Before investigating ligand bias at CB_1R and CB_2R, we characterised the binding of our three novel compounds at these two receptors using a FRET-based homogenous time-resolved (HTRF) competition binding assay. Binding was characterised in two ways, via saturation binding and competition binding. Both experiments utilised terbium-labelled HEK293TR-SNAP-CB_1R and HEK293TR-SNAP-CB_2R membranes and a fluorescent tracer called D77.

To calculate the affinity of these compounds for the receptors we first calculated the affinity of the tracer using saturation binding. In the saturation binding experiments, increasing concentrations of the fluorescent tracer were added to assay wells alongside a fixed quantity of the membranes. Membranes expressed the receptor of interest in order to calculate the tracer affinity before experimentation on the unlabelled compounds (Davenport & Russell, 1996). Importantly, specific receptor binding is calculated in these assays through the subtraction of non-specific binding from total binding. That is, binding from "all pockets" except the orthosteric binding site (e.g. non-specific binding (NSB)) was quantified and removed from binding to "all pockets", therefore determining specific receptor binding to the orthosteric site. Non-specific binding of the tracer was defined in the presence of a high-affinity antagonist, namely rimonabant for CB_1Rs and SR-144,528 for CB_2Rs.

In addition to determining specific binding, saturation experiments also enabled us to determine the ligand concentration at half the receptor sites at equilibrium, which is given by the dissociation rate constant, or K_d value. Saturation binding experiments using radioligands can be used to determine the maximum number of receptor sites (B_{max}), but this value was not determined in these experiments and is a minor drawback of HTRF.

After carrying out saturation binding experiments to calculate the K_d of the tracer, we considered the binding affinity of novel compounds in competition binding experiments. This technique involved using a fixed concentration of the fluorescent ligand determined by the saturation binding experiments, alongside increasing concentrations of the compounds of interest. By carrying out these experiments we were able to study the binding of a series of novel compounds and compare them to the reference compounds rimonabant and SR-144,528. Competition binding experiments followed a similar protocol, using radioligands to study the kinetics of unlabelled compounds (Sykes and Charlton, 2018).

3.2 Results

Saturation binding experiments

Saturation binding experiments enabled the K_d values of the tracer D77 for CB_1R and CB_2R to be determined by subtracting the amount of nonspecific binding from the total binding observed at increasing concentrations of tracer. The K_d value is the concentration of tracer which occupies half of the receptor sites at equilibrium. For CB_1R, we calculated that the K_d value was 446nM, such that 446nM of the D77 ligand were required to occupy half the receptor sites. In contrast, we determined a K_d value of 545nM for CB_2R, which may indicate weaker D77 binding to CB_2R compared to CB_1R, where the K_d value is lower and a smaller amount of the fluorescent ligand is required to occupy half the receptor sites at equilibrium. Saturation plots for the fluorescent tracer D77 are shown in Figure 6A and B. 900nM of D77 was then used for competition binding experiments at CB_1R and CB_2R respectively.

Competition binding experiments

Competition binding experiments allow the calculation of the inhibition constant (K_i) values for the reference and novel compounds tested on CB_1R- and CB_2R-expressing membranes. This, therefore, quantifies the concentration of competing ligands which would occupy half of the receptor with no fluorescent tracer present. Initially, IC_{50} values were calculated and then used in the Cheng-Prusoff equation to calculate the K_i values for the compounds profiled. These values were then converted into a negative logarithmic value ($\log[K_i]$ or pK_i).

At CB_1R, the respective pK_i values for the novel compounds 005, 009 and 025 were all <6, suggesting weak affinity binding to CB_1R compared with the reference compound rimonabant, which had a pK_i value of 8.87 ± 0.14, and is a CB_1R antagonist. In contrast, the pK_i values at CB_2R for the novel compounds 005, 009 and 025 were 7.59 ± 0.10, 6.25 ± 0.10 and 7.79 ± 0.08, respectively, suggesting a higher affinity for CB_2R compared to CB_1R. SR-144,528 was the reference compound for CB_2R, and we determined a pK_i value of 8.72 ± 0.10.

The pK_i values at CB_2R compared to CB_1R are indicative of the strength of binding, with compound 025 being the novel compound with the highest measurable affinity. This information is graphed as percentage (%) specific binding (see Figure 6C and D and Table 2).

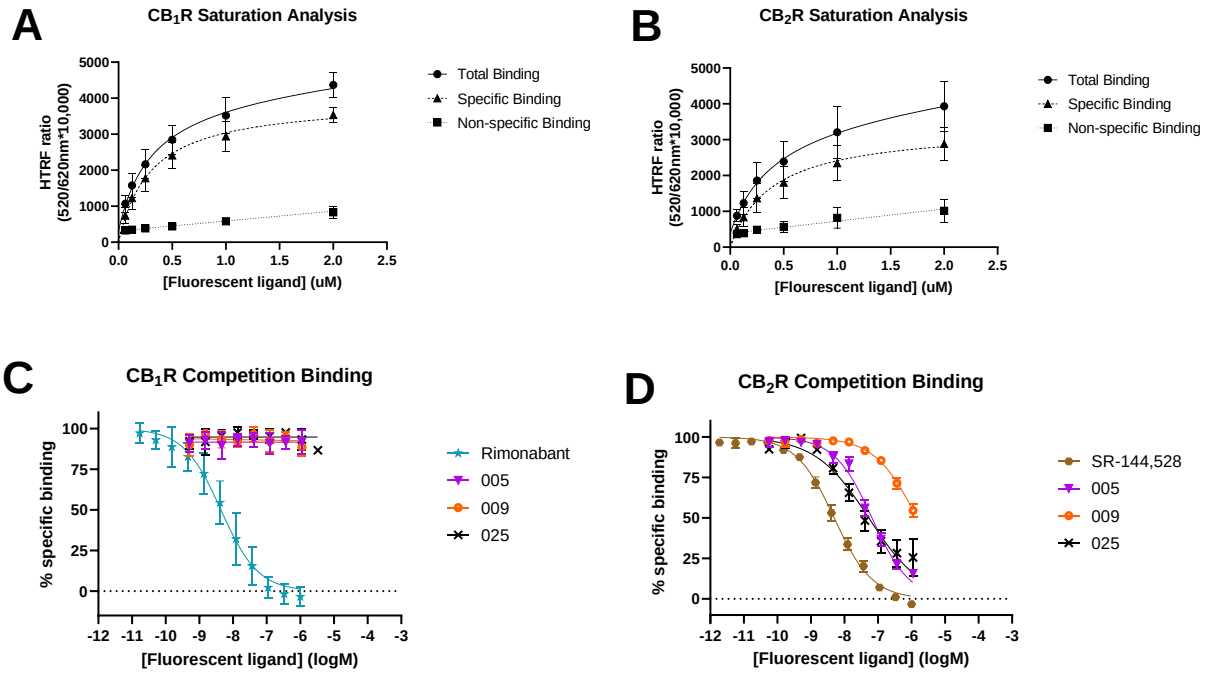

CB_1R competition binding experiments					
	Rimonabant	SR-144,528	005	009	025
pK_i	8.87 ± 0.14	-	< 6	< 6	< 6

CB_2R competition binding experiments					
	Rimonabant	SR-144,528	005	009	025
pK_i	-	8.72 ± 0.10	7.59 ± 0.10	6.25 ± 0.10	7.79 ± 0.08

Figure 6 (top): Saturation binding of the D77 tracer and competition binding assays for novel compounds at cannabinoid receptor-1 (CB_1R) and cannabinoid receptor-2 (CB_2R). (A) D77 CB_1R saturation analysis; **(B)** D77 CB_2R saturation analysis. **(C)** CB_1R competition binding and; **(D)** CB_2R competition binding data using a fixed concentration of tracer (900nM). Competition binding data have been constrained to 100% and 0% for maximal and minimal binding. Averaged data in the plots are shown as mean ± SEM, n≥3. Table 2 contains inhibition constant values as a negative logarithmic value (pK_i) for reference and novel ligands tested at CB_1R and CB_2R. Data are average of n≥3 (mean ± SEM).

3.3 Discussion

In these initial saturation experiments, we were able to determine the K_d values of the tracer D77 for both CB_1R and CB_2R by using increasing concentrations of the tracer.

The kinetics of D77 binding have already been established in the lab by a previous PhD student, so I did not characterise this myself. Competition binding experiments allowed us to derive the pK_i value of the novel compounds for CB_2R from the calculated IC_{50} values via the Cheng-Prusoff equation, enabling us to better understand their respective receptor affinities and selectivity values.

In these initial experiments, the compounds were diluted directly in DMSO and added to the 384-well plate containing the assay buffer, fluorescent probe and membranes. The assay buffer contained HBSS with 0.5% BSA and 0.02% F-127 (pluronic acid) to prevent non-specific binding and to stabilise the cell membranes, and 5 mM HEPES to stabilise the assay buffer. The assay buffer containing 2% DMSO was also used as a vehicle control in order to quantify receptor binding in the absence of any compound (total binding). It is unlikely that this buffer was unsuitable and accountable for the lack of CB_1R binding since the same buffer was suitable for our proceeding experiments. In proceeding functional experiments, these compounds were first diluted in DMSO, and then added to assay buffer before addition to the assay plates.

These experiments employed three novel compounds taken forward for profiling following *in silico* docking scoring predictions. Such computational studies are designed to support the discovery and development of novel druggable chemotypes to target CB_1R and CB_2R. The three novel compounds identified appeared to have a greater affinity for CB_2R compared to CB_1R, which is significant in the context of drug discovery for CB_2R due to the challenges involved in developing effective CB_2R-specific drugs (An *et al.,* 2020). Despite these findings, the competition binding experiments indicate that at concentrations above 1 µM, the compounds become more insoluble. This is often the case with highly lipophilic compounds, especially those with similar chemical properties to endogenous cannabinoids which are also highly lipophilic (Makriyannis *et al.,* 2005). The structural design of drugs as potential novel compounds to target the CB_2R that mimic endogenous cannabinoids in their ability to reach the receptor binding site and subsequently activate second messenger responses in cells may prove advantageous.

3.4 Conclusions

To conclude, initial binding studies enabled us to determine the specific binding of the fluorescent tracer and allowed us to study the affinity of the novel ligands for either CB_1R or CB_2R. Via competitive binding studies, we identified that the novel ligands have a higher affinity for CB_2R compared to CB_1R. However, competition binding experiments do not provide any information concerning compound efficacy

and do not distinguish the compounds as either an agonist, inverse agonist or antagonist. Since the compounds did not appear to bind CB_1R, the proceeding functional assays (mini-G (mG) and β-arrestin assays) were carried out on CB_2R-expressing cells only, to investigate the extent of ligand-CB_2R bias.

Chapter Four: Using biosensors to characterise cannabinoid ligand-receptor activity, using RET techniques.

4.1 Introduction

Following competition binding studies, we carried out functional assays using biosensors to better characterise ligand efficacy, and to study receptor activation and G protein activity. Firstly, a stable cell line of HEK293TR-CB_2R cells expressing mini-G (mG) proteins was created as previously outlined (Carpenter and Tate 2016). The engineered Gα subunit has three major modifications whereby (i) the N-terminus is truncated; (ii) the α-helical domain has been removed and; (iii) the α5 helix in the C-terminus is mutated in order to stabilize the receptor upon guanine nucleotide-binding (Wan *et al.,* 2018). Since mG proteins mimicking the endogenous G protein are stable and fluorescently active, they are useful tools when studying G protein structure-activity and can also be used as biosensors upon receptor activation. The truncated mG protein was tagged with a venus acceptor fluorophore, whilst the receptor C-terminus was tagged with a NanoLuc™ donor fluorophore. We also studied β-arrestin recruitment through a similar means, in which the C-terminus of HEK293TR-CB_2R cells was also tagged with NanoLuc™, and the β-arrestin protein was tagged with a venus acceptor fluorophore.

Agonist-receptor binding will ideally result in an increase in the bioluminescence resonance energy transfer (BRET) signal, since either the mG protein or β-arrestin protein will be recruited to the receptor following receptor activation. These experiments were done in order to investigate if the reference ligands and novel ligands of interest, once bound to the receptor, were biased in their ability to recruit the mG protein or β-arrestin protein. We used HEK293TR-CB_2R cells following the initial competition binding studies, since the novel compounds did not appear to bind to CB_1R, but did appear to have a good affinity for CB_2R. We ideally wanted to see that while binding to CB_2R, the novel compounds (005, 009 and 025) would preferentially recruit the mG protein or β-arrestin to a lesser or greater extent, thereby suggesting a degree of bias once bound to CB_2R.

Later, we used a $G\alpha_i$ protein tricistronic activity (Gi-CASE) biosensor described previously (Schihada *et al.,* 2021), in order to investigate the functional activity of the heterotrimeric G protein in response to compound-receptor binding. Transfection of the Gi-CASE plasmid into GPCR-expressing cells results in the tagging of both the Gα subunit with a NanoLuc™ fluorophore and the gamma subunit of the Gβγ dimer with a venus acceptor fluorophore. Therefore, using the Gi-CASE biosensor in standard BRET experimentation is a good indicator of agonist-binding at receptors since receptor activation will proceed with G protein activation and the dissociation of

the Gα subunit from Gβγ. This should cause a reduced BRET signal due to a reduction in the resonance energy transfer between the donor and acceptor fluorophores, based on the increased spatial proximity (Dale *et al.,* 2019).

In addition, using a Gi-CASE biosensor can also be a useful tool for investigating ligand bias based on how compounds are able to activate the G protein differentially once recruitment has occurred. Therefore, this biosensor was important to completing our studies of signalling bias, using a more native receptor activation system. Gi-CASE biosensor experiments were first carried out by transiently transfecting the plasmid into CB_2R-expressing HEK293TR cells (the plasmid is not fully integrated into the cell's genome), which were then stimulated with HU-210, a non-selective CB_1R and CB_2R agonist. We then stably transfected the Gi-CASE biosensor into HEK293TR cells expressing one of either a full-length CB_1R, a truncated (91-472) CB_1R, or a full-length CB_2R. We then investigated receptor activation using reference compounds and novel compounds. Truncated CB_1R cells mimicked the CB_1R receptors in the CB_1R binding assay because these truncated receptors have a smaller N-terminus and there is, therefore, a reduced distance between the fluorescent ligand and the donor terbium fluorophore attached to via the SNAP-tag labelled CB_1 receptors. This was necessary as we did not observe CB_1R binding in our initial binding experiments, due most likely to their poor affinity and compound solubility. Initial experiments in cells stably expressing the Gi-CASE biosensor involved characterising receptor function using known CB_1R and CB_2R synthetic agonists including HU-210, HU-308, and the inverse agonists rimonabant and SR-144,528. Proceeding experiments used these compounds in conjunction with the endogenous cannabinoids AEA, 2-AG, and the novel compounds 005, 009 and 025.

All cells were tested following a 48-72 hour incubation period after the cells had been plated and grown in a cell culture medium with antibiotics and tetracycline to induce cannabinoid receptor expression. When running the functional assays, plated cells were prepared in assay buffer which contained HBSS with 0.5% BSA and 5 mM HEPES, identical to the binding experiments.

4.2 Results

Mini G protein recruitment findings

In order to study G protein recruitment to the receptor on the plasma membrane, we followed a previously outlined protocol which uses modified G proteins known as mini G (mG) proteins which are fluorescently active (Carpenter & Tate, 2016). In a similar

fashion, fluorescent β-arrestin proteins were also utilized. Cultured HEK293TR-CB_2R cells expressing either of these two proteins were plated using a standard protocol and were incubated for 48 hours in full cell culture medium containing 10% foetal calf serum (FCS). After 48 hours the cell culture medium was aspirated off, washed and changed to assay buffer, and the cells were stimulated with reference compounds including HU-308, AEA, 2-AG and SR-144,528, as well as the three novel compounds. The raw EC_{50} values for each compound were recorded as a negative logarithmic value (log[EC_{50}]; pEC_{50}). When stimulating the cells tested with HU-308, AEA, 2-AG, we recorded pEC_{50} values of 7.3 ± 0.1, 6.3 ± 0.4 and 5.2 ± 0.2 (figure 7), respectively. For the novel compounds 005 and 025, we recorded pEC_{50} values of 7.5 ± 0.2 and 8.2 ± 0.3, respectively (figure 8). No response was observed with compound 009 or the inverse agonist SR-144,528.

As for the maximal response (E_{max}) of each compound, this was standardised against that achieved by HU-308, which is a CB_2R-selective agonist (Hanus *et al.,* 1999), which had an E_{max} value of 86.9 ± 7.8 % in these experiments. For the endogenous agonists AEA and 2-AG, E_{max} values of 54.9 ± 10.4 and 90.6 ± 4.6 %, respectively, were recorded. In contrast, for the novel compounds 005 and 025, a lower maximum response was recorded, with E_{max} values of 19.2 ± 1.3 and 30.7 ± 4.7 % being observed (figure 7). Again, no response was observed for compound 009 or SR-144,528. The mG data collected at CB_2R are summarised in Table 3. In the data presented, error bars indicate experiment-to-experiment variation relative to the response of 3 μM HU-308. HU-308 was the positive control for each concentration of drug tested. A separate control was used for each concentration-response curve which was independent of the reference curve.

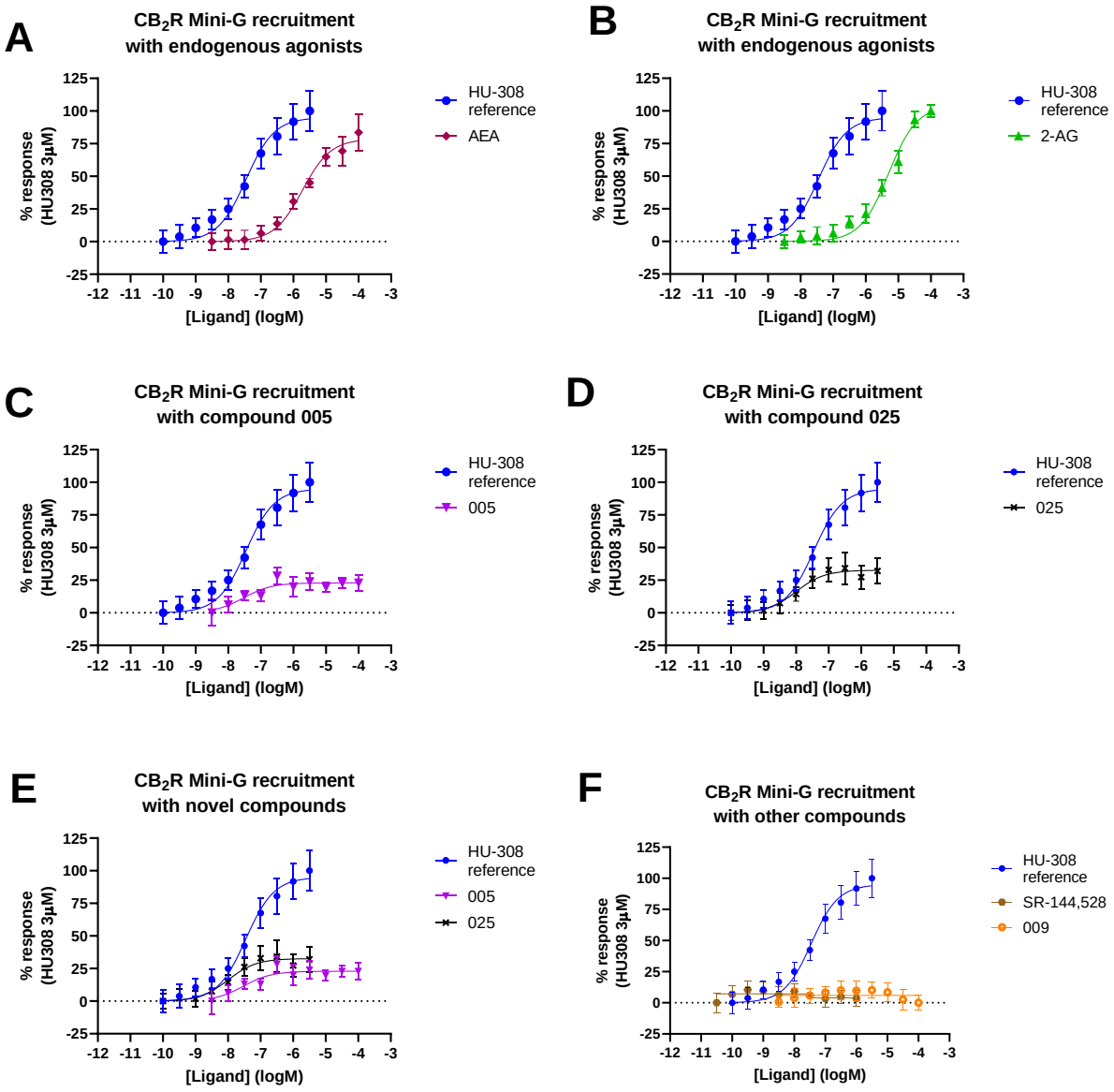

Figure 7: **Results of mini-G (mG) protein recruitment for cannabinoid receptor-2 (CB_2R)-expressing HEK293TR cells, upon stimulation with reference and novel compounds.** mG recruitment following stimulation with **(A)** the endogenous agonist anandamide (AEA), **(B)** (2-AG), **(C)** compound 005 and **(D)** compound 025. **(E)** Comparison of mG recruitment for compounds 005 and 025. **(F)** mG responses to compound 009 and the inverse agonist SR-144,528, both of which failed to recruit the mG protein. Data have been constrained to 100% and 0% for maximal and minimal binding. Maximal responses are given as a percentage (%) of the maximal response elicited by HU-308, which is a CB_2R-selective agonist. Data are normalised against 3 µM HU-308 response and are averaged (mean ± S.E.M.) from an n≥3.

Mini-G protein recruitment		
Compound	CB_2R pEC_{50}	CB_2R E_{max} (%)
HU-308	7.3 ± 0.1	86.9 ± 7.8
AEA	6.3 ± 0.4	54.9 ± 10.4
2-AG	5.2 ± 0.2	90.6 ± 4.6
SR-144,528	No fit	No fit
005	7.5 ± 0.2	19.2 ± 1.3
009	No fit	ND
025	8.2 ± 0.3	30.7 ± 4.7

Table 3: **Summary table of results from mini G protein recruitment assays in cannabinoid receptor-2 (CB_2R)-expressing HEK293TR cells, in the presence of reference and novel compounds.** Half maximal effective concentration (EC_{50}) expressed as a negative logarithmic value (log[EC_{50}]; pEC_{50}). Maximal responses (E_{max}) to agonist stimulation are given as a percentage (%) of the response elicited by 3 μM HU-308, which is a selective CB_2R agonist. Data are averaged (mean ± S.E.M) across n≥3.

β-arrestin recruitment findings

Following stimulation with the synthetic agonists HU-308, and AEA and 2-AG both endocannabinoids, we recorded pEC_{50} values of 7.1 ± 0.2, 7.2 ± 0.2 and 5.8 ± 0.1, respectively (figure 8). For the novel compounds 005 and 025, pEC_{50} values of 7.4 ± 0.4 and 8.5 ± 0.3 were observed. No response was observed for SR-144,528 or compound 009. When recording E_{max} values, responses were again standardised against HU-308, which had a maximal response of 98.54 ± 2.9 % in these experiments. For AEA and 2-AG, E_{max} values of 24.0 ± 2.3 and 89.1 ± 4.6 % of the HU308 maximal response (100%) were recorded. The responses for the novel compounds were also visually lower, and we recorded E_{max} values for compounds 005 and 025 of 14.2 ± 2.6 and 21.9 ± 3.6 as a percentage of the HU-308 response, respectively (figure 8). Again, no response was recorded for the inverse agonist SR-144,528 or compound 009. A summary of the β-arrestin recruitment is given is Table 4.

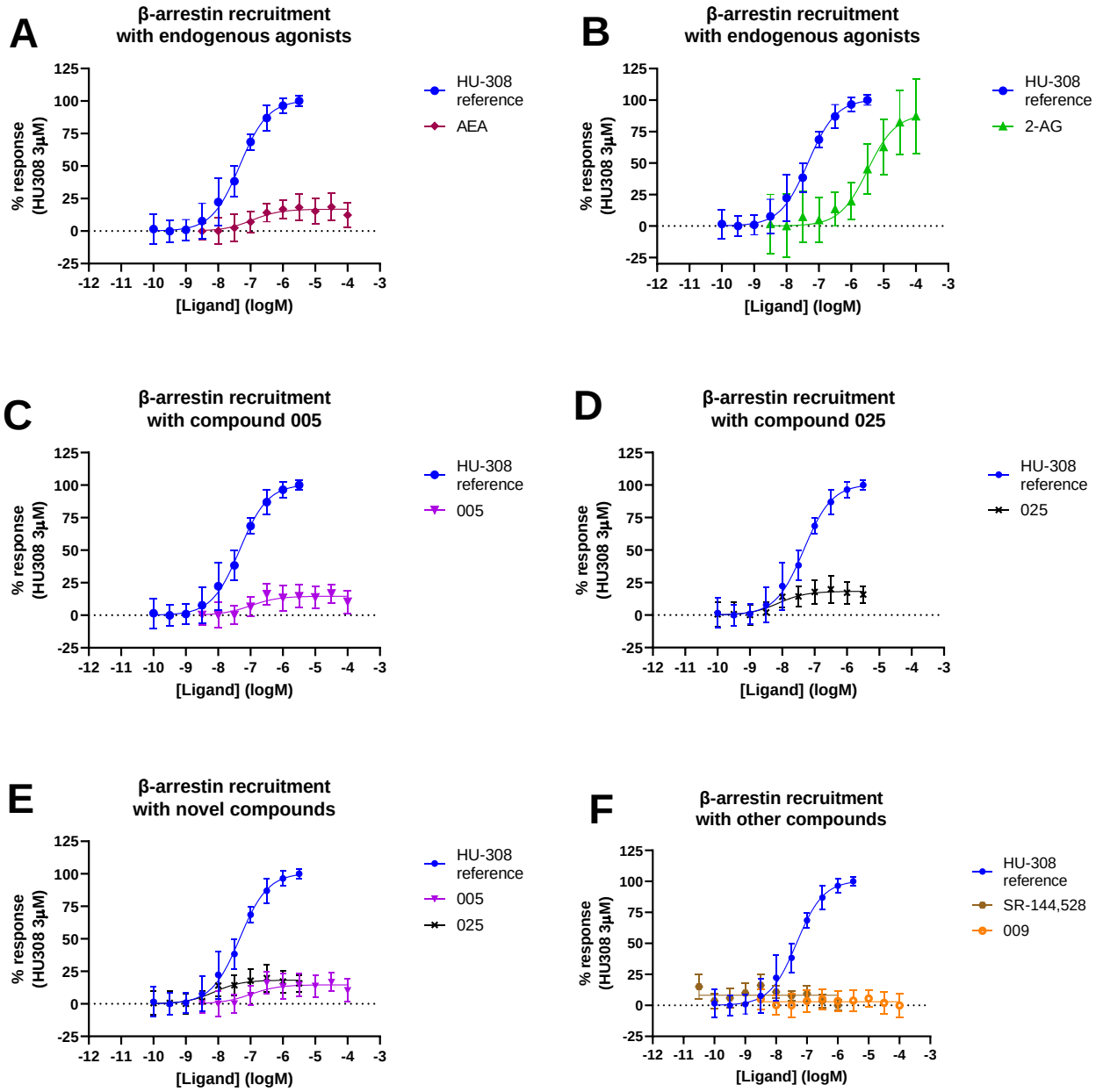

Figure 8: **Results of β-arrestin protein recruitment for cannabinoid receptor-2 (CB_2R)-expressing HEK293TR cells, upon stimulation with reference and novel compounds.** β-arrestin recruitment following stimulation with **(A)** the endogenous agonist anandamide (AEA). **(B)** 2-arachidonoylglycerol (2-AG), **(C)** compound 005 and **(D)** compound 025. **(E)** Comparison of β-arrestin recruitment between compounds 005 and 025. **(F)** β-arrestin responses to compound 009 and the inverse agonist SR-144,528, both of which failed to recruit the β-arrestin protein. Data have been constrained to 100% and 0% for maximal and minimal binding All responses were a percentage (%) of the response elicited by HU-308, which is a CB_2R-selective agonist. Data are normalised against 3 μM HU-308 response and are average (mean ± S.E.M.) from an n≥3.

β-arrestin recruitment		
Compound	CB_2R pEC_{50}	CB_2R E_{max} (%)
HU-308	7.1 ± 0.2	98.5 ± 2.9
AEA	7.2 ± 0.2	24.0 ± 2.3
2-AG	5.8 ± 0.1	89.1 ± 4.6
SR-144,528	No fit	No fit
005	7.4 ± 0.4	14.2 ± 2.6
009	No fit	ND
025	8.5 ± 0.3	21.9 ± 3.6

Table 4: **Summary table of results from β-arrestin protein recruitment assays in cannabinoid receptor-2 (CB_2R)-expressing HEK293TR cells, in the presence of reference and novel compounds.** Half maximal effective concentration (EC_{50}) expressed as a negative logarithmic value (log[EC_{50}]; pEC_{50}). Maximal responses (E_{max}) to agonist stimulation are given as a percentage (%) of the response elicited by 3 μM HU-308, which is a selective CB_2R agonist. Data are averaged (mean ± S.E.M) across n≥3.

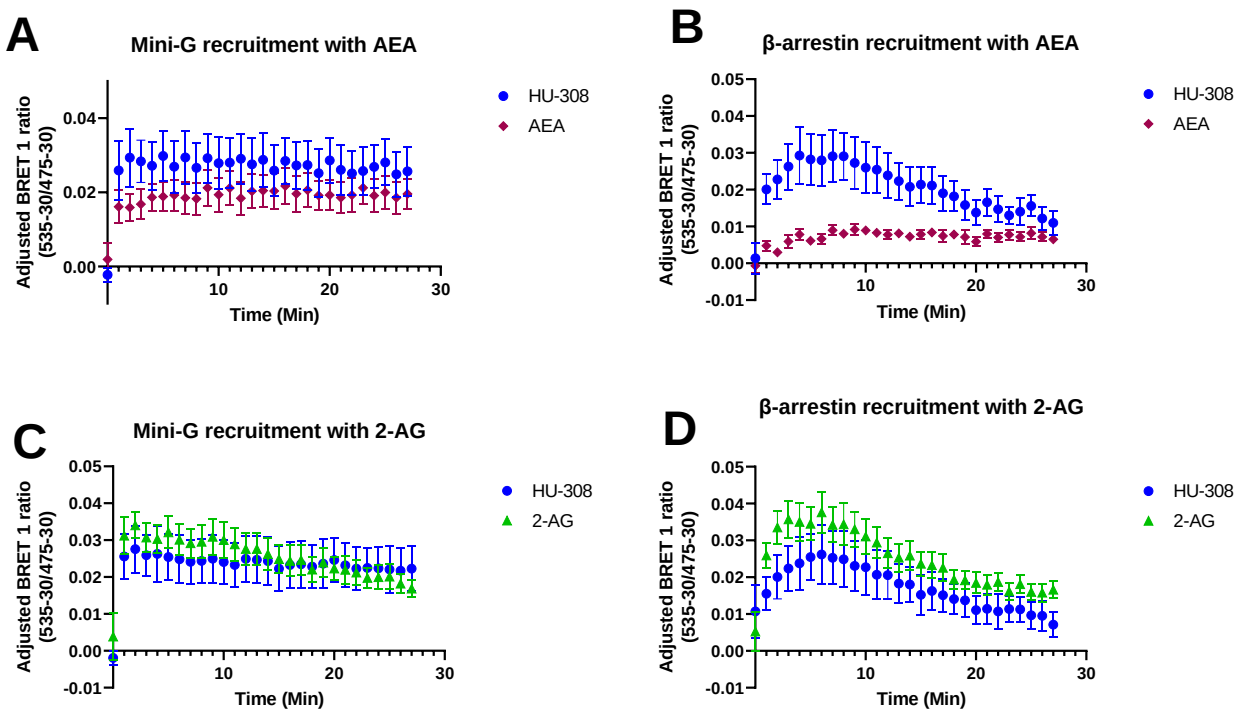

***Figure 9 (above): Response* time-courses of endogenous ligands compared directly with HU308, when used to stimulate HEK293TR cells expressing cannabinoid receptor-2 (CB_2R) in a mini-G (mG) protein and β-arrestin recruitment assay.** CB_2R stimulation with **(A)** AEA in the mini-G protein recruitment assay and **(B)** AEA in the β-arrestin recruitment assay. CB_2R stimulation with **(C)** 2-AG in the mG recruitment assay and **(D)** 2-AG in the β-arrestin assay. Data are averaged (mean ± SEM), across n≥3.

Mini-G (mG) protein and β-arrestin protein recruitment experiments also highlighted that the response to 2-AG, the endogenous ligand, appears to decay over the course of both assays. This data can be seen in figure 9, which is a time-course of the response throughout the duration of the assay with 2-AG relative to 3 μM HU-308 positive control. The 2-AG response decayed over time which is potentially likely due to the ligand's instability and its metabolism. We found that HU-308 does not appear to decay in the mG assay but does decay in the β-arrestin assay (figure 9).

Gi-CASE: preliminary transient transfection assays

The use of $G\alpha_i$ protein tricistronic activity sensors (Gi-CASE) for studying G protein activation is a novel technique and uses biosensors developed recently (Schihada *et al.,* 2021). Here, we initially carried out transient transfections of the Gi-CASE plasmid in order to establish the best concentration of plasmid to use in our investigations into G protein activation. Importantly, the Gi-CASE biosensor was solely used as a marker of receptor activation and was not used to assess downstream signalling. We found that between 400-600 ng/μL of the plasmid was optimal in obtaining a BRET response following stimulation with 10 μM HU-210, a synthetic non-selective agonist at CB_1R and CB_2R. Above these concentrations, the dose-response becomes less pronounced (see figure 10).

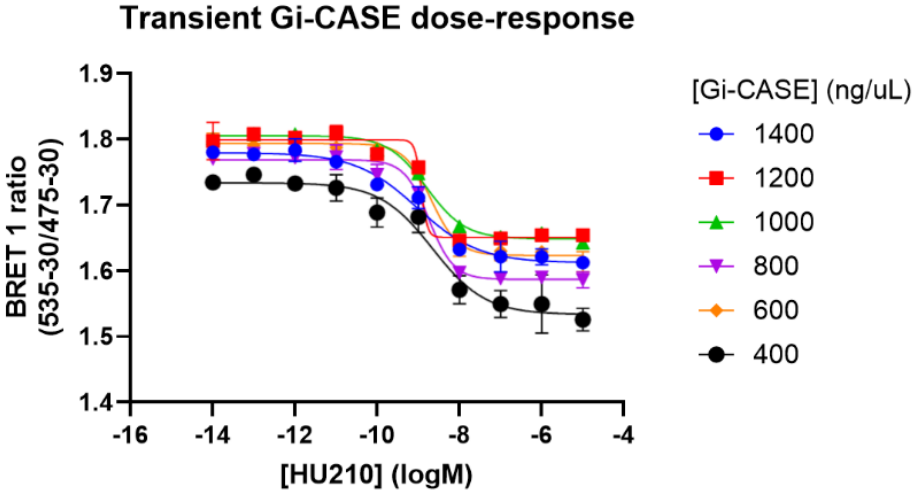

Figure 10 (above): **Preliminary data from transiently transfecting a novel G_{ai} tricistronic activity sensor (Gi-CASE) into HEK293TR-CB_2R cells.** Six separate transfection ratio conditions were used. Gi-CASE DNA was equalised with salmon sperm DNA. Meaned data ± S.E.M, representative of (n≥3).

Gi-CASE: stable cell line assays

(i) Reference compounds

After finding a response via transient transfection of the Gi-CASE plasmid into HEK293TR-CB_2R cells, we attempted to create stable cell lines expressing the full-length CB_1R, truncated CB_1R (91-472) and the CB_2R, with the Gi-CASE plasmid. After the stable cell lines had been established through selection with the appropriate selection agent, which in this case was Geneticin®, a series of reference compounds were tested against the cells. Specifically, we used reference compounds including HU-210 (CB_1R and CB_2R receptor agonist), HU-308 (CB_2R agonist), rimonabant (CB_1R inverse agonist) and SR-144,528 (CB_2R inverse agonist), to characterise CB_1R and CB_2R functional activity.

We found that HU-210 had a greater maximal response at CB_1R compared to HU-308, whereas rimonabant had a potent inverse agonist effect on both CB_1R and CB_2R which resulted in an increase in BRET signal (figure 11). CB_1R inverse agonist responses were noticeably more potent for rimonabant reflecting its higher reported affinity for CB_1R (Porcu *et al.,* 2018; Wu *et al.,* 2011). SR-144,528 had a weak partial agonist effect on CB_1R, but this could not be properly quantified due to its low potency. Similar albeit less-pronounced profiles were seen with truncated CB_1R cells, whereas HU-308 caused a strong increase in BRET signal as a CB_2R-selective agonist (figure 11). A summary of the responses for Gi-CASE assays with reference compounds is given in table 5.

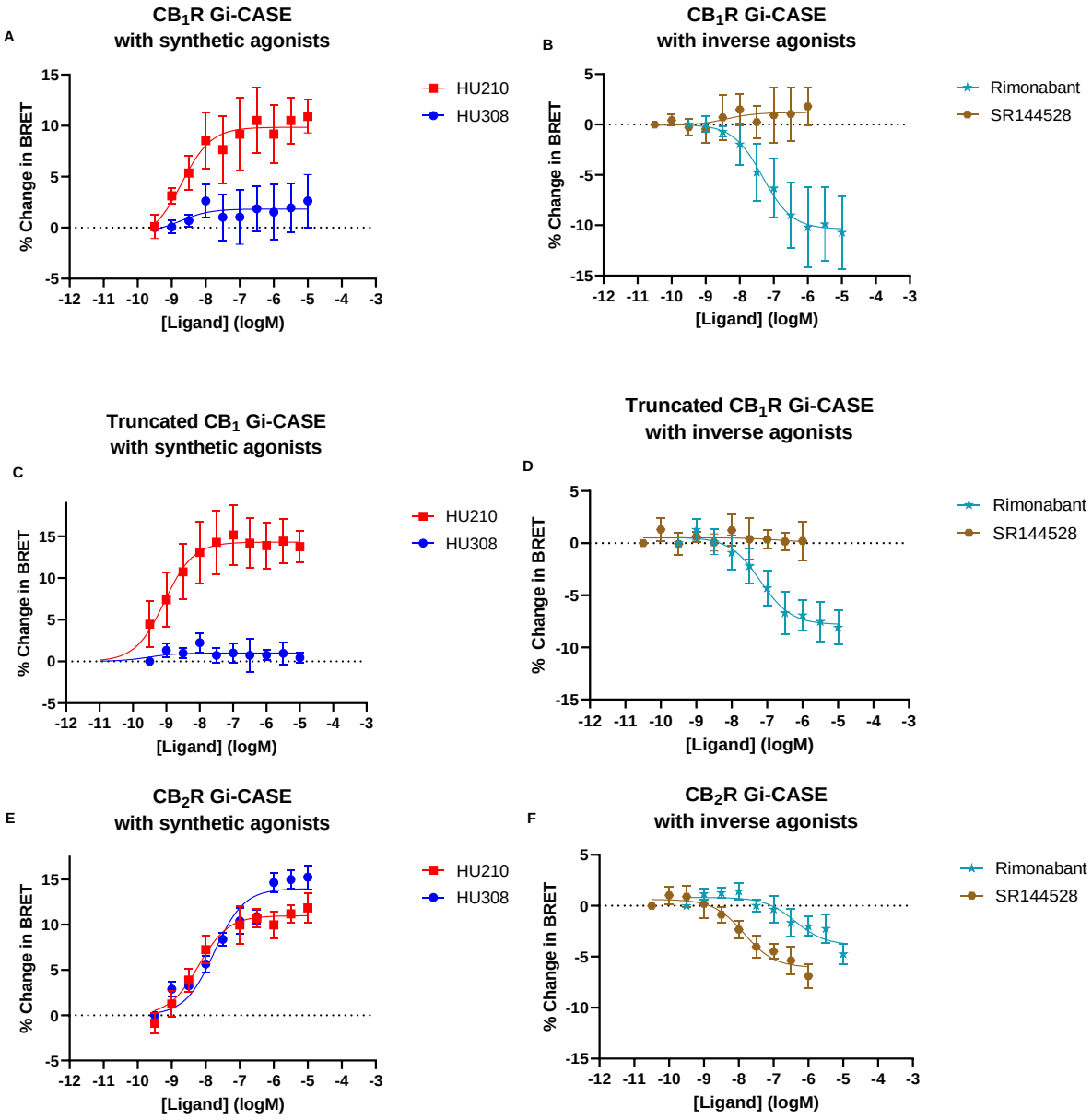

Figure 11: **Reference agonist stimulation of HEK293TR cells expressing cannabinoid receptor-1 (CB_1R), truncated (91-472) CB_1R and cannabinoid receptor-2 (CB_2R), all expressing a novel G protein activity biosensor (Gi-CASE).** Agonist stimulation using a non-selective CB_1R and CB_2R a synthetic agonist HU-210 and CB_2R-selective synthetic agonist HU-308 at **(A)** full-length CB_1R cells, at **(C)** at truncated CB_1R cells and at **(E)** full-length CB_2R cells. Inverse agonist stimulation using CB_1R-antagonist rimonabant and CB_2R-selective antagonist SR-144,528 at **(B)** full-length CB_1R cells, at **(D)** truncated CB_1R cells and at **(F)** full-length CB_2R cells. Responses are relative to positive controls including 10μM HU-210 for CB_1Rs and 10 μM HU-308 for CB_2Rs.

Full-length CB_1R with reference compounds

	HU-210	HU-308	Rimonabant	SR-144,528
pEC_{50}	8.8 ± 0.1	8.1 ± 0.4	7.2 ± 0.4	No fit
E_{max} (%)	10.5 ± 1.8	1.5 ± 1.9	-14.1 ± 2.9	ND

Truncated CB_1R with reference compounds

	HU-210	HU-308	Rimonabant	SR-144,528
pEC_{50}	9.2 ± 0.3	8.2 ± 0.5	7.1 ± 0.4	No fit
E_{max} (%)	14.6 ± 1.6	1.1 ± 1.0	-8.2 ± 1.5	ND

Full-length CB_2R with reference compounds

	HU-210	HU-308	Rimonabant	SR-144,528
pEC_{50}	8.2 ± 0.4	7.9 ± 0.1	5.2 ± 1.4	7.5 ± 0.2
E_{max} (%)	14.0 ± 1.6	13.6 ± 0.6	-6.0 ± 1.1	-6.9 ± 0.9

***Table 5*: Summary table for HEK293TR cells expressing cannabinoid receptor-1 (CB_1R), truncated (91-472) CB_1R and cannabinoid receptor-2 (CB_2R) after stimulation with a series of reference agonists.** Synthetic cannabinoid receptor agonists HU-210 and HU-308 were used, as well as rimonabant which is a CB_1R inverse agonist, and SR-144,528 which is a CB_2R-selective inverse agonist. Data are averaged (mean ± S.E.M) from n≥3. Data are expressed as a percentage change in BRET relative to positive controls including 10μM HU-210 for CB_1Rs and 10 μM HU-308 for CB_2Rs.

(ii) Novel compounds

After characterising CB_1R and CB_2R with the reference compounds, we tested the novel compounds including compounds 005, 009 and 025 which were derived from *in silico* docking. We also took forward AEA and 2-AG as the endogenous ligands and HU-210 and SR-144,528 as reference compounds from which to compare the response of the novel ligands. The endogenous ligands and HU-210, being non-selective, had a similar agonist effect at both receptors. SR-144,528 had a small agonist effect at all CB_1Rs (see figure 12 and 13) despite being an inverse agonist at CB_2R (see figure 14). As for the novel compounds, 005 elicited a partial-agonist response at both receptors based on the observed decrease in BRET (see figures 12-14). Compound 009 failed to recruit mG or β-arrestin but here caused an increase in the BRET signal, which in this experimental framework may indicate an inverse agonist effect of the compound (see figure 12-14). Interestingly, compound 025 had

a fuller agonist effect on CB_2R (figure 14), which was not observed at the other receptors. The agonist response of the compounds at CB_1Rs was compared to HU-210, a non-selective agonist at CB_1R and CB_2R. However, experiments for CB_2R used HU-308 which is a CB_2R-selective agonist. A summary of the data for novel compounds in the Gi-CASE experiments is given in table 6.

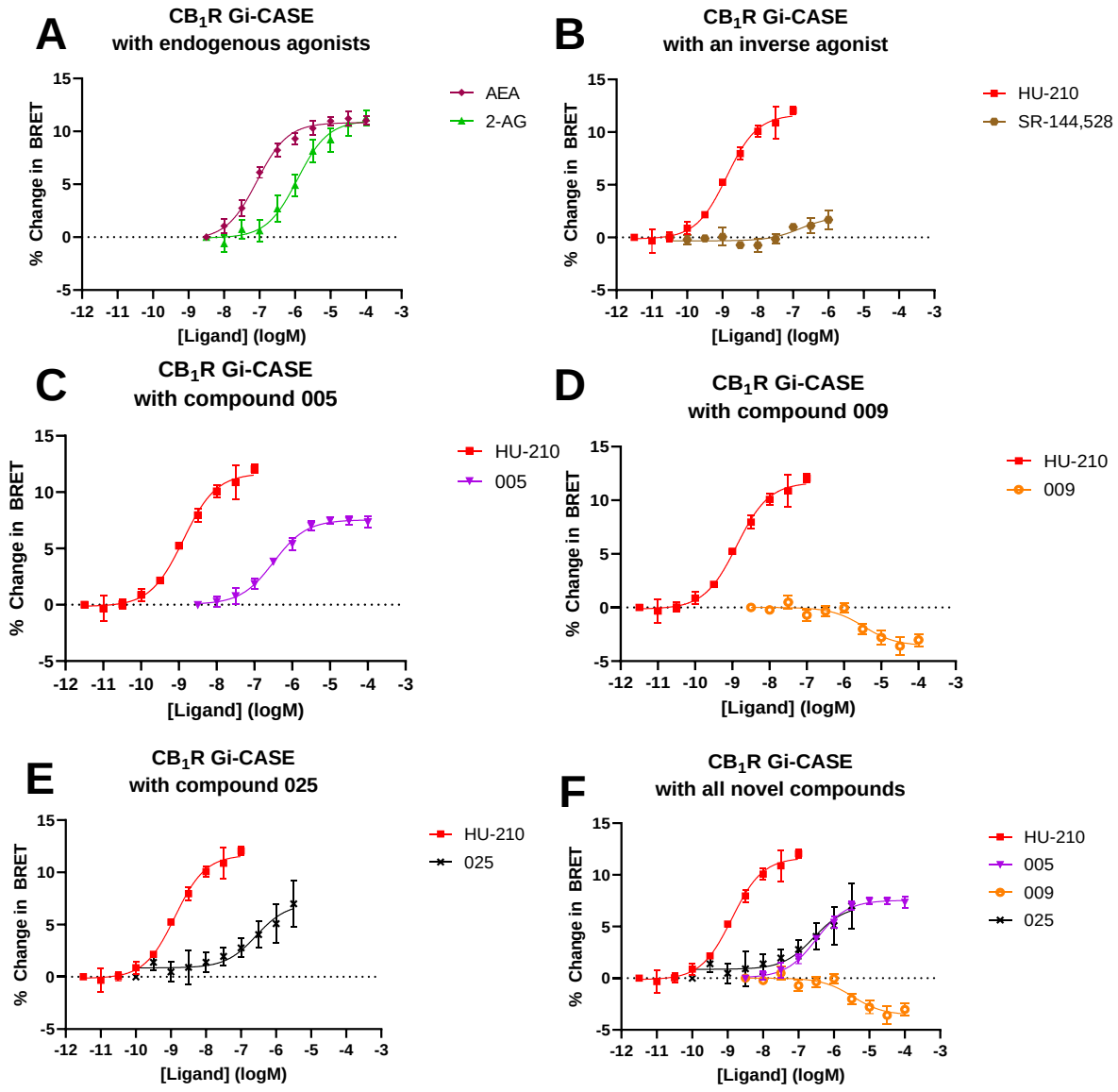

Figure 12: **Functional assays of HEK293TR cells expressing cannabinoid receptor-1 (CB_1R) and a novel G protein activity biosensor. (A)** Agonist stimulation of CB_1R cells with two endogenous agonists anandamide (AEA) and 2-arachidonoylglycerol (2-AG). **(B)** Stimulation of CB_1R cells with synthetic agonist HU-210 and inverse agonist SR-144,528. **(C)** Agonist response elicited at CB_1R by novel compound 005 compared to synthetic agonist HU-210. **(D)** Agonist response elicited at CB_1R by novel compound 009 compared to synthetic agonist HU-210. **(E)** Agonist response elicited at CB_1R by novel compound 025 compared to synthetic agonist HU-

210. **(F)** Collated novel compound responses of all novel compounds relative to agonist response at CB_1R by synthetic agonist HU-210. Data at averaged (mean ± SEM) across n≥3. Data are percentage (%) change in BRET relative to the response with 10 µM HU-210 as a positive control.

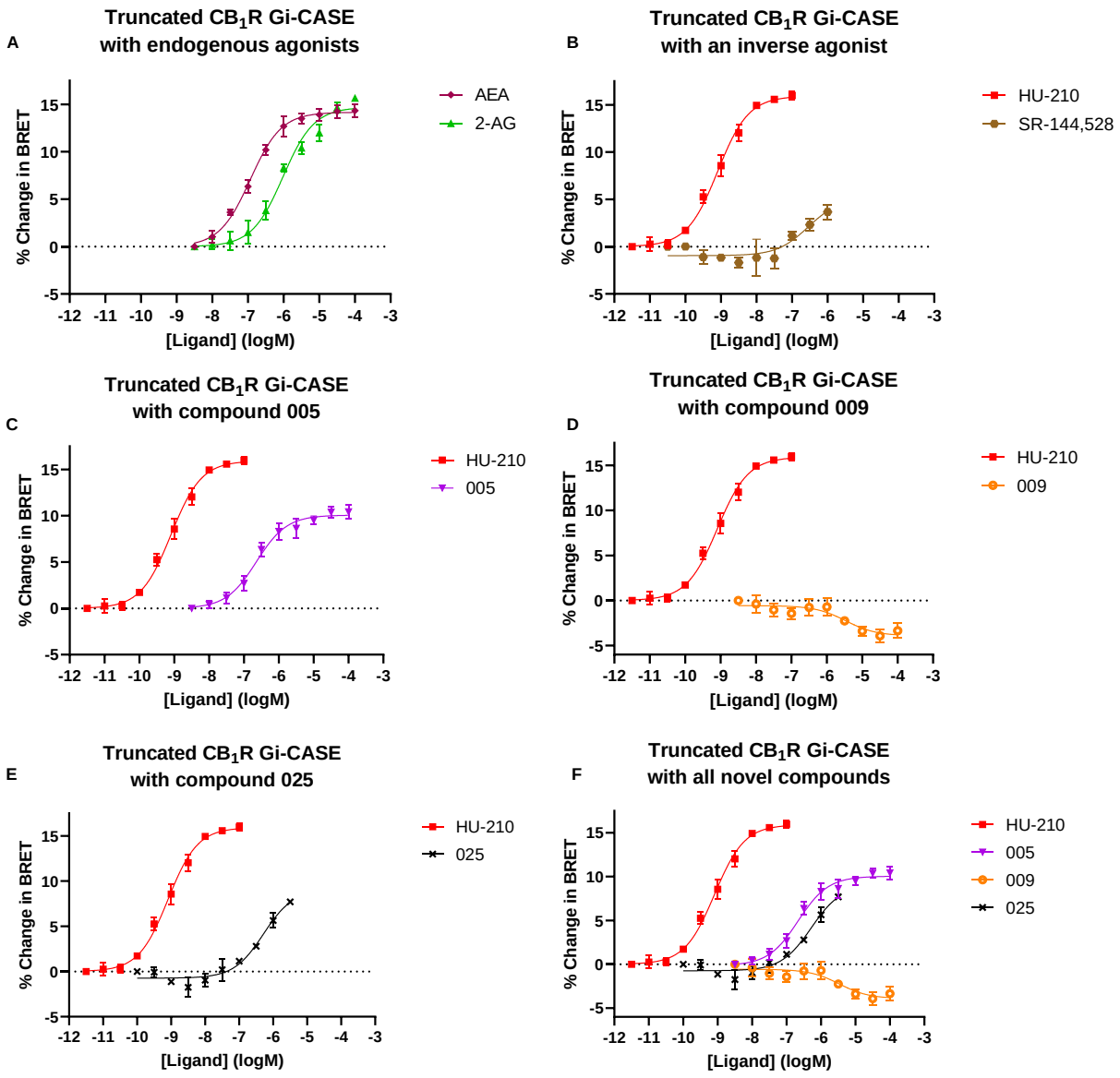

Figure 13: **Functional assays of HEK293TR cells expressing a truncated (91-472) cannabinoid receptor-1 (tCB_1R) and a novel G protein activity biosensor.** **(A)** Agonist stimulation of tCB_1R cells with two endogenous agonists anandamide (AEA) and 2-arachidonoylglycerol (2-AG). **(B)** Stimulation of tCB_1R cells with synthetic agonist HU-210 and inverse agonist SR-144,528. **(C)** Agonist response elicited at tCB_1R by novel compound 005 compared to synthetic agonist HU-210. **(D)** Agonist response elicited at tCB_1R by novel compound 009 compared to synthetic agonist HU-210. **(E)** Agonist response elicited at tCB_1R by novel compound 025 compared to synthetic agonist HU-210. **(F)** Collated novel compound responses of all novel compounds relative to agonist response at tCB_1R by synthetic agonist HU-210. Data are percentage (%) change in BRET, and are averaged (mean ± SEM) across n≥3 and relative to the response with 10 µM HU-210 as a positive control.

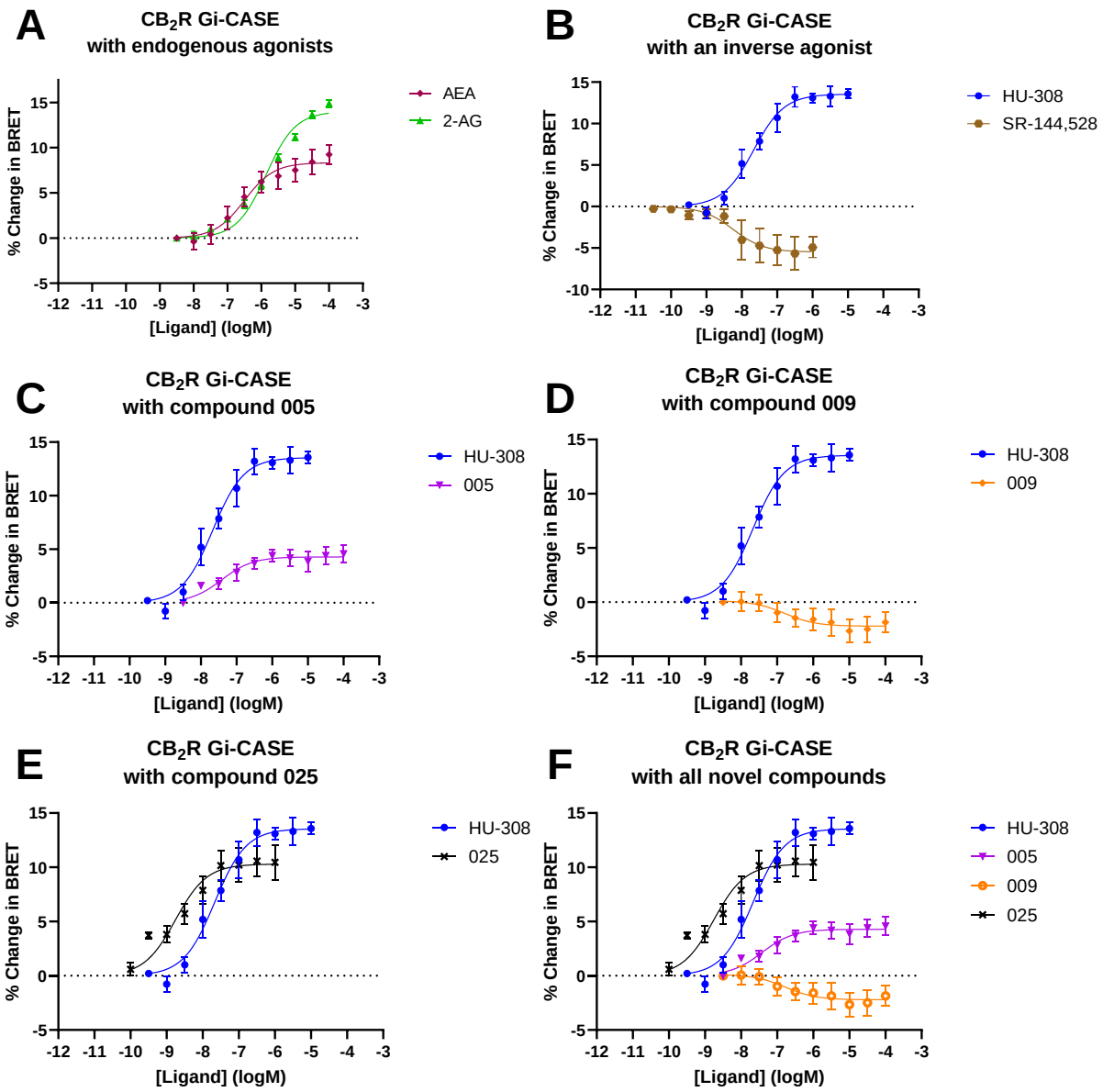

Figure 14: **Functional assays of HEK293TR cells expressing cannabinoid receptor-2 (CB_2R) and a novel G protein activity biosensor. (A)** Agonist stimulation of CB_2R cells with two endogenous agonists anandamide (AEA) and 2-arachidonoylglycerol (2-AG). **(B)** Stimulation of CB_2R cells with synthetic agonist HU-308 and inverse agonist SR-144,528. **(C)** Agonist response elicited at CB_2R by novel compound 005 compared to synthetic agonist HU-308. **(D)** Agonist response elicited at CB_2R by novel compound 009 compared to synthetic agonist HU-308. **(E)** Agonist response elicited at CB_2R by novel compound 025 compared to synthetic agonist HU-308. **(F)** Collated novel compound responses of all novel compounds relative to agonist response at CB_2R by synthetic agonist HU-308. Data are percentage (%) change in BRET, and are averaged (mean ± SEM) across n≥3, and are relative to the response of 10 μM HU-308 as a positive control.

Full-length CB_1R Gi-CASE cells tested with reference and novel ligands							
	HU-210	AEA	2-AG	SR-144,528	005	009	025
pEC_{50}	8.8 ± 0.1	7.0 ± 0.1	5.8 ± 0.2	7.3 ± 0.6	6.5 ± 0.1	5.5 ± 0.1	6.9 ± 0.1
E_{max}	11.1 ± 0.8	10.8 ± 0.5	10.7 ± 0.6	3.5 ± 2.0	7.3 ± 0.4	-3.3 ± 0.3	7.0 ± 1.0
Truncated (91-472) CB_1R Gi-CASE cells tested with reference and novel ligands							
	HU-210	AEA	2-AG	SR-144,528	005	009	025
pEC_{50}	8.2 ± 0.4	6.9 ± 0.6	6.0 ± 0.1	5.9 ± 0.2	6.5 ± 0.2	6.5 ± 0.5	6.2 ± 0.1
E_{max}	15.1 ± 0.8	14.2 ± 0.6	14.7 ± 0.3	6.0 ± 1.2	10.0 ± 0.6	-3.2 ± 0.3	8.9 ± 0.6
Full-length CB_2R Gi-CASE cells tested with reference and novel ligands							
	HU-308	AEA	2-AG	SR-144,528	005	009	025
pEC_{50}	7.9 ± 0.5	6.4 ± 0.3	6.1 ± 0.1	7.2 ± 1.5	7.4 ± 0.3	6.8 ± 0.5	8.6 ± 0.1
E_{max}	13.2 ± 1.2	8.4 ± 1.2	14.2 ± 0.5	-6.0 ± 0.5	4.4 ± 0.8	-2.9 ± 0.8	9.8 ± 1.2

Table 6: **Agonist stimulation responses using reference and novel compounds, tested on HEK293TR cells expressing either cannabinoid receptor-1 (CB_1R), truncated CB_1R or cannabinoid receptor-2 (CB_2R), as well as a novel G protein activity biosensor (Gi-CASE).** Reference compounds include the synthetic agonists HU-210 and HU308, the endogenous cannabinoid receptor agonists anandamide (AEA) and 2-arachidonoylglycerol (2-AG) and an inverse agonist SR-144,528. Novel compounds include compounds 005, 009 and 025, derived from *in silico* docking scoring. Data are averaged (mean ± SEM) across n≥3 and are relative to positive controls including 10 μM HU-210 for CB_1Rs or HU-308 for CB_2Rs.

4.3 Discussion

After characterising ligand binding at CB_1R and CB_2R, we considered if the novel compounds were biased towards either G protein signalling or β-arrestin signalling using mini-g (mG) and β-arrestin recruitment assays. We then used Gi-CASE biosensor assays to study functional G protein activity in response to drug stimulation. The principles behind the two assays vary. The mG recruitment assay uses a minimal G protein in which the GTPase activity has been disabled to prevent the exchange of nucleotides (Wan *et al.,* 2018). This also means that the mG proteins forms stable receptor complexes (Carpenter & Tate, 2016) and the BRET response is irreversible in the presence of an agonist. In addition, the mG assay only elucidates G protein activation and recruitment without quantifying differences in downstream signalling, which does not allow for the study of systems bias where there are stoichiometric differences in the abundance of G protein or β-arrestin (Smith *et al.,* 2018). In contrast, the Gi-CASE assay involves using the fluorescent G protein where the catalytic component is still intact (Schihaha *et al.,* 2021), making G protein activation more dynamic and able to reach a true equilibrium, and the BRET response is therefore less binary. The mG and β-arrestin recruitment assays were used to study ligand bias comparing G protein or β-arrestin recruitment to the receptor, while the Gi-CASE assays considers ligand bias by studying G protein activation in response to drug stimulation.

A series of reference compounds were used in both sets of experiments as positive controls and when evaluating the reliability of the assays as a means to assess the novel compounds. Reference compounds include HU-210, a full agonist at CB_1R and CB_2R (Ottani & Giuliani, 2001), and HU-308, a CB_2R-selective agonist (Hall *et al.,* 2022). In addition, SR-144,528 and rimonabant were used as purported antagonists at CB_2R and CB_1R, respectively (Fong & Heymsfield, 2009; Porcu *et al.,* 2018; Portier *et al.,* 1998). 2-AG, a full agonist at both receptors (Sugiura & Waku, 2000) and AEA a partial agonist at both receptors (Pete & Narouze, 2021), were also used.

The mG protein and β-arrestin recruitment experiments showed the novel ligands to be relatively unbiased in their ability to recruit either the mG protein or β-arrestin upon receptor activation. This is due to the similarity in the change in the BRET signal elicited by the binding of each novel ligand to CB_2R, when compared with the maximal response achieved by the reference compound and CB_2R agonist, HU-308. Potency values were given as pEC50 values, which were similar for all compounds across both assays.

HU-308 had a maximal response for β-arrestin recruitment (table 4) but was less than 100% for G-protein activation in the mG recruitment assay (table 3), despite the compound being a selective-CB_2R agonist. This was likely due to inherent errors within the assay (using control wells for normalisation rather than the control curve for normalisation), as HU-308 should in theory have a maximal response approximately equal to 100% for both G protein and β-arrestin activation. Rimonabant and SR-144,528 are both reported as antagonists and inverse agonists in the literature (Fong & Heymsfield, 2009; Porcu *et al.,* 2018; Portier *et al.,* 1998), and are therefore not appropriate reference compounds to use in mG and β-arrestin recruitment assays, which require an agonist response for mG or β-arrestin recruitment. The proceeding Gi-CASE experiments demonstrate that SR-144,528 has an inverse agonist response, which is sufficient to inhibit receptor constitutive activity and would in theory block agonist-stimulated mG or β-arrestin recruitment. There is no constitutive activity in either the mG or β-arrestin assay at CB_2R, meaning SR-144,528 appears as a neutral antagonist.

The mG and β-arrestin recruitment assays confirmed that 2-AG is nearly a full agonist at both CB_1R and CB_2R, and that AEA is a partial agonist as reported in the literature (Sugiura & Waku, 2000; Pete & Narouze, 2021). The mG response of 2-AG appears to decay over time based on the diminished percentage change in response. Since the percentage change in BRET signal diminishes over time, it suggests that 2-AG is progressively less able to bind and elicit CB_2R activation, reducing G protein activation. The decay in the 2-AG response may also indicate preferential signalling via β-arrestin to enable more rapid receptor internalisation and mG response inhibition. The other endocannabinoid, AEA, does not appear to decay in either the mG or β-arrestin recruitment assay, which may indicate preferred signalling through the G protein, but this could also be a reflection of how 2-AG is a full agonist at both CB_1R and CB_2R, while AEA is not. Nevertheless, the decay in response does not solely indicate ligand bias, but should be considered future experiments using 2-AG and AEA because of the time-dependent change in response between the first five minutes of compound addition and at the end of the microplate being read.

In the Gi-CASE experiments, HU-210 and HU-308 along with rimonabant and SR-144,528 were used as positive controls to characterise CB_1R and CB_2R prior to stimulation with the novel compounds. The responses of HU-210 showed it to be selective at both receptors, while HU-308 seems to be CB_2R-selective in agreement with the literature (Ottani & Giuliani, 2001; Hall *et al.,* 2022). That said, the pEC_{50} values of HU-308 remain the same at both CB_1R and CB_2R despite it having a higher

E_{max} at CB_2R (table 5). CB_1R and CB_2R may have a similar coupling efficiency to the G protein (Kim *et al.,* 2020), based on the similar pEC_{50} values observed between CB_1R and CB_2R for HU-308 in the initial Gi-CASE experiments with the known compounds (table 5). The low response to HU-308 in CB_1R could also be the result of fixing the slope to 1, meaning that the response may not be entirely real.

SR-144,528 also appeared to be an inverse agonist at CB_2R and had some agonist effects at CB_1R and the truncated CB_1R. Rimonabant appeared to be an inverse agonist at both full-length and truncated CB_1R, and CB_2R, which contrasts the understanding of it as an antagonist and selective for CB_1R (Boyd & Flemming, 2005). Rimonabant as an inverse agonist agrees with the idea that it can bind the receptor but may also cause the accumulation of inactive G protein hence the increase in BRET signal. The same is true of SR-144,528 binding to the CB_2R in the Gi-CASE assay. The observed differences in potency between the competition binding and Gi-CASE experiments may arise due to using membranes used initially versus whole cells in the functional assays.

In the CB_1R Gi-CASE assays, AEA appeared to behave as a fuller agonist and a partial agonist at CB_2R. When testing the novel compounds in the Gi-CASE assays, we did not identify any ligand bias but identified 005 and 025 to be agonists and 009 to be an inverse agonist. Signalling bias was not studied at CB_1R on the basis that the novel compounds did not appear to bind to the receptor. However, using the Gi-CASE biosensors at CB_1R and CB_2R highlighted binding by the novel compounds to both receptors, contrasting our ligand binding experimental findings that they were CB_2R-specific. This also sheds light onto the coupling efficiency of CB_1R versus CB_2R since the competition binding experiments depicted no binding but in these experiments there is a clear response among all the compounds at both receptors, suggesting that the G protein itself can enhance ligand affinity.

4.4 Conclusions

The mG and β-arrestin recruitment assays and Gi-CASE assays failed to identify ligand bias among the reference or novel compounds. It seems that compounds 005 and 025 are agonists at both CB_1R and CB_2R, whereas compound 009 displays inverse agonism. These conclusions are drawn following the characterisation of receptor binding using reference agonists including HU-210 and HU-308, the endogenous agonists AEA and 2-AG, and inverse agonists including rimonabant and SR-144,528. The novel ligands seem to be slightly more potent at CB_2R, but they do not appear to be biased towards either the G protein or β-arrestin protein.

Chapter 5: Characterising CB_1R and CB_2R internalisation, using confocal microscopy and DERET assays.

5.1 Introduction

Gi-CASE experiments elucidated G protein activation, so we complemented this with studies of receptor internalisation in order to gain a complete pharmacological profile of the compounds and gain insights into β-arrestin function, which initiates receptor internalisation (Ahn *et al.,* 2003). We first used confocal microscopy to study receptor internalisation (Miyashita, 2004; He *et al.,* 2019), stimulating green fluorescent protein (GFP)-tagged HEK293TR-CB_2R-cells with an agonist HU-308 and an inverse agonist SR-144-528, and hypothesised that ligand-receptor binding would lead to a dose-dependent increase in the abundance of intracellular vesicles of the internalised receptor, before testing the novel compounds 005, 009 and 025. Studies of internalisation were then complemented with diffusion-enhanced resonance energy transfer (DERET) assays, and it was hoped that agonist binding would lead to a dose-dependent increase in the FRET signal. This is because receptor internalisation into the cytoplasmic domain should reduce quenching of the fluorescent terbium donor fluorophore attached via a SNAP-tag to the N-terminus of the receptor located on the outside of the cell, enabling prolonged signal emission (Levoye *et al.,* 2015).

All cells were tested following a 48-hour incubation period after the cells had been plated and grown in a cell culture medium with antibiotics. Cells expressing CB_2R were used with confocal microscopy to study receptor internalisation. These cells were treated with tetracycline to induce receptor expression and were cultured in a cell growth medium for 48 hours. They were then prepared for experimentation and stimulated with reference and novel compounds, before being fixed and stored in assay buffer (HBSS, 0.5% BSA and 5mM HEPES) prior to imaging. For the DERET assay, both full-length CB_1R and CB_2R cells were used. After plating, the cells were prepared for terbium labelling, proceeded by wash steps to remove residual free terbium. The cells were then stimulated with compounds in an assay buffer consisting of HBSS, 0.1% BSA and 5 mM HEPES, with fluorescein dye added.

5.2 Results

GFP-based internalisation assay

Initially, receptor internalisation was studied using confocal microscopy using HEK293TR-CB_2R cells expressing a green fluorescent protein (GFP) tag. We expected that agonist stimulation to cause a dose-dependent increase in the rate of receptor internalisation. Internalised CB_2Rs should be seen as visible granules in the cytosol, as opposed to cells treated with vehicle which should display mainly a visible fluorescent outline of surface receptors on the outer leaflet of the plasma membrane.

As a preliminary experiment (n=1), we stimulated the CB_2R cells with HU-308 and SR-144,528, which are agonists and inverse agonists at CB_2R, respectively. DMSO was also used as a vehicle control. After 1 hour of stimulation, the cells were fixed with Hoechst stain and the cells were stored in assay buffer prior to visualisation. We did not see any observable difference in CB_2R internalisation with either compound at any concentration compared to the vehicle control.

We then stimulated three separate plates of cells with the reference compounds (HU-308 and SR-144,528) alongside the novel ligands (005, 009 and 025) for 60 minutes. The cells were then fixed in the same way as in the preliminary experiment. A small decrease in signal could be seen in cells treated with HU-308 and compound 005, but this was not seen with compound 025 or compound 009. Furthermore, significant internalisation was observed in DMSO-treated cells, where often more granules of internalised receptors, were seen. Overall, there was no observable difference in receptor internalisation between any of the used compounds compared to the buffer control, to warrant any further analysis of the images (see figure 15).

For all experiments, GFP counts were considerably low, and the degree of staining in cells was very inconsistent. Because no imaging analysis was carried out, we followed up these findings with diffusion-enhanced resonance energy transfer (DERET) assays.

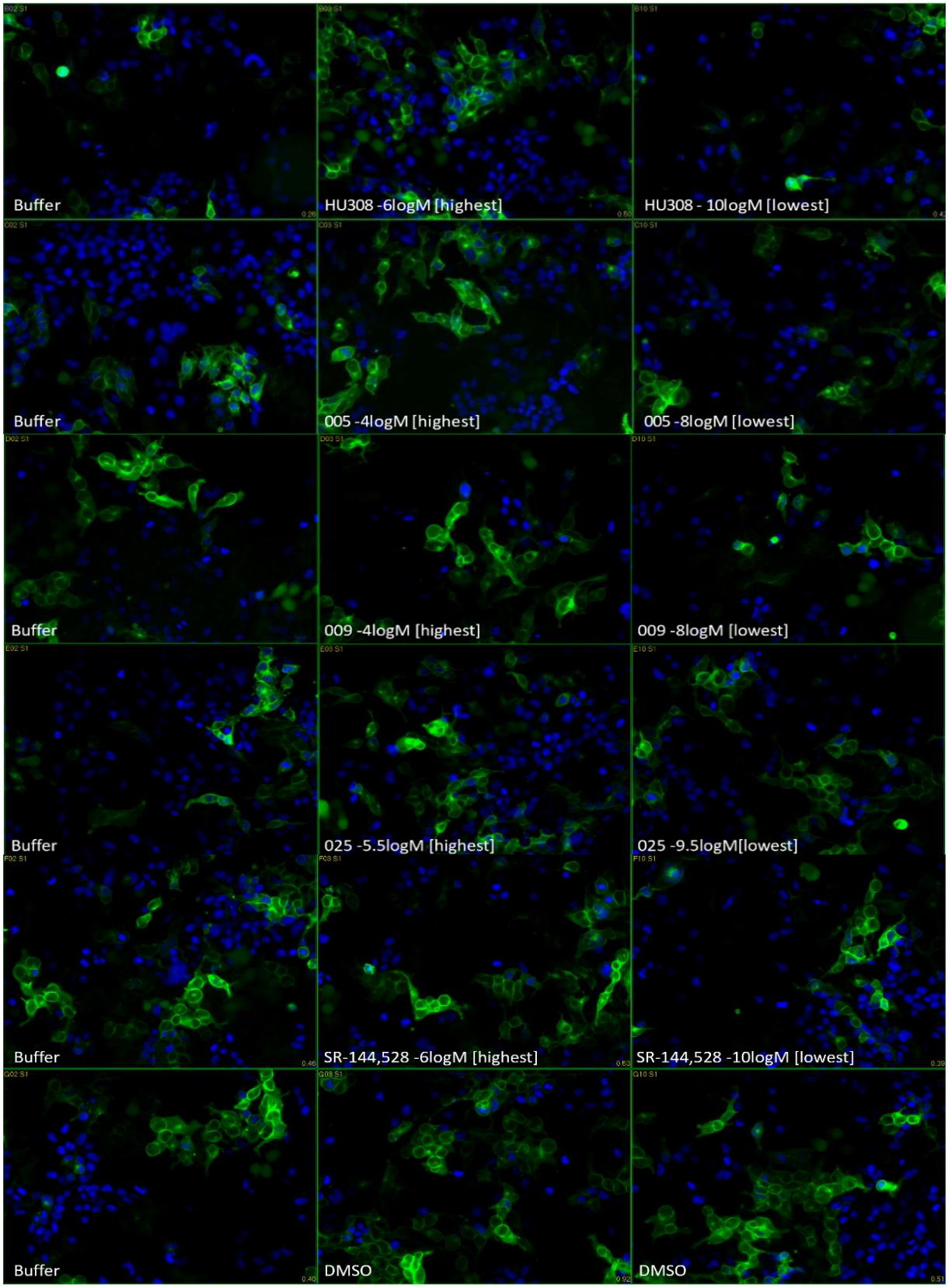

Figure 15: **Confocal imaging investigating receptor internalisation using cannabinoid receptor-2 (CB_2R)-expressing HEK293TR cells.** HEK293TR-CB_2R cells were stimulated for one hour with reference compounds and the three novel compounds, as well as a dimethyl sulfoxide (DMSO) blank. Green staining indicates green fluorescent protein (GFP) tagged CB_2R. Blue denotes Hoechst staining of cell

nuclei. No analysis of receptor internalisation was undertaken due to inconsistent cell staining and counts.

DERET assays for internalisation

DERET assays were carried out on SNAP-tagged HEK293TR cells expressing CB_1R and CB_2R to gain a full pharmacological profile of the novel compounds and to study the effects of β-arrestin recruitment, which eventually leads to receptor internalisation. As a result, DERET assays also enabled us to study bias among the compounds, by identifying if the ligands cause greater receptor internalisation at one receptor over another. The findings could also be potentially compared with the agonist responses in the Gi-CASE assays measuring G protein activity.

In the DERET assays, we stimulated CB_1R and CB_2R cells with refence compounds including 10 μM of the synthetic agonists HU-210, HU-308, and 1 μM of the inverse agonist SR-144,528. We also used the two endocannabinoids AEA and 2-AG, and the three novel compounds including compounds 005, 009 and 025. The DERET assay is based on a protocol described previously (Levoye *et al.,* 2015). Typically, the DERET assay involves the irreversible attachment of a terbium cryptate label (SNAP-Lumi4-Tb) to confluent cells expressing a SNAP-tagged receptor, pre-washed in PBS and a solution containing 1:4 ratio of LABMED:deionised water, before adding 50 μL/well of 100 nM terbium cryptate solution and placing in a humidified incubator (37 °C, 5% CO_2) for 1 hour. The cells are then washed several times in PBS to remove the terbium label, after which the fluorescein dye (10 μM in DMSO) mixed with 90 μL/well assay buffer (HBSS, 0.1% BSA, 5 mH HEPES) is added.

The addition of fluorescein dye at high concentrations causes the terbium label to become saturated with dye. However, agonist stimulation and the eventual internalisation of the receptor into the cytosolic domain is expected to cause a dose-dependent increase in signal, since the terbium label is no longer quenched by the high concentration of fluorescein dye on the outside of the cell, which prevents energy transfer from the terbium donor (Levoye *et al.,* 2015). Here, the cells were stimulated, and the plate was read each minute for 1 hour at 37 °C, before analysing the concentration response curves for agonist stimulating the CB_1R and CB_2R containing cells, the data for which is available in figures 16 and 17, respectively. A summary of the DERET assay data is given in table 7.

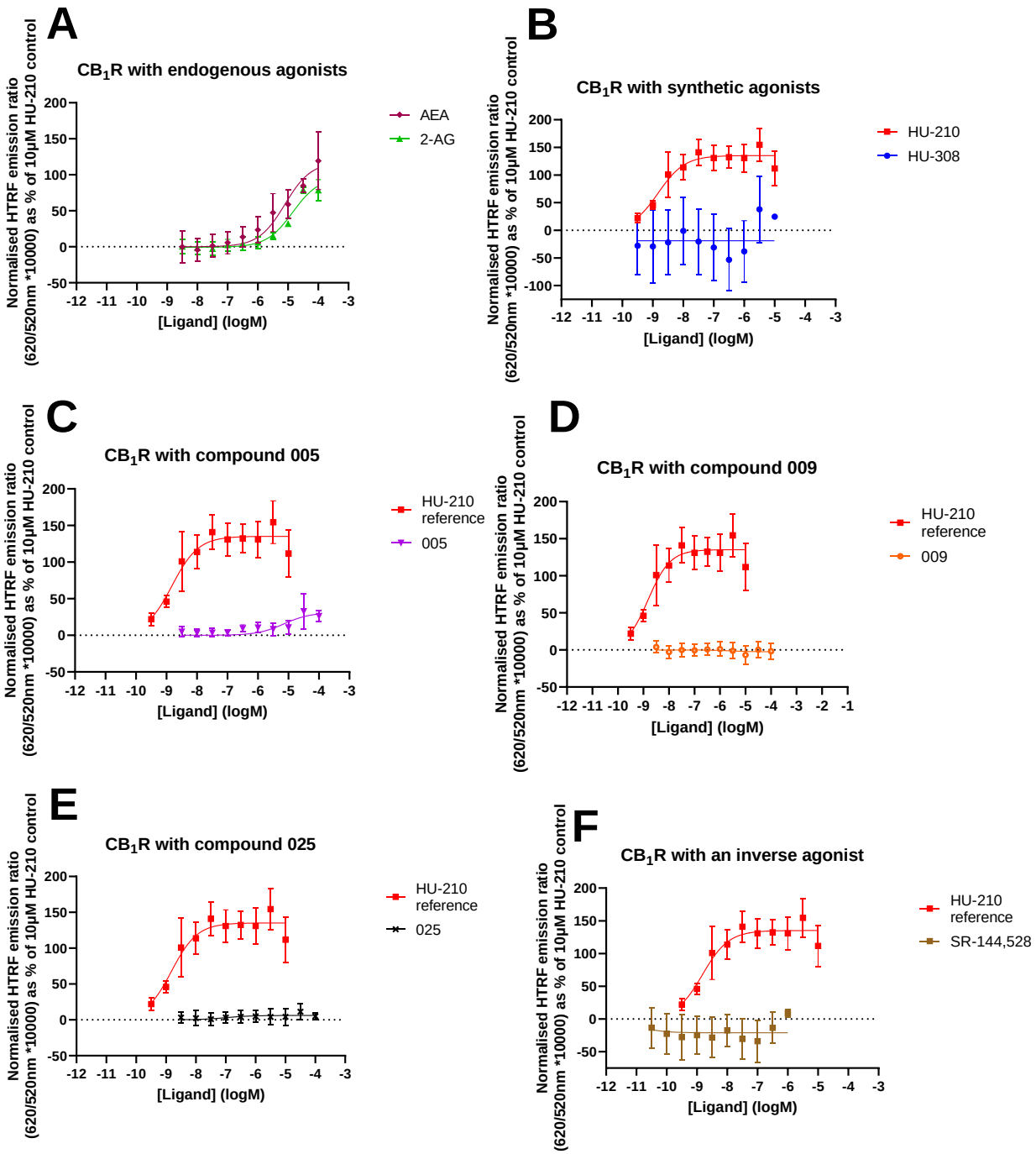

Figure 16: **Diffusion-enhanced resonance energy transfer (DERET) assays carried out on HEK293TR cells expressing cannabinoid receptor-1 (CB_1R) to elucidate receptor internalisation upon agonist stimulation. (A)** CB_1R internalisation following stimulation with endogenous agonists anandamide (AEA) and 2-arachidonoylglycerol (2-AG). **(B)** CB_1R internalisation following stimulation with synthetic agonists HU-210 and HU-308. **(C)** CB_1R internalisation following stimulation with novel compound 005. **(D)** CB_1R internalisation following stimulation with novel compound 009. **(E)** CB_1R internalisation following stimulation with novel compound 025. **(F)** CB_1R internalisation following stimulation with an inverse agonist SR-144,528. Data are given as a HTRF emission ratio (620/520*10,000), are normalised to 10 µM Hu-210 as a control and averaged (mean ± SEM), across n=3.

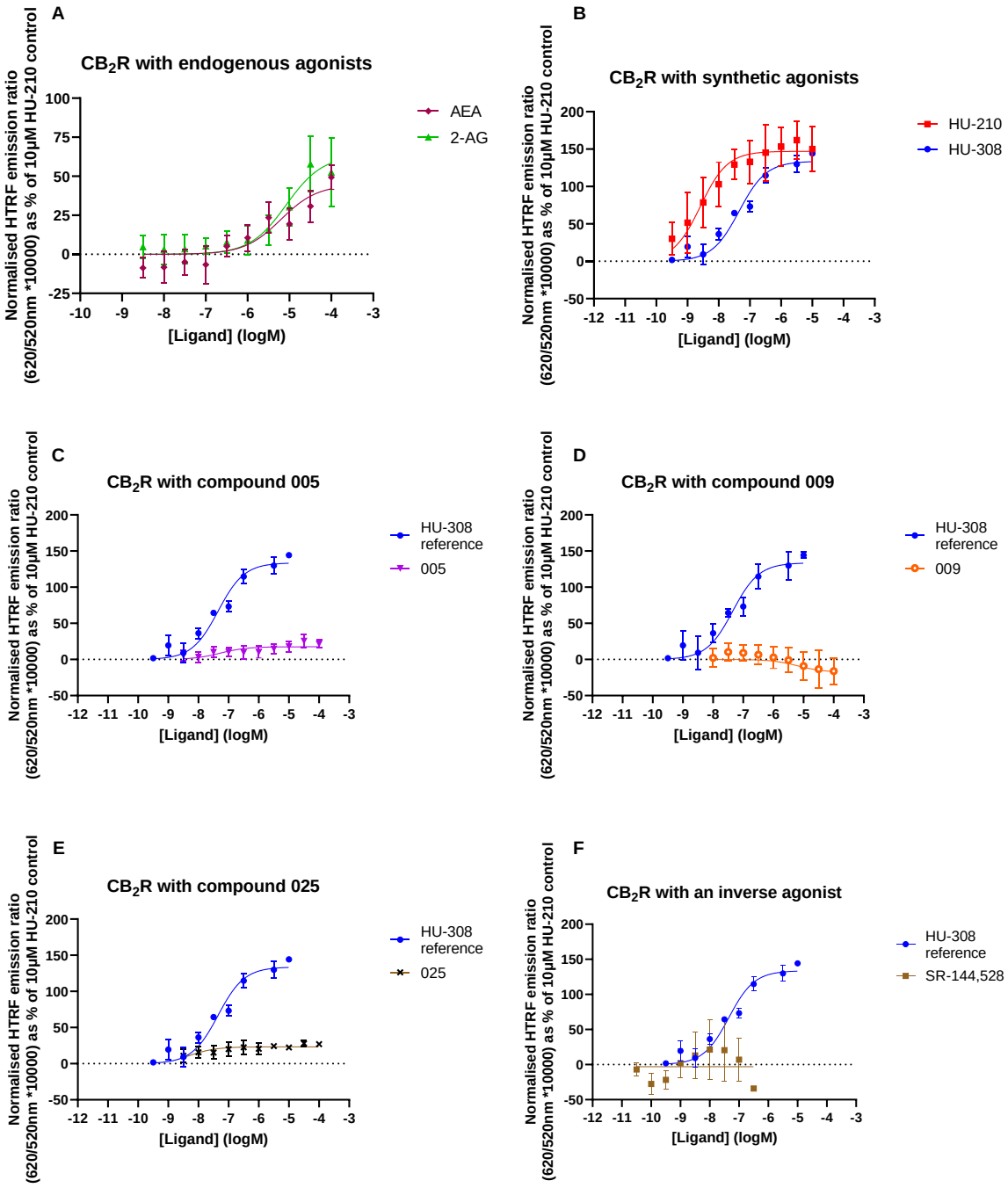

Figure 17: **Diffusion-enhanced resonance energy transfer (DERET) assays carried out on HEK293TR cells expressing cannabinoid receptor-2 (CB_2R) to elucidate receptor internalisation upon agonist stimulation. (A)** CB_2R internalisation following stimulation with endogenous agonists anandamide (AEA) and 2-arachidonoylglycerol (2-AG). **(B)** CB_2R internalisation following stimulation with synthetic agonists HU-210 and HU-308. **(C)** CB_2R internalisation following stimulation with novel compound 005. **(D)** CB_2R internalisation following stimulation with novel compound 009. **(E)** CB_2R internalisation following stimulation with novel compound 025. **(F)** CB_2R internalisation following stimulation with an inverse agonist SR-144,528. Data are given as a HTRF emission ratio (620/520*10,000), are normalised to 10 µM HU-308 as a control and averaged (mean ± SEM), across n=3.

	Agonist stimulation of HEK293TR cells expressing CB_1R with reference and novel ligands (percentage of control 10 μM HU-210)							
	HU-210	HU-308	AEA	2-AG	SR-144,528	005	009	025
pEC_{50}	9.1 ± 2.0	No fit	5.7 ± 0.8	5.1 ± 0.2	No fit	5.3 ± 0.4	No fit	7.9 ± 1.0
E_{max} (%)	137.5 ± 14.0	ND	104.1 ± 12.3	80.4 ± 6.3	ND	31.5 ± 6.2	-13.4 ± 0.7	12.9 ± 6.4
	Agonist stimulation of HEK293TR cells expressing CB_2R with reference and novel ligands (percentage of control 10 μM HU-308)							
	HU-210	HU-308	AEA	2-AG	SR-144,528	005	009	025
pEC_{50}	8.6 ± 0.4	7.4 ± 0.1	5.3 ± 0.7	4.8 ± 0.4	9.0 ± 1.2	6.7 ± 1.4	5.2 ± 0.5	8.5 ± 0.7
E_{max} (%)	148.2 ± 25.8	133.2 ± 4.5	49.2 ± 0.7	105.0 ± 2.2	-16.7 ± 11.5	27.0 ± 4.1	-21.0 ± 12.8	29.1 ± 2.7

Table 7: **Summary table for data extracted from diffusion-enhanced resonance energy transfer (DERET) assays carried out on HEK293TR cells expressing cannabinoid receptor-1 (CB_1R) and cannabinoid receptor-2 (CB_2R).** Reference compounds include synthetic agonists HU-210 and HU-308, an inverse agonist SR-144,528 and two endogenous agonists including anandamide (AEA) and 2-arachidonoylglycerol (2-AG). Three novel compounds were also tested against CB_1R and CB_2R including compounds 005, 009 and 025. Extracted data include the half maximal effective concentration as a negative logarithmic value (log[EC_{50}]; pEC_{50}) and the maximum response as an indicator of compound efficacy (E_{max}) relative to the maximal response of 10 μM HU-210 for CB_1R and 10 μM HU-308 for CB_2R. Data are normalised and averaged (mean ± SEM) across n=3.

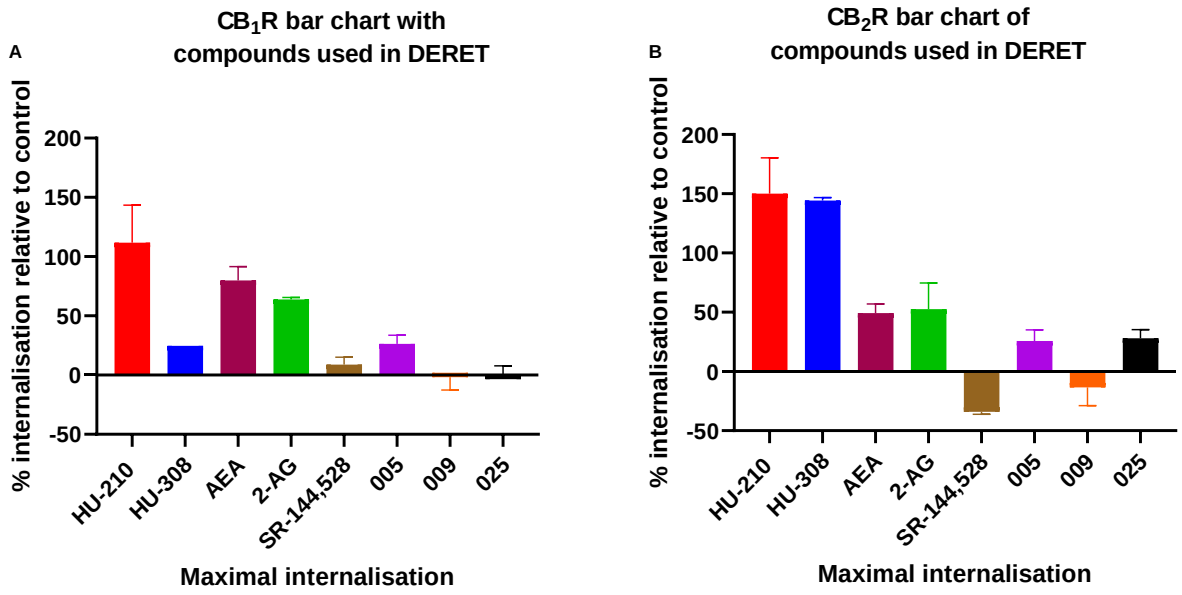

Figure 18: **Bar chart comparing the maximum degree of cannabinoid receptor-1 (CB_1R) and cannabinoid receptor-2 (CB_2R) internalisation triggered by agonist stimulation relative to the reference compound, in a diffusion-enhanced resonance energy transfer (DERET) assay.** Reference compounds include 10μM HU-210 and HU-308 as positive controls, 100μM anandamide (AEA) and 2-arachidonoylglycerol (2-AG), and 1μM SR-144,528. Novel ligands include 100μM compound 005 and 025 and 33μM compound 009. **(A)** Bar chart comparing agonist-induced internalisation at CB_1R. **(B)** Bar chart comparing agonist-induced internalisation at CB_2R. Data are given as a percentage (%) response relative to the maximal response of 10μM HU-210 for CB_1R and 10μM HU-308 for CB_2R. Data are normalised and averaged (mean ± SEM) from n=3, using the highest concentration of compound used.

DERET assays for SNAP-tagged CB_1R and CB_2R expressed in HEK293-TR cells allowed us to better understand the pharmacological profile of the reference and novel ligands and further allowed us to consider β-arrestin function and resulting receptor internalisation following agonist stimulation. For all compounds, the FRET signal increased over the course of the assay, with end readings taken to determine compound potency values (pEC_{50}). The use of the synthetic agonist HU-308 saw an absence of FRET signal at CB_1R (figure 16), but a robust agonist response at CB_2R (figure 17).

HU-210 stimulated an agonist response at both receptors and was used as a reference agonist from which to compare the agonist response of the novel compounds at CB_1R. HU-308 was the reference agonist for CB_2R. Sometimes the maximal response of the reference compounds was over 100% which was likely the result of variability in the assay. No response was seen following stimulation with SR-144,528 at either receptor.

The agonist responses brought about by the two endogenous agonists AEA and 2-AG were fairly similar between CB_1R and CB_2R, although the maximum FRET response of 2-AG at CB_2R was higher than that at CB_1R (figure 18). For the novel compounds, compound 005 had a fairly similar agonist response at both CB_1R and CB_2R, but the dose-response curve appears to be left-shifted at CB_2R compared to CB_1R, the same scenario was observed for compound 025 (figures 16 and 17). A fuller response was also seen with compound 009 at CB_2R compared to CB_1R, yet this compound appears to cause a decrease in signal as opposed to an increase which was seen with compounds 005 and 025.

5.3 Discussion

In order to better characterise the reference and novel ligands at CB_1R and CB_2R, we studied receptor internalisation using confocal microscopy and DERET assays. Confocal microscopy involved stimulating the CB_2R labelled with a GFP tag for 1 hour at 37° C, before fixing. In contrast, the DERET assays studied both CB_1R and CB_2R internalisation, by stimulating SNAP-tagged CB_1R and CB_2R expressed in HEK293-TR cells which were previously terbium labelled (SNAP-Lumi4-Tb).

Confocal microscopy failed to substantially highlight CB_2R internalisation following stimulation with either the reference compounds (HU-308 and SR-144,528) or the novel ligands (compounds 005, 009 and 025) at any concentration, compared with the buffer control. That said, a small difference in receptor internalisation may be seen in cells treated with HU-308 and 005, but this was not sufficient to warrant analysis. This is because GFP staining was somewhat sporadic, and the cells appeared to exhibit receptor internalisation even in the absence of any agonist. Sporadic receptor internalisation, particularly at the cannabinoid receptors, is likely the result of constitutive activity, which is apparent among GPCRs (Schmidt *et al.,* 2020; Teitler *et al.,* 2002). Constitutive activity causes receptor activation and hence internalisation, without formal receptor activation through agonist stimulation.

Using confocal microscopy, constitutive activity is reflected by the presence of granules of internalised receptors in the absence of agonist (Slice *et al.,* 1998). In buffer-treated cells, we observed granules of internalised receptor, the abundance of which was sometimes higher than in agonist-treated cells, suggesting a high amount of constitutive activity in CB_2Rs, which aligns with the literature (Fong, 2014). The inconsistencies in GFP staining in agonist-treated cells is difficult to explain since the Hoechst staining of the live cell nuclei appeared to be homogenous across the wells. However, the constitutive activity of CB_2R and hence the rapidity of receptor

internalisation may mean that receptors are degraded within the 1 hour stimulation period, resulting in the degradation of the GFP tags and therefore the observed lack of signal despite Hoechst staining being consistent. It is also possible that by having a mixed population, GFP-CB_2R expression was considerably low. Future studies of receptor internalisation using confocal microscopy should involve time-course assays to more accurately map receptor internalisation and recycling back to the membrane over the course of an hour, rather than capturing receptor internalisation at a single time point after stimulation. We also should include CB_1Rs in future experiments, based on the agonist responses seen by the novel compounds with CB_1R cells expressing the Gi-CASE biosensors.

We continued to study cannabinoid receptor internalisation using DERET assays, and hypothesised that agonist-induced receptor internalisation would cause an increase in the FRET signal by reducing the quenching of the fluorescent terbium donor fluorophore attached to the N-terminus of the receptor via the SNAP tag (Levoye *et al.,* 2015). We expected agonist responses of both the reference and novel compounds to reflect previous functional assays since full agonists may more strongly induce receptor internalisation, and better reduce terbium quenching versus partial agonists. In contrast, inverse agonists may bind the receptor but potentially inhibiting receptor internalisation, hence maintaining terbium quenching.

We found that HU-210, 2-AG and AEA increase the FRET signal, similarly as in the mG, β-arrestin and Gi-CASE assays, whereas the response of HU-308 is CB_2R-specific and consolidates it as a CB_2R-selective agonist (Hall *et al.,* 2022). The response for AEA and 2-AG was less pronounced considering that these are the endogenous ligands for CB_1R and CB_2R (Devane *et al.,* 1992; Mechoulam *et al.,* 1995), which may provide more information about the coupling of β-arrestin in response to AEA and 2-AG. Some reports suggest how 2-AG can elicit β-arrestin-dependent activation of signalling pathways (Delgado-Peraza *et al.* 2016; Ibsen *et al.,* 2019), which may account for how the 2-AG response decays over time, which is also seen in the mG and β-arrestin recruitment assays (figure 10). 2-AG metabolism could also reduce its effectiveness in causing receptor internalisation over the 60-minute assay period.

The graphs suggest compound 025 is more potent at causing CB_2R internalisation compared to CB_1R, however, the fitted data in table 7 suggests otherwise due to large errors associated with the data fitting. Internalisation was reduced following stimulation with SR-144,528 and compound 009 at CB_2R, indicative of their inverse agonism, but the compound 009 response was diminished in CB_1R. Compound 005 appeared to

cause internalisation at both CB_1R and CB_2R. Interestingly, SR-144,528 caused a small degree of internalisation at CB_1R, and complements the slight increase in BRET signal seen at CB_1R in the Gi-CASE assays relative to the HU-210 positive control (figure 12 and 13), the reasons for which are unclear since SR-144,528 is a CB_2R inverse agonist (Bouaboula *et al.,* 1999).

5.4 Conclusions

Confocal microscopy elucidated constitutive activity at CB_1Rs and CB_2Rs but did not allow us to gain insights into the novel compounds of interest. However, the results of the DERET assays consolidated the mechanisms of action of the novel compounds by reflecting our findings from previous functional assays, suggesting that compound 005 is an agonist at CB_1R and CB_2R, while compound 025 could be more selective for CB_2R, despite the errors with data fitting. Compound 009 is an inverse agonist, which is more selective for CB_2R compared to CB_1R.

Chapter 6: Developing a novel membrane-based biosensor assay via G protein lipidation.

6.1 Introduction

After completing our investigation into biased signalling and finding that the novel and reference compounds are unbiased, we tried to develop a membrane-based biosensor assay for the future screening of novel hits at the cannabinoid receptors, which could be hopefully applied to other GPCRs. The assay involves attaching lipid groups to the to specific amino acid residues of the G protein, thus increasing its affinity for the inner leaflet of the phospholipid bilayer. Proteins can interact with lipids via the attachment of fatty acids, sterols, isoprenoids, phospholipids, and glycosylphosphatidylinositol (GPI) anchors to the protein, increasing their hydrophobicity to readily interact with lipids (Resh, 2013).

For this side project, we lipidated the G protein by promoting cysteine palmitoylation and glycine myristoylation at the extreme N-terminus of the intracellular Gα subunit (Jiang *et al.,* 2018). Cysteine palmitoylation is a post-translational modification involving the addition of palmitic acid, a 16-carbon fatty acid, to cysteine residues at extreme N-terminus, requiring palmitoyl transferases (Hodson *et al.,* 2015). For most G proteins, the N-terminus amino acid sequence of the Gα subunit contains cysteine residues, readily enabling cysteine palmitoylation. In contrast, glycine myristoylation involves the addition of myristic acid, a 14-carbon fatty acid, to glycine residues immediately right of an initiating methionine at the start of an amino acid sequence. The methionine is typically cleaved prior to myristoylation using methionine aminopeptidase, exposing the glycine to myristoylation (Wright *et al.,* 2010). Myristoylation is favoured when serine and lysine are the sixth and seventh amino acid residues inwards from the N-terminus (Wright *et al.,* 2010). Therefore, myristoylation should happen when the N-terminus of a given amino acid is as follows: methionine-glycine-X-X-X-serine-lysine (M-G-X-X-X-S-K, X is a non-polar amino acid) (Zhang *et al.,* 2021). In this project, we tried to enhance cysteine palmitoylation and glycine myristoylation by substituting numerous amino acid residues at the N-terminus to promote G protein lipidation with the plasma membrane to create a membrane-based assay of functional G protein activity.

HEK293TR cells expressing CB_1R, truncated (91-472) CB_1R and CB_2R with the Gi-CASE plasmid developed previously (Schihada *et al.,* 2021). The Gi-CASE and Gs-CASE plasmids were changed such that $G\alpha_i$ and $G\alpha_s$ proteins had the N-terminus sequence MGCCCSK (methionine-glycine-cysteine-cysteine-cysteine-serine-lysine) to maximise the extent of glycine myristoylation as well as enhance cysteine palmitoylation. The Gq-CASE plasmid was also modified with the sequence MGLESSK (methionine-glycine-leucine-glutamine-serine-serine-lysine) so that $G\alpha_q$ proteins would

be targeted for myristoylation. The sequence contains two cysteine residues downstream of the MGXXXSK motif, suggesting that palmitoylation readily happens to the N-terminus of this protein (Marrari *et al.,* 2007).

Creating a second lipid anchor was considered by targeting the C-terminus of the Gγ portion of the G protein. However, the C-terminus of Gγ often contains a CaaX motif (Noguera-Salvà *et al.,* 2017), which includes cysteine, two aliphatic amino acids, and a specific amino acid (Marshal, 1993) to enable cysteine prenylation. Cysteine prenylation involves covalently attaching farnesyl or geranylgeranyl isoprenoids to the cysteine based on the identity of the final specific amino acid (Palsuledesai & Distefano, 2015). This suggests that the Gγ C-terminus can be lipidated without intervention. A summary of the alterations carried out at $G\alpha_i$, $G\alpha_s$ and $G\alpha_q$ is given in table 8.

We first created stable cell lines of full-length CB_1Rs, truncated (91-472) CB_1Rs and full-length CB_2Rs with the modified $G\alpha_i$, $G\alpha_s$ and $G\alpha_q$ plasmids, before generating membrane batches of the cells. As preliminary experiments, cell membranes were then stimulated with HU-210, HU-308, AEA, 2-AG, rimonabant and SR-144,528, as well as the three novel compound (n=1). We later transiently transfected the plasmids into whole cells expressing CB_1R and CB_2R and stimulated with HU-210, HU-308 and SR-144,528 (n=1). We hypothesised that agonist responses would be similar to those recorded in our previous Gi-CASE experiments involving whole cells, indicating the possibility to miniaturise the Gi-CASE assay to study functional G protein activity.

G protein subunit	Original N-termini sequence	Existing lipid modifications	New N-termini sequence	New lipid modifications
α_i	M**G**C**C**TL**S**AEDKAAVERSKMID-	Palmitoylation Myristoylation	M**G**C**C**C**S**K […]	Triple palmitoylation Myristoylation unchanged
α_s	MGCLGNSKTEDQRNEEDAQR-	Palmitoylation only		Triple palmitoylation Myristoylation
α_q	MTLESIMACCLSEEAKEARR-	Palmitoylation only	M**G**LESSK […]	Palmitoylation unchanged Myristoylation
	C-termini sequence			
γ_1	-KGIPEDKNPFKELKGGCVIS	Farnesylation	N/A	No change
γ_2	-TPVPASENPFREKKFFCAIL	Geranylgeranylation	N/A	No change

Table 8: **Table summarising the amino acid changes made to the N-termini of the alpha (α) subunit of G proteins, including stimulatory ($G\alpha_s$), inhibitory ($G\alpha_i$) and phospholipase C-coupled ($G\alpha_q$) proteins.** Amino acid changes were brought about by targeting novel G protein biosensors which encode each G protein. $G\alpha_i$ and $G\alpha_s$ proteins were altered to express the sequence MGCCCSK (methionine-glycine-cysteine-cysteine-cysteine-serine-lysine) to enable myristoylation and enhance existing palmitoylation, while $G\alpha_q$ proteins were altered to express the sequence MGLESSK (methionine-glycine-leucine-glutamine-serine-serine-lysine) to enable myristoylation since palmitoylation already occurs. The C-termini of the gamma (γ) subunit of the G protein was left unaltered since a CAAX (cysteine-aliphatic amino acid-aliphatic amino acid-X specific amino acid) motif is present on most phenotypes, which naturally leads to lipidation via the addition of prenyl groups in either farnesylation or geranylgeranylation.

6.2 Results

We tested batches of membrane preparations of cells stably expressing the modified biosensor, with various reference agonists including HU-210, HU-308, rimonabant and SR-144,528. We also tested the membranes with the novel compounds 005, 009 and 025. Agonist stimulation of membrane preparations of cells expressing CB_1R, truncated CB_1R and CB_2R with the lipidated Gi-, Gs- and Gq-CASE biosensors did not elicit any detectable BRET signal (n=1) with any of these compounds. It is not clear why this was the case, but it is possible that the lipidation modifications were not sufficient to securely hold the G proteins to the membrane once whole cells were made into membrane preparations. Since we saw no detectable signal at all, we did not consider repeating this assay using the same membrane batches.

Because we had well-characterised receptor binding and functional G protein activity using the original Gi-CASE biosensor, we instead transiently transfected whole cells expressing CB_1Rs and CB_2Rs with the modified Gi-CASE biosensor to compare agonist responses with those obtained previously. After culturing the cells for 48 hours, whole cells expressing CB_1R and the modified biosensor were stimulated with HU-210 and HU-308, and CB_2R cells expressing the modified biosensor were stimulated with HU-308 and SR-144,528. We found that HU-210 caused a dose-dependent decrease in the BRET signal whereas HU-308 appears to cause an increase in the BRET signal, which was more robust at CB_2R compared to CB_1R (figure 19) (n=1). Dose-response curves were normalised relative to 10 µM HU-210 for CB_1Rs or 10 µM HU-308 for CB_2Rs. No response was seen with SR-144,528 at CB_2R. It is important to note that the results of this experiment, which are summarised in table 9, are only from one experiment as a preliminary study into membrane-based assays.

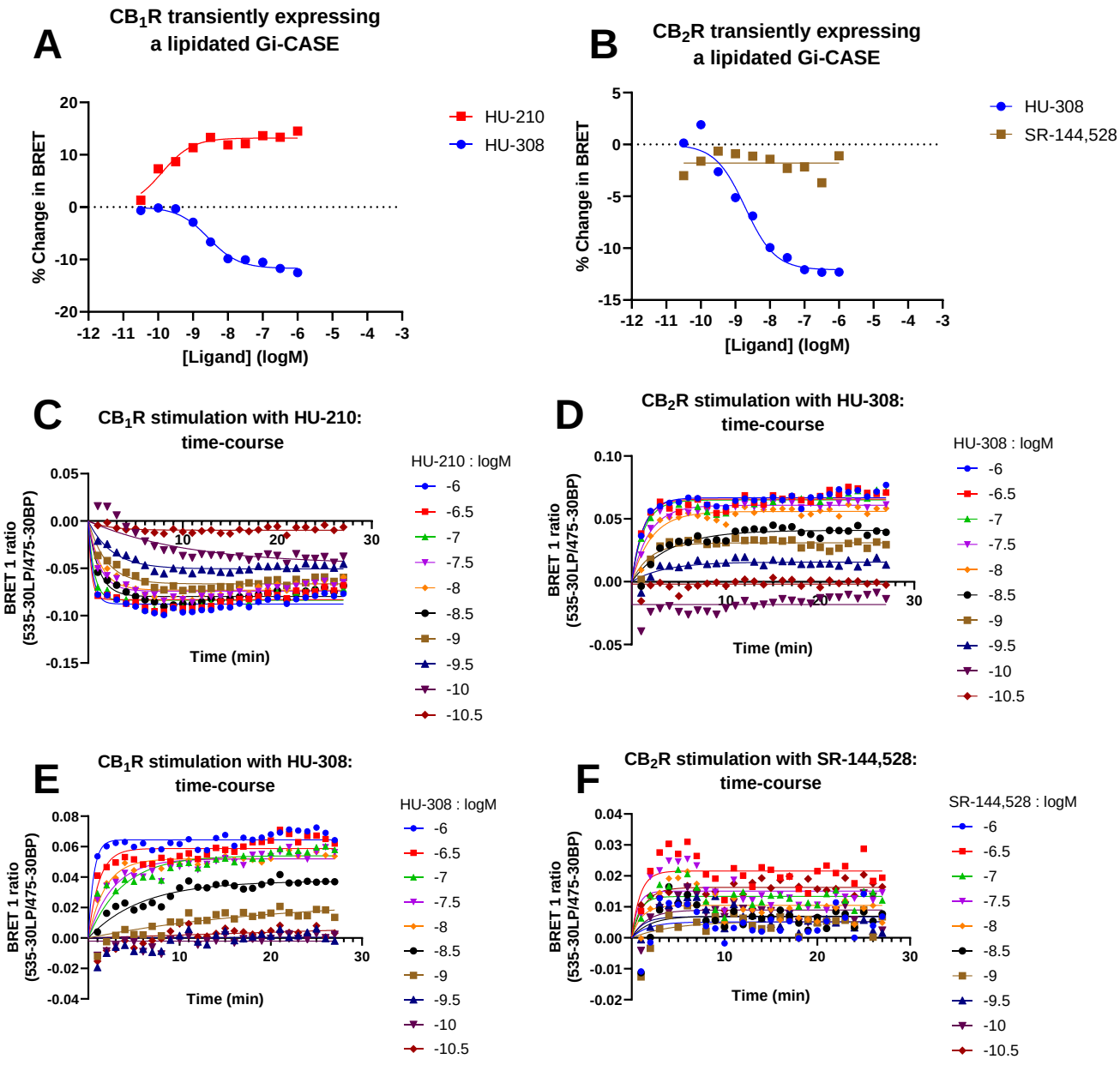

Figure 19: **Agonist stimulation of HEK293TR cells expressing cannabinoid receptor-1 (CB_1R) and cannabinoid receptor-2 (CB_2R), transiently expressing a novel G protein activity biosensor (Gi-CASE). (A)** Dose-response of CB_1R stimulated with synthetic agonists HU-210 and HU-308. Data are normalised to 10 µM HU-210. **(B)** Dose-response of CB_2R stimulated with HU-308 and an inverse agonist SR-144,528, data are normalised to 10 µM HU-308. **(C)** Time-course of CB_1R stimulation with HU-210. **(D)** Time-course of CB_2R stimulation with HU-308. **(E)** Time-course of CB_1R stimulation with HU-308. **(F)** Time-course of CB_2R stimulation with SR-144,528. Data are given as a ratio of 535-30 long-pass (LP)/475-30 broad pass (BP), using the final five readings from n=1 (mean of readings ± SEM).

	CB_1R		CB_2R	
	HU-210	HU-308	HU-308	SR-144,528
pEC_{50}	9.9	8.6	-8.7	No fit
E_{max}	13.2	-11.7	-12.1	ND

Table 9: **Summary table of agonist responses elicited by reference compounds HU-210, HU-308 and SR-144,528 when tested against HEK293TR cells expressing cannabinoid receptor-1 (CB_1R) and cannabinoid receptor-2 (CB_2R), transiently expressing a lipidated biosensor of G protein activity.** Half effective inhibitory concentration (EC_{50}) is given as a logarithmic value (log[EC_{50}]; pEC_{50}) and the maximal response (E_{max}) is also given. Data are a normalised to 10 µM HU-210 for CB_1Rs and 10 µM HU-308 for CB_2Rs average of the final five readings from n=1.

6.3 Discussion

By creating membrane-tethered yet fluorescently active $G\alpha_i$, $G\alpha_s$ and $G\alpha_q$ proteins, this could create a reliable and high-throughput means to screen novel hits for cannabinoid receptors and other GPCRs without using whole cells, the culturing of which can be laborious and inefficient, with more variability in receptor expression compared to using membrane batches. The [^{35}S]GTPγS assay is an example of a membrane-based assay to study G protein activity for GPCRs coupling through inhibitory G ($G\alpha_i$) proteins, which may be favourable for these GPCRs because $G\alpha_i$ may readily undergo lipidation (Vögler *et al.,* 2008). This assay is less feasible in for $G\alpha_s$-coupled GPCRs, whose G protein may be less strongly associated with the lipid membrane and is less abundant (Milligan, 1988). In addition, the assay uses radioactive materials and requires cell membrane permeabilization or alternatively preparing membranes, but does not allow for the real-time study of G protein activation (Harrison & Traynor, 2003). As a result, we attempted to create a membrane-based assay of G protein activation by lipidating a fluorescently active G protein, using Gi-CASE plasmids created previously (Schihada *et al.,* 2021).

We transfected the modified Gi-CASE, Gs-CASE and Gq-CASE biosensors into CB_1R, truncated (91-472) CB_1R- and CB_2R-expressing HEK293TR cells, before culturing and eventually harvesting into membranes. Initially, we stimulated the receptor membranes with a series of reference compounds (HU-210, HU-308, AEA, 2-AG and SR-144,528) and the novel compounds (005, 009 and 025), but we failed to observe any BRET signal at all. It is not clear why this was the case.

We then transiently transfected whole cells expressing full-length CB_1R and CB_2R with the modified Gi-CASE plasmid and stimulated the cells with HU-210, HU-308 and SR-144,528. An agonist response was seen upon treatment with HU-210 based on the observed decrease in BRET. These findings were also seen in whole CB_1R and CB_2R cells expressing the biosensor. However, HU-308 stimulation appears to lead to an increase in BRET signal at CB_1R and CB_2R, indicative of receptor binding but no G protein dissociation, suggesting it as an inverse agonist and contrasts it as a CB_2R-selective agonist (Hall *et al.,* 2022). A difference in response was also observed with SR-144,528 which is typically a CB_2R inverse agonist (Bouaboula *et al.,* 1999). The reason for the difference in HU-308 and SR-144,528 response is not clear, but continued experimentation would enable us to better characterise this and to optimise this assay as a screening method for novel agonists.

While we did not achieve a response in our initial experiments on the membranes, we did observe a response when the cells transiently expressed the modified Gi-CASE plasmid, suggesting that tethering the G protein to the membrane does not considerably affect G protein activation and dissociation. For example, it was suggested that anchoring the G protein to the membrane prevents its dissociation and could hence account for observing no response. It is also possible that the cells were not stably expressing the G protein when they were harvested and that cell centrifugation damaged the cell membranes, clarifying the importance of repeating and optimising these assays.

6.4 Conclusions

In conclusion, the membrane-based biosensor assay is still in its infancy, and we need to understand why the G protein appears to be lost when cell membranes are prepared. Nevertheless, observing a response in whole cells transiently transfected with the modified G protein biosensor is promising, despite some differences in agonist responses. Collectively, continued assay optimisation and troubleshooting will enable us to develop a robust and reliable membrane-based biosensor assay for identifying novel agonists based on G protein activation.

Chapter Seven: General discussion

In this investigation, we considered whether stimulating the cannabinoid receptors with novel and known agonists would cause the preferential activation of G protein or β-arrestin signalling pathways. This project identified that the novel compounds, taken froward from *in silico* docking, can bind both CB_1R and CB_2R, but are more selective for CB_2R. This observation was seen following the competition binding studies which showed that all three compounds exhibited little binding at CB_1R compared to higher affinity binding at CB_2R. These initial experiments first involved determining the dissociation rate constant (K_d) of the fluorescent tracer D77 using saturation binding experiments and were followed by competition binding experiments, to characterise unlabelled compound binding in membranes expressing CB_1R and CB_2R.

In addition, we did not conclude that the novel compounds were biased at the cannabinoid receptors, based on the results of the functional assays. Functional assays involved running mini-G (mG) and β-arrestin recruitment assays of CB_2R-expressing cells, using a range of reference compounds, including HU-308 as a known agonist. Agonist binding featured as an increase in BRET signal by inducing the recruitment of either the venus-tagged mG or β-arrestin proteins to the receptor, enabling resonance energy transfer between the donor-labelled receptor and acceptor-labelled mG or β-arrestin protein (Carpenter & Tate, 2016). The novel ligands failed to show a difference in BRET response and pEC_{50} values in either mG or β-arrestin recruitment assay, suggesting they are unbiased ligands. The positive control HU-308 had a pEC_{50} value of 7.3 ± 0.1 and 7.1 ± 0.2 respectively, which is similar to the value of 7.29 ± 0.51, obtained by Soethoudt *et al.* using a [^{35}S]-GTPγS assay (Soethoudt *et al.,* 2017).

The mG and β-arrestin recruitment assays studied the effect of the endocannabinoids AEA and 2-AG. For AEA, the β-arrestin maximal response was 24% of the HU-308 reference, which was visibly lower compared to in the mG recruitment assay where its response was 54.9% of the reference agonist HU-308. However, AEA appeared to be more potent in the β-arrestin assay since the pEC_{50} was 7.2 compared to 6.3 in the mG assay. A similar response was observed with 2-AG, whereby the β-arrestin response was more potent (pEC_{50} 5.8 vs. 5.2), even though the maximal responses was nearly the same. Soethoudt *et al.* (2017) found that AEA is relatively balanced in its preference for either the G protein or the β-arrestin protein, while 2-AG seems to be biased towards β-arrestin recruitment (Soethoudt *et al.,* 2017). However, our observations seemed to suggest that AEA favours mG recruitment based on the maximal response, more so than β-arrestin.

Gi-CASE assays of functional G protein activity then proceeded the mG and β-arrestin recruitment assays. Gi-CASE assays were performed in cells expressing CB_1R, truncated CB_1R and CB_2R to study how G protein activation was affected by agonist stimulation and to see if truncation of the CB_1R receptor affected ligand responses. The Gi-CASE biosensor was an appropriate biosensor to study the functional activity of $G\alpha_i$-coupled receptors, although the Gs-CASE biosensor would be required for studying $G\alpha_s$-coupled GPCRs including the β_2-adrenoceptor (Wenzel-Seifert & Seifert, 2000). The assay was first characterised using reference compounds including HU-210, HU-308, rimonabant and SR-144,528, before including the three novel compounds. The pEC_{50} values for HU-210 at truncated and full-length CB_1Rs (8.8 ± 0.1 and 9.2 ± 0.3, respectively) was higher than the pEC_{50} of 8.3 seen in rat cerebellar membranes previously (Salo *et al.,* 2006), and is higher than that observed when HU-210 is tested against CB_2Rs in our assay (pEC_{50} of 8.2 ± 0.4). HU-308 was the positive control used in assays involving CB_2Rs, which in the mG and β-arrestin assay had a pEC_{50} of 7.3 ± 0.1 and 7.1 ± 0.2, respectively. These values are lower than those obtained in the Gi-CASE membrane assay (pEC_{50} of 7.9 ± 0.1), and lower than the pEC_{50} value of 7.46 ± 0.15, derived from the same intact cell assay (Scott-Dennis *et al.,* 2023).

Rimonabant and SR-144,528, since they are inverse agonists, did not elicit an agonist response in either the mG or β-arrestin assays. However, these two compounds were included in the Gi-CASE assays in order to study their effect on G protein activation. In truncated and full-length CB_1Rs, rimonabant, which binds more strongly at CB_1R compared to CB_2R (pKi of 8.5 versus 6; unpublished data from Veprintsev lab), had a pEC_{50} of 7.2 ± 0.4 and 7.1 ± 0.4, respectively, values of which are similar to those seen in intact-cells as described in the original assay (Schihada *et al.,* 2021). In contrast, SR-144,528 was used as a CB_2R-specific inverse agonist (pK_i of 8.7 at CB_2R versus 6.7 at CB_1R), which in the Gi-CASE assay had a pEC_{50} values of 7.5 ± 0.2 when first characterising the assay, which is similar to values of 7.8 and 7.7 obtained in [^{35}S]-GTPγS and cAMP assays previously (Soethoudt *et al.,* 2017)

Gi-CASE assays included CB_1Rs, and whilst none of the novel compounds appeared to bind the receptor in the initial binding experiments, the Gi-CASE assays showed that the novel compounds affected G protein activity and thus bound to the receptor. Differential binding at CB_1R versus CB_2R could reflect differences in G protein coupling efficiency at CB_1R compared to CB_2R but could also indicate that the novel compounds exhibit allosteric activity and bind to different binding sites on CB_1R compared with CB_2R, which complements recent reports for CB_1R (Laprairie *et al.,* 2017; Shao *et al.,* 2019).

Differences in compound binding could also be due to differences in compound solubility between the assays. For example, the compounds in the competition binding experiments were diluted in 100% DMSO before adding to the assay plate, whereas their addition in the Gi-CASE assays involved diluting in DMSO as well as in assay buffer (1/10) before adding to the assay plate. Therefore, diluting in assay buffer may be an important intermediary step, which may have some effect on final assay concentrations. DMSO may also be damaging for cells and tissues despite its widespread use in pharmacological studies (Verheijen *et al.,* 2019), which may account for the absence of binding in the CB_1R membranes compared to whole-cell experiments.

The Gi-CASE functional assay indicated that compounds 005 appears to be a full agonist for CB_1R and CB_2R, whereas compound 025 appears to be more selective for CB_2R. Interestingly, compound 025 appears to elicit a more potent agonist response at CB_2R compared to at CB_1R, where the pEC_{50} at CB_2R is 8.6, versus 6.9 at CB_1R. However, the difference in the percentage decrease in BRET signal between CB_1R and CB_2R is only marginally different. In contrast, compound 009 may be an inverse agonist, since competition binding experiments with the fluorescent tracer D77 at CB_2R indicated binding to the same binding site as the other compounds, but this compound causes G protein accumulation and the continued excitation of the acceptor in the Gi-CASE assay.

Our investigation into biased signalling only used HEK293TR cells, which may have prevented us from identifying bias as oppose to if a range of cell types had been used. Phenotypic and cell-specific differences in drug response following stimulation, which is reported to affect the treatment of tumour cells for example, (Roots *et al.,* 2007; Niepel *et al.,* 2019), may result in different abundancies of G protein and β-arrestin protein that could cause systems bias between cell types. Using different cell types is an important consideration for the future screening of these novel compounds when detecting bias.

Drug selectivity, at least in terms of functional responses, could be affected by differences in CB_1R and CB_2R expression between the cells (Tirona *et al.,* 2011). In our experiments, we did not standardise receptor expression, which prevents the proper comparison of the novel compounds' potencies. However, the assays described in this investigation are designed to avoid the problems of signal amplification where receptor number becomes an issue. For example, the observation that compound 025 is more selective for CB_2R compared to CB_1R, and that the response of compound 005 as a

weak partial is agonist, may differ when receptor expression is increased as this would not only increase the number of binding sites but also effector proteins coupled to the receptor, enabling a higher signalling response signal amplification.

Functional assays to study G protein activation and signalling bias were then complemented with studies into receptor internalisation to elucidate β-arrestin activity and to gain a fuller pharmacological profile of the compounds tested. Confocal microscopy was applied to study GFP-labelled CB_2R cells, which were fixed after stimulation for 1 hour of stimulation with HU-308, AEA, 2-AG, SR-144,528 and compounds 005, 009 and 025. Agonist activity should cause a dose-dependent increase in receptor internalisation (Wu *et al.,* 2008), the opposite of which should be observed with inverse agonists, which in this case included compound 009 and SR-144,528. Receptor internalisation is indicated by the appearance of granules in the cytosol as vesicles containing the receptor, and there should be minimal GFP-labelled receptors outlining the cell (Slice *et al.,* 1998). However, we failed to reliably observe this, and agonist-induced receptor internalisation was often similar to cells treated with our DMSO-containing buffer (vehicle control). It is most plausible that CB_2R constitutive activity accounts for our findings, and it is accepted that the cannabinoid receptors are highly constitutively active (Fong, 2014), suggesting the need for time-course assays to study internalisation at shorter time intervals. In addition, the assay set-up included half-log dilutions of the reference and novel compounds, meaning that we had a small window from which to study receptor internalisation, compared to using log dilutions in future. It is also important to study receptor internalisation at CB_1Rs given the Gi-CASE response observed despite an apparent lack of binding in the competition binding experiments.

DERET assays were also used to study receptor internalisation and we found a similar inverse agonist response in compound 009 and similar agonist responses for compounds 005 and 025. The positive control for CB_1Rs was HU-210, with a pEC_{50} of 9.1 ± 2.0, and HU-308 was the positive control for CB_2Rs and had a pEC_{50} value of 7.4 ± 0.1. While the HU-308 pEC_{50} value is similar to those obtained in the other functional assays of this investigation and the literature, the pEC_{50} of HU-210 seems to be higher with greater error. In addition, the responses of the endogenous compounds AEA and 2-AG also deviates in the DERET assay compared to the other functional assays in this investigation. For AEA, we obtained pEC_{50} values of 5.7 ± 0.8 and 5.3 ± 0.7 for CB_1R and CB_2R respectively, and 5.1 ± 0.2 and 4.8 ± 0.4 for 2-AG at CB_1R and CB_2R, respectively. By comparison, the Gi-CASE assay obtained pEC_{50} values of 7.0 ± 0.1 and 6.4 ± 0.3 for AEA at CB_1R and CB_2R, respectively, and 5.8 ± 0.2 and 6.1 ± 0.1 for

2-AG at CB_1R and CB_2R, respectively. The reason for the lower pEC_{50} values is unclear but could be based on the framework of the DERET assay which involves receptor internalisation over a longer time period versus G protein activation in the Gi-CASE assay (Levoye *et al.,* 2015). These differences in pEC_{50} values between the assays might be partly explained by the metabolism of the endocannabinoids (Basavarajappa, 2007). Furthermore, the cells were washed multiple times with PBS before incubating with the fluorescent label, which caused a number of cells to be removed from the plate and required the assay to be optimised. As a result, the DERET assay could be repeated in future for better reliability and troubleshooting, which may help to obtain drug responses in-line with our previous experiments.

As a side project, we attempted to miniaturise the whole-cell Gi-CASE assay by creating a membrane-based assay with a lipidated and fluorescently active G protein. Miniaturising the Gi-CASE assay would allow the high-throughput screening of novel agonists by considering G protein activation in membranes rather than whole cells. The assay requires troubleshooting and optimisation because existing data only comes from preliminary experiments, but initial experiments in cells transiently transfected with the biosensor show some response.

Discovering novel agonists for the cannabinoid receptors, especially CB_2R, is valuable due to the importance of the endocannabinoid system in multiple physiological functions and the significance of these receptor in a number of pathological states. When developing novel drugs to target the receptors, deriving compounds which exhibit a level of bias for the cannabinoid receptors may enable these novel drugs to have fewer side effects by being more pathway-specific. This investigation studied the effect of three novel compounds from *in silico* docking but did not find any of them to be biased. However, the investigation suggests that the novel compounds are more selective for CB_2R than CB_1R, that two of these compounds appear to be partial agonists, while one appears to be an inverse agonist. Continued pre-clinical profiling of these compounds will better elucidate their selectivity for CB_2R, and it may also be worthwhile testing these compounds against other cannabinoid-like receptors.

Acknowledgements

I would like to thank my supervisors Professor Dmitry Veprintsev, Dr David Sykes and Dr Eline Koers for their continued support and expertise throughout this project. I would also like to thank the current and previous PhD students and post-doctoral researchers in the Veprintsev lab and the broader cell signalling community at the University of Nottingham, for their help and advice for which I am very grateful.

References

Ahn S, Nelson CD, Garrison TR, Miller WE, Lefkowitz RJ. (2003). Desensitization, internalization, and signaling functions of beta-arrestins demonstrated by RNA interference*. Proc Natl Acad Sci U S A*. **100**(4):1740-4.

Aittaleb M, Boguth CA, Tesmer JJ. (2010). Structure and function of heterotrimeric G protein-regulated Rho guanine nucleotide exchange factors. *Mol Pharmacol*. **77**(2):111-25.

An D, Peigneur S, Hendrickx LA, Tytgat J. (2020). Targeting Cannabinoid Receptors: Current Status and Prospects of Natural Products. *Int J Mol Sci.* **21**(14):5064.

Banerjee AA, Mahale SD. (2015). Role of the Extracellular and Intracellular Loops of Follicle-Stimulating Hormone Receptor in Its Function. Front Endocrinol (Lausanne). **6**:110.

Basavarajappa BS. (2007). Critical enzymes involved in endocannabinoid metabolism. *Protein Pept Lett*. **14**(3):237-46.

Berger M, Amminger GP, McGregor IS. (2022). Medicinal cannabis for the treatment of anxiety disorders. *Aust J Gen Pract*. **51**(8):586-592.

Blanton H, Armin S, Muenster S, Abood M, Benamar K. (2022). Contribution of G Protein-Coupled Receptor 55 to Periaqueductal Gray-Mediated Antinociception in the Inflammatory Pain. *Cannabis Cannabinoid Res*. **7**(3):274-278.

Blum K, Morgan J, Cadet JL, Baron D, Carney PR, Khalsa J, Badgaiyan RD, Gold MS. (2021). Psychoactive Drugs Like Cannabis -Induce Hypodopaminergic Anhedonia and Neuropsychological Dysfunction in Humans: Putative Induction of Dopamine Homeostasis via Coupling of Genetic Addiction Risk Severity (GARS) testing and Precision Pro-dopamine Regulation (KB220). *Neurology (ECronicon)*. **13**(4):86-92.

Bouaboula M, Desnoyer N, Carayon P, Combes T, Casellas P. (1999) Gi protein modulation induced by a selective inverse agonist for the peripheral cannabinoid receptor CB2: implication for intracellular signalization cross-regulation. *Mol Pharmacol*. **55**(3):473-80.

Boyd ST, Fremming BA. (2005). Rimonabant--a selective CB1 antagonist. *Ann Pharmacother*. **39**(4):684-90.

Brini M, Calì T, Ottolini D, Carafoli E. (2014). Neuronal calcium signaling: function and dysfunction. *Cell Mol Life Sci*. **71**(15):2787-814.

Carpenter B, Tate CG. (2016). Engineering a minimal G protein to facilitate crystallisation of G protein-coupled receptors in their active conformation. *Protein Eng Des Sel*. **29**(12):583-594.

Casey SL, Mitchell VA, Sokolaj EE, Winters BL, Vaughan CW. (2022). Intrathecal Actions of the Cannabis Constituents Δ(9)-Tetrahydrocannabinol and Cannabidiol in a Mouse Neuropathic Pain Model. *Int J Mol Sci*. **23**(15):8649.

Chaudhary PK, Kim S. (2021). The GRKs Reactome: Role in Cell Biology and Pathology*. Int J Mol Sci*. **22**(7):3375.

Chen CZ, Southall N, Xiao J, Marugan JJ, Ferrer M, Hu X, Jones RE, Feng S, Agoulnik IU, Zheng W, Agoulnik AI. (2013). Identification of small-molecule agonists of human relaxin family receptor 1 (RXFP1) by using a homogenous cell-based cAMP assay.*Biomol Screen.* **18**(6):670-7.

Coffa S, Breitman M, Spiller BW, Gurevich VV. (2011). A single mutation in arrestin-2 prevents ERK1/2 activation by reducing c-Raf1 binding. Biochemistry. **50**(32): 6951-8.

Costa AM, Russo F, Senn L, Ibatici D, Cannazza G, Biagini G. (2022). Antiseizure Effects of Cannabidiol Leading to Increased Peroxisome Proliferator-Activated Receptor Gamma Levels in the Hippocampal CA3 Subfield of Epileptic Rats. *Pharmaceuticals (Basel)*. **15**(5):495.

Dale NC, Johnstone EKM, White CW, Pfleger KDG. (2019) NanoBRET: The Bright Future of Proximity-Based Assays. *Front Bioeng Biotechnol*. **7**:56.

Davenport, A.P., Russell, F.D. (1996). Radioligand Binding Assays: Theory and Practice. In: Mather, S.J. (eds) Current Directions in Radiopharmaceutical Research and Development. Developments in Nuclear Medicine, vol 30. Springer, Dordrecht. https://doi.org/10.1007/978-94-009-1768-2_11

Delgado-Peraza F, Ahn KH, Nogueras-Ortiz C, Mungrue IN, Mackie K, Kendall DA, Yudowski GA. (2016). Mechanisms of Biased β-Arrestin-Mediated Signaling Downstream from the Cannabinoid 1 Receptor. *Mol Pharmacol*. **89**(6):618-29.

Devane WA, Hanus L, Breuer A, Pertwee RG, Stevenson LA, Griffin G, Gibson D, Mandelbaum A, Etinger A, Mechoulam R. (1992). Isolation and structure of a brain constituent that binds to the cannabinoid receptor. *Science*. **258**(5090):1946-9.

Du Y, Ren P, Wang Q, Jiang SK, Zhang M, Li JY, Wang LL, Guan DW. (2018). Cannabinoid 2 receptor attenuates inflammation during skin wound healing by inhibiting M1 macrophages rather than activating M2 macrophages. *J Inflamm (Lond).* **15**:25.

Fong TM, Heymsfield SB. (2009). Cannabinoid-1 receptor inverse agonists: current understanding of mechanism of action and unanswered questions. *Int J Obes (Lond).* **33**(9):947-55.

Fong TM. (2014). Constitutive activity in cannabinoid receptors. *Adv Pharmacol*. **70**:121-33.

Gilissen J, Geubelle P, Dupuis N, Laschet C, Pirotte B, Hanson J. (2015). Forskolin-free cAMP assay for Gi-coupled receptors. *Biochem Pharmacol*. **98**(3):381-91.

Gillis A, Christie MJ. (2021). Opioid overdose and tolerance: is the recruitment of β-arrestin to the μ-receptor involved? *Neuropsychopharmacol.* **46**:2226–2227.

Guerrero-Alba R, Barragán-Iglesias P, González-Hernández A, Valdez-Moráles EE, Granados-Soto V, Condés-Lara M, Rodríguez MG, Marichal-Cancino BA. (2019). Some Prospective Alternatives for Treating Pain: The Endocannabinoid System and Its Putative Receptors GPR18 and GPR55. *Front Pharmacol.* **9**:1496.

Haider RS, Matthees ESF, Drube J, Reichel M, Zabel U, Inoue A, Chevigné A, Krasel C, Deupi X, Hoffmann C. (2022). β-arrestin1 and 2 exhibit distinct phosphorylation-dependent conformations when coupling to the same GPCR in living cells. *Nat Commun.* **13**(1):5638.

Hall S, Faridi S, Trivedi P, Sultana S, Ray B, Myers T, Euodia I, Vlatten D, Castonguay M, Zhou J, Kelly M, Lehmann C. (2022). Selective CB_2 Receptor Agonist, HU-308, Reduces Systemic Inflammation in Endotoxin Model of Pneumonia-Induced Acute Lung Injury. *Int J Mol Sci.* **23**(24):15857.

Hanus L, Breuer A, Tchilibon S, Shiloah S, Goldenberg D, Horowitz M, Pertwee RG, Ross RA, Mechoulam R, Fride E. (1999). HU-308: a specific agonist for CB(2), a peripheral cannabinoid receptor. *Proc Natl Acad Sci U S A*. **96**(25):14228-33.

Harrison C, Traynor JR. (2003). The [35S]GTPgammaS binding assay: approaches and applications in pharmacology. *Life Sci.* **4**(4):489-508.

He F, Ye ZY, Zhao LD, Yin BC, Ye BC. (2019). Probing exosome internalization pathways through confocal microscopy imaging. *Chem Commun (Camb).* **55**(93):14015-14018.

He Y, Jia H, Yang Q, Shan W, Chen X, Huang X, Liu T, Sun R. (2023). Specific Activation of CB2R Ameliorates Psoriasis-Like Skin Lesions by Inhibiting Inflammation and Oxidative Stress. *Inflammation*. Online ahead of print.

Hendrik Schmidt J, Perslev M, Bukowski L, Stoklund M, Herborg F, Herlo R, Lindegaard Madsen K. (2020). Constitutive internalization across therapeutically targeted GPCRs correlates with constitutive activity. *Basic Clin Pharmacol Toxicol*. 126 Suppl 6:116-121.

Hernández-Hernández E, García-Fuster MJ. (2022). Dose-Dependent Antidepressant-Like Effects of Cannabidiol in Aged Rats. *Front Pharmacol*. **13**:891842.

Heydenreich FM, Miljuš T, Jaussi R, Benoit R, Milić D, Veprintsev DB. (2017). High-throughput mutagenesis using a two-fragment PCR approach. *Sci Rep*. **7**(1):6787.

Hofer AM. (2012). Interactions between calcium and cAMP signaling. *Curr Med Chem.* **19**(34):5768-73.

Howlett AC. (2005). Cannabinoid receptor signaling. *Handb Exp Pharmacol*. (168):53-79.

Hu GM, Mai TL, Chen CM. (2017). Visualizing the GPCR Network: Classification and Evolution. *Sci Rep*. **7**(1):15495.

Ibsen MS, Finlay D, Patel M, Javitch JA, Glass M, Grimsey NL. (2019). Cannabinoid CB1 and CB2 Receptor-Mediated Arrestin Translocation: Species, Subtype, and Agonist-Dependence. *Front. Pharmacol.* **10**:350.

Jiang H, Zhang X, Chen X, Aramsangtienchai P, Tong Z, Lin H. (2018). Protein Lipidation: Occurrence, Mechanisms, Biological Functions, and Enabling Technologies. Chem Rev. **118**(3):919-988.

Kakkar R, Raju RV, Sharma RK. (1999). Calmodulin-dependent cyclic nucleotide phosphodiesterase (PDE1). *Cell Mol Life Sci*. **55**(8-9):1164-86.

Kamato D, Thach L, Bernard R, Chan V, Zheng W, Kaur H, Brimble M, Osman N, Little PJ. (2015). Structure, Function, Pharmacology, and Therapeutic Potential of the G Protein, Gα/q,11. *Front Cardiovasc Med.* **2**:14.

Karila L, Roux P, Rolland B, Benyamina A, Reynaud M, Aubin HJ, Lançon C. (2014). Acute and long-term effects of cannabis use: a review. *Curr Pharm Des.* **20**(25):4112-8.

Katritch V, Cherezov V, Stevens RC. (2013). Structure-function of the G protein-coupled receptor superfamily. *Annu Rev Pharmacol Toxicol*. **53**:531-56.

Kelly E. (2013). Efficacy and ligand bias at the μ-opioid receptor. *Br J Pharmacol*. **169**(7):1430-46.

Kenakin T, Christopoulos A. (2013). Signalling bias in new drug discovery: detection, quantification and therapeutic impact. *Nat Rev Drug Discov*. **12**(3):205-16.

Kenakin T. (2019). Biased Receptor Signaling in Drug Discovery. *Pharmacol Rev*. **71**(2):267-315.

Kim HR, Xu J, Maeda S, Duc NM, Ahn D, Du Y, Chung KY. (2020). Structural mechanism underlying primary and secondary coupling between GPCRs and the Gi/o family. *Nat Commun.* **11**(1):3160.

LaPrairie RB, Bagher AM, Kelly ME, Dupre DJ, Denovan-Wright EM. (2014). Type 1 Cannabinoid Receptor Ligands Display Functional Selectivity in a Cell Culture Model of Striatal Medium Spiny Projection Neurons. *J. Biol. Chem.* **289**:24845–24862

LaPrairie RB, Bagher AM, Kelly MEM, Denovan-Wright EM. (2015). Biased Type 1 Cannabinoid Receptor Signaling Influences Neuronal Viability in a Cell Culture Model of Huntington Disease. *Mol. Pharmacol.* **89**:364–375.

Laprairie RB, Kulkarni PM, Deschamps JR, Kelly MEM, Janero DR, Cascio MG, Stevenson LA, Pertwee RG, Kenakin TP, Denovan-Wright EM, Thakur GA. (2017). Enantiospecific Allosteric Modulation of Cannabinoid 1 Receptor. *ACS Chem Neurosci*. **8**(6):1188-1203.

Levoye A, Zwier JM, Jaracz-Ros A, Klipfel L, Cottet M, Maurel D, Bdioui S, Balabanian K, Prézeau L, Trinquet E, Durroux T, Bachelerie F. (2015). A Broad G Protein-Coupled Receptor Internalization Assay that Combines SNAP-Tag Labeling, Diffusion-Enhanced Resonance Energy Transfer, and a Highly Emissive Terbium Cryptate. *Front Endocrinol (Lausanne)*. **6**:167.

Liu QR, Aseer KR, Yao Q, Zhong X, Ghosh P, O'Connell JF, Egan JM. (2022). Anti-Inflammatory and Pro-Autophagy Effects of the Cannabinoid Receptor CB2R: Possibility of Modulation in Type 1 Diabetes. *Front Pharmacol*. **12**:809965.

Makriyannis A, Tian X, Guo J. (2005). How lipophilic cannabinergic ligands reach their receptor sites. *Prostaglandins Other Lipid Mediat*. **77**(1-4):210-218.

Mansoury M, Hamed M, Karmustaji R, Al Hannan F, Safrany ST. (2021). The edge effect: A global problem. The trouble with culturing cells in 96-well plates. *Biochem Biophys Rep*. **26**:100987.

Manzanares J, Julian M, Carrascosa A. (2006). Role of the cannabinoid system in pain control and therapeutic implications for the management of acute and chronic pain episodes. *Curr Neuropharmacol*. **4**(3):239-57.

Marrari Y, Crouthamel M, Irannejad R, Wedegaertner PB. (2007). Assembly and trafficking of heterotrimeric G proteins. *Biochemistry*. **46**(26):7665-77.

Marshall CJ. (1993). Protein prenylation: a mediator of protein-protein interactions. *Science.* **259**(5103):1865-6.

Milligan G. (1988). Techniques used in the identification and analysis of function of pertussis toxin-sensitive guanine nucleotide binding proteins. *Biochem J.* **255**(1):1-13.

Miyashita T. (2004). Confocal microscopy for intracellular co-localization of proteins. *Methods Mol Biol.* **261**:399-410.

Mohammad Nezhady MA, Rivera JC, Chemtob S. (2020). Location Bias as Emerging Paradigm in GPCR Biology and Drug Discovery. *iScience*. **23**(10):101643.

Mohan ML, Vasudevan NT, Gupta MK, Martelli EE, Naga Prasad SV. (2012). G-protein coupled receptor resensitization-appreciating the balancing act of receptor function. *Curr Mol Pharmacol*. PMID: 22697395.

Morcuende A, García-Gutiérrez MS, Tambaro S, Nieto E, Manzanares J, Femenia T. (2022). Immunomodulatory Role of CB2 Receptors in Emotional and Cognitive Disorders. *Front Psychiatry*. **13**:866052.

Mullard A. (2020). FDA approves first GPCR biased agonist. *Nat Rev Drug Discov.* **19**(10):659.

Muller C, Morales P, Reggio PH. (2019). Cannabinoid Ligands Targeting TRP Channels. *Front Mol Neurosci*. **11**:487.

Niepel M, Hafner M, Duan Q, Wang Z, Paull EO, Chung M, Lu X, Stuart JM, Golub TR, Subramanian A, (2017). Ma'ayan A, Sorger PK. Common and cell-type specific responses to anti-cancer drugs revealed by high throughput transcript profiling. *Nat Commun.* **8**(1):1186.

Ogura Y, Parsons WH, Kamat SS, Cravatt BF. (2016). A calcium-dependent acyltransferase that produces N-acyl phosphatidylethanolamines. *Nat Chem Biol*. **12**(9):669-71.

Ottani A, Giuliani D. (2001). Hu 210: a potent tool for investigations of the cannabinoid system. CNS Drug Rev. **7**(2):131-45.

Palsuledesai CC, Distefano MD. (2015). Protein prenylation: enzymes, therapeutics, and biotechnology applications. *ACS Chem Biol*. **10**(1):51-62.

Penumarti A, Abdel-Rahman AA. (2014). The novel endocannabinoid receptor GPR18 is expressed in the rostral ventrolateral medulla and exerts tonic restraining influence on blood pressure. *J Pharmacol Exp Ther*. **349**(1):29-38.

Pete DD, Narouze SN. (2021). Endocannabinoids: Anandamide and 2-Arachidonoylglycerol (2-AG). In: Narouze, S.N. (eds) Cannabinoids and Pain. Springer, Cham.

Porcu A, Melis M, Turecek R, Ullrich C, Mocci I, Bettler B, Gessa GL, Castelli MP. (2018). Rimonabant, a potent CB1 cannabinoid receptor antagonist, is a $G\alpha_{i/o}$ protein inhibitor. *Neuropharmacology*. **133**:107-120.

Portier M, Rinaldi-Carmona M, Pecceu F, Combes T, Poinot-Chazel C, Calandra B, Barth F, le Fur G, Casellas P. (1999). SR 144528, an antagonist for the peripheral cannabinoid receptor that behaves as an inverse agonist. *J Pharmacol Exp Ther*. **288**(2):582-9.

Ranjan R, Pandey S, Shukla AK. (2017). Biased Opioid Receptor Ligands: Gain without Pain. *Trends Endocrinol Metab*. **28**(4):247-249.

Resh MD. (2013). Covalent lipid modifications of proteins. *Curr Biol.* **23**(10):R431-5.

Roots I, Laschinski G, Arjomand-Nahad F, Kirchheiner J, Schwarz D, Brockmöller J, Cascorbi I, Gerloff T. (2007). Genotype and phenotype relationship in drug metabolism. *Ernst Schering Res Found Workshop*. (59):81-100.

Schihada H, Shekhani R, Schulte G. (2021). Quantitative assessment of constitutive G protein-coupled receptor activity with BRET-based G protein biosensors. *Sci Signal.* **14**(699):eabf1653.

Scott-Dennis MJ, Rafani FA, Yicheng Y, Perera T, Harwood C, Guba W, Rufer AC, Grether U, Veprintsev DB, Sykes DA. (2023). Development of a membrane-based Gi-

CASE biosensor assay for profiling compounds at cannabinoid receptors. [Manuscript submitted for publication].

Seamon KB, Padgett W, Daly JW. (1981). Forskolin: unique diterpene activator of adenylate cyclase in membranes and in intact cells. *Proc Natl Acad Sci U S A.* **78**(6):3363-7.

Senese NB, Kandasamy R, Kochan KE, Traynor JR. (2020). Regulator of G-Protein Signaling (RGS) Protein Modulation of Opioid Receptor Signaling as a Potential Target for Pain Management. *Front Mol Neurosci*. **13**:5.

Sengmany K, Hellyer SD, Albold S, Wang T, Conn PJ, May LT, Christopoulos A, Leach K, Gregory KJ. (2019). Kinetic and system bias as drivers of metabotropic glutamate receptor 5 allosteric modulator pharmacology. *Neuropharmacology.* **149**:83-96.

Shao Z, Yan W, Chapman K, Ramesh K, Ferrell AJ, Yin J, Wang X, Xu Q, Rosenbaum DM. (2019). Structure of an allosteric modulator bound to the CB1 cannabinoid receptor. *Nat Chem Biol*. **15**(12):1199-1205.

Shenoy SK, Drake MT, Nelson CD, Houtz DA, Xiao K, Madabushi S, Reiter E, Premont RT, Lichtarge O, Lefkowitz RJ. (2006). beta-arrestin-dependent, G protein-independent ERK1/2 activation by the beta2 adrenergic receptor. *J Biol Chem*. **281**(2):1261-73.

Slice LW, Yee HF Jr, Walsh JH. (1998). Visualization of internalization and recycling of the gastrin releasing peptide receptor-green fluorescent protein chimera expressed in epithelial cells. *Recept Channels*. **6**(3):201-12.

Smith JS, Lefkowitz RJ, Rajagopal S. (2018). Biased signalling: from simple switches to allosteric microprocessors. *Nat Rev Drug Discov.* **17**(4):243-260.

Soethoudt M, Grether U, Fingerle J, Grim TW, Fezza F, de Petrocellis L, Ullmer C, Rothenhäusler B, Perret C, van Gils N, Finlay D, MacDonald C, Chicca A, Gens MD, Stuart J, de Vries H, Mastrangelo N, Xia L, Alachouzos G, Baggelaar MP, Martella A, Mock ED, Deng H, Heitman LH, Connor M, Di Marzo V, Gertsch J, Lichtman AH, Maccarrone M, Pacher P, Glass M, van der Stelt M. (2017). Cannabinoid CB_2 receptor ligand profiling reveals biased signalling and off-target activity. *Nat Commun*. **8**:13958.

Sugiura T, Waku K. (2000). 2-Arachidonoylglycerol and the cannabinoid receptors. Chem Phys Lipids. **108**(1-2):89-106.

Sun D, Ostermaier MK, Heydenreich FM, Mayer D, Jaussi R, Standfuss J, Veprintsev DB. (2013). AAscan, PCRdesign and MutantChecker: a suite of programs for primer design and sequence analysis for high-throughput scanning mutagenesis. *PLoS One*. **8**(10):e78878.

Sykes DA, Dowling MR, Charlton SJ. (2010). Measuring receptor target coverage: a radioligand competition binding protocol for assessing the association and dissociation rates of unlabeled compounds. *Curr Protoc Pharmacol*. Chapter 9:Unit 9.14.

Teitler M, Herrick-Davis K, Purohit A. (2002). Constitutive activity of G-protein coupled receptors: emphasis on serotonin receptors. *Curr Top Med Chem*. **2**(6):529-38.

Tirona RG. (2011). Molecular mechanisms of drug transporter regulation. *Handb Exp Pharmacol.* (201):373-402.

Titus S, Neumann S, Zheng W, Southall N, Michael S, Klumpp C, Yasgar A, Shinn P, Thomas CJ, Inglese J, Gershengorn MC, Austin CP. (2008). Quantitative high-throughput screening using a live-cell cAMP assay identifies small-molecule agonists of the TSH receptor. *J Biomol Screen*. **13**(2):120-7.

Turcotte C, Blanchet MR, Laviolette M, Flamand N. (2016). The CB_2 receptor and its role as a regulator of inflammation. *Cell Mol Life Sci*. **73**(23):4449-4470.

Verheijen M, Lienhard M, Schrooders Y, Clayton O, Nudischer R, Boerno S, Timmermann B, Selevsek N, Schlapbach R, Gmuender H, Gotta S, Geraedts J, Herwig R, Kleinjans J, Caiment F. (2019). DMSO induces drastic changes in human cellular processes and epigenetic landscape in vitro. *Sci Rep*. **9**(1):4641.

Vögler O, Barceló JM, Ribas C, Escribá PV. (2008). Membrane interactions of G proteins and other related proteins. *Biochim Biophys Acta*. **1778**(7-8):1640-52.

Wan Q, Okashah N, Inoue A, Nehmé R, Carpenter B, Tate CG, Lambert NA. (2018). Mini G protein probes for active G protein-coupled receptors (GPCRs) in live cells. *J Biol Chem*. **293**(19):7466-7473.

Wang T, Li Z, Cvijic ME, Zhang L, Sum CH. (2017). Measurement of cAMP for Gαs- and Gαi Protein-Coupled Receptors (GPCRs). In: Markossian S, Grossman A, Brimacombe K, et al., editors. Assay Guidance Manual [Internet]. Bethesda (MD): Eli Lilly & Company and the National Center for Advancing Translational Sciences. Available from: https://www.ncbi.nlm.nih.gov/books/NBK464633/.

Wen Y, Wang Z, Zhang R, Zhu Y, Lin G, Li R, Zhang J. (2023). The antinociceptive activity and mechanism of action of cannabigerol. *Biomed Pharmacother*. **158**:114163.

Wenzel-Seifert K, Seifert R. (2000). Molecular analysis of beta(2)-adrenoceptor coupling to G(s)-, G(i)-, and G(q)-proteins. *Mol Pharmacol.* **58**(5):954-66.

Wilkerson JL, Alberti LB, Thakur GA, Makriyannis A, Milligan ED. (2022). Peripherally administered cannabinoid receptor 2 (CB_2R) agonists lose anti-allodynic effects in TRPV1 knockout mice, while intrathecal administration leads to anti-allodynia and reduced GFAP, CCL2 and TRPV1 expression in the dorsal spinal cord and DRG. *Brain Res*. **1774**:147721.

Wright MH, Heal WP, Mann DJ, Tate EW. (2010). Protein myristoylation in health and disease. *J Chem Biol.* **3**(1):19-35.

Wu DF, Yang LQ, Goschke A, Stumm R, Brandenburg LO, Liang YJ, Höllt V, Koch T. (2008). Role of receptor internalization in the agonist-induced desensitization of cannabinoid type 1 receptors. *J Neurochem*. **104**(4):1132-43.

Wu HM, Yang YM, Kim SG. (2011). Rimonabant, a cannabinoid receptor type 1 inverse agonist, inhibits hepatocyte lipogenesis by activating liver kinase B1 and AMP-activated protein kinase axis downstream of Gα i/o inhibition. *Mol Pharmacol*. **80**(5):859-69.

Xiang X, Wang X, Wu Y, Hu J, Li Y, Jin S, Wu X. (2022). Activation of GPR55 attenuates cognitive impairment, oxidative stress, neuroinflammation, and synaptic dysfunction in a streptozotocin-induced Alzheimer's mouse model. *Pharmacol Biochem Behav*. **214**:173340.

Zhang Y, Qin Z, Sun W, Chu F, Zhou F. (2021). Function of Protein S-Palmitoylation in Immunity and Immune-Related Diseases. *Front Immunol*. **12**:661202.

Zhou Y, Xu Y, Yang J, Yu Z, Wang W, Yuan M, Wang Y, Bai Q, Li Z. Spinal cannabinoid receptor 2 activation alleviates neuropathic pain by regulating microglia and suppressing P2X7 receptor. *Front Mol Neurosci*. **16**:1061220.

Zhu X, Finlay DB, Glass M, Duffull SB. (2020). Evaluation of the profiles of CB 1 cannabinoid receptor signalling bias using joint kinetic modelling. *Br. J. Pharmacol.* ***177***:3449–3463.